

Distribution Agreement

In presenting this thesis or dissertation as a partial fulfillment of the requirements for an advanced degree from Emory University, I hereby grant to Emory University and its agents the non-exclusive license to archive, make accessible, and display my thesis or dissertation in whole or in part in all forms of media, now or hereafter known, including display on the world wide web. I understand that I may select some access restrictions as part of the online submission of this thesis or dissertation. I retain all ownership rights to the copyright of the thesis or dissertation. I also retain the right to use in future works (such as articles or books) all or part of this thesis or dissertation.

Signature:

Paul. R. Evans II

Date

RGS14 limits postsynaptic calcium to block CA2 synaptic plasticity

By

Paul Robert Evans II
Doctor of Philosophy

Graduate Division of Biological and Biomedical Sciences
Neuroscience

John R. Hepler, PhD
Advisor

Gary J. Bassell, PhD
Committee Member

Randy A. Hall, PhD
Committee Member

Stephen F. Traynelis, PhD
Committee Member

James Q. Zheng, PhD
Committee Member

Accepted:

Lisa A. Tedesco, Ph.D.
Dean of the James T. Laney School of Graduate Studies

Date

RGS14 limits postsynaptic calcium to block CA2 synaptic plasticity

By

Paul Robert Evans II
B.S., Emory University, 2010

Advisor: John R. Hepler, PhD

An abstract of
a dissertation submitted to the Faculty of the
James T. Laney School of Graduate Studies of Emory University
in partial fulfillment of the requirements for the degree of
Doctor of Philosophy

Graduate Division of Biological and Biomedical Sciences
Neuroscience
2016

Abstract

RGS14 limits postsynaptic calcium to block CA2 synaptic plasticity

By Paul Robert Evans II

The regulators of G protein signaling (RGS) proteins are a diverse family of proteins that function as central components of G protein and other signaling pathways. RGS14 is an unusual RGS protein that acts as a multifunctional scaffolding protein to integrate signaling events and pathways essential for synaptic plasticity, including conventional and unconventional G protein signaling and mitogen-activated protein kinase (MAPK). In primate and rodent brain, RGS14 is highly expressed in pyramidal neurons in hippocampal area CA2. However, the protein distribution and spatiotemporal expression patterns of RGS14 in mouse brain during postnatal development have not been described. We find that RGS14 mRNA/protein are upregulated in mouse brain during early postnatal development until reaching highest, sustained levels in adulthood. Our findings also reveal a dynamic localization of RGS14 protein in mouse brain. CA2 pyramidal neurons differ dramatically from neighboring regions CA1/CA3 in that they lack a capacity for long-term potentiation (LTP) of synaptic transmission, which is highly correlated with memory formation. While we previously identified RGS14 as a critical factor limiting CA2 plasticity and hippocampus-dependent learning and memory, the mechanisms by which RGS14 blocks synaptic plasticity in CA2 remained unknown. Independent studies attributed this lack of plasticity to robust calcium (Ca^{2+}) buffering and extrusion in CA2 spines relative to CA1. However, RGS14 has not been implicated in Ca^{2+} signaling required synaptic potentiation. Here we provide the first evidence that RGS14 natively associates with key members of Ca^{2+} signaling pathways in mouse brain. Additionally, the nascent LTP found in CA2 neurons of mice lacking RGS14 requires Ca^{2+} -stimulated pathways. Our results further show RGS14 impairs CA2 spine structural plasticity, the activity-dependent enlargement of spines associated with synaptic potentiation. Finally, we find that CA2 neurons lacking RGS14 display robust spine structural plasticity and significantly larger spine Ca^{2+} transients than WT CA2 or CA1 controls. Our findings define a previously unknown role of RGS14 in the regulation of Ca^{2+} signaling in neurons. Moreover, we provide strong evidence that RGS14 limits spine Ca^{2+} levels during synaptic activity to restrict plasticity in area CA2.

RGS14 limits postsynaptic calcium to block CA2 synaptic plasticity

By

Paul Robert Evans II
B.S., Emory University, 2010

Advisor: John R. Hepler, PhD

A dissertation submitted to the Faculty of the
James T. Laney School of Graduate Studies of Emory University
in partial fulfillment of the requirements for the degree of
Doctor of Philosophy

Graduate Division of Biological and Biomedical Sciences
Neuroscience
2016

Table of Contents

	<u>Page</u>
Chapter 1: Introduction	1
1.1 Overview of G protein/GPCR/RGS signaling	2
1.2 Molecular characterization of Regulator of G protein Signaling 14 (RGS14)	3
1.2.1 RGS14 protein architecture	3
1.2.2 RGS14 bridges conventional, unconventional, and MAPK signaling	5
1.2.3 Cellular regulation of RGS14	10
1.3 RGS14 naturally limits learning and synaptic plasticity in hippocampal CA2	12
1.3.1 RGS14 suppresses LTP and spatial learning	12
1.3.2 LTP as a model of memory formation and typical mechanisms	14
1.3.3 Possible mechanisms by which RGS14 suppresses plasticity in hippocampal CA2	17
1.3.4 Connecting CA2 – redefining anatomical substrates of learning	20
1.4 Overall hypothesis and objective of this dissertation	26
Chapter 2: Postnatal developmental expression of RGS14 in the mouse brain	29
2.1 Introduction	30
2.2 Experimental Procedures	32
2.3 Results	38
2.4 Discussion	55
Chapter 3: RGS14 limits postsynaptic calcium to block CA2 synaptic plasticity	63
3.1 Introduction	64
3.2 Experimental Procedures	64

3.3 Results	76
3.4 Discussion	100
Chapter 4: Discussion	106
4.1 RGS14 expression during early postnatal development: the aging conspiracy against plasticity in CA2	107
4.2 RGS14 regulation of Ca ²⁺ signaling in CA2 spines	108
4.3 Working model of CA2 plasticity regulation by RGS14	109
4.4 Defining mnemonic functions for CA2 and RGS14	113
4.5 Roles for CA2 in human behavior and disease	117
4.6 RGS14: more than just a suppressor of learning and memory?	121
4.7 Summary and Perspectives	123
References	126

Index of Figures and Tables

	<u>Page</u>
Figure 1.1 – RGS14 domain structure and identified binding partners	4
Figure 1.2 – Area CA2 at the intersection of multiple hippocampal circuits	22
Table 2.1 – Primary antibodies used in this chapter	33
Figure 2.1 – Characterization of the epitope, specificity, and sensitivity of the RGS14 mouse monoclonal antibody	41
Figure 2.2 – RGS14 mRNA and protein are upregulated in mouse brain during postnatal development	44
Table 2.2 – Regional brain localization of RGS14	45
Figure 2.3 – RGS14 immunolabeling in anterior olfactory nucleus (AON) of postnatal mouse brain	47
Figure 2.4 – RGS14 immunoreactivity in postnatal mouse piriform cortex	48
Figure 2.5 – RGS14 immunoreactivity in postnatal mouse orbital cortex	50
Figure 2.6 – RGS14 immunoreactivity in postnatal mouse entorhinal cortex	51
Figure 2.7 – RGS14 immunolabeling is transiently expressed in postnatal mouse neocortex	53
Figure 2.8 – RGS14 immunolabeling in postnatal mouse hippocampus	54
Table 3.1 – RGS14 natively interacts with G protein, calcium-activated plasticity signaling, and actin cytoskeleton pathways in mouse brain	77
Figure 3.1 – RGS14 directly interacts with Ca ²⁺ /CaM and CaMKII	84
Figure 3.2 – Further characterization of the RGS14•Ca ²⁺ /CaM interaction	86
Figure 3.3 – Nascent CA2 LTP in RGS14 KO mice follows similar mechanisms to	89

CA1

Figure 3.4 – Supplemental immunostaining and input/output curve	91
Figure 3.5 – RGS14 impairs spine structural plasticity	94
Figure 3.6 – Multiposition Imaging of Spines with High Throughput Automation (MISHA)	96
Figure 3.7 – RGS14 restricts CA2 spine Ca^{2+} levels	98
Figure 3.8 – Similar changes in dendritic Ca^{2+} levels during spine structural plasticity	99
Figure 4.1 – Postsynaptic signaling regulating plasticity in hippocampal CA2 pyramidal neurons	112

Chapter 1:
Introduction¹

¹ A portion of this chapter has been published. Evans PR, Dudek SM, and Hepler JR (2015) Regulator of G Protein Signaling 14 (RGS14): A Molecular Break on Synaptic Plasticity Linked to Learning and Memory. *Prog Mol Biol Transl Sci.* 133:169-206.

1.1 Overview of G protein/GPCR/RGS signaling

Established models propose that agonist binding to a G protein-coupled receptor (GPCR) induces a conformational change in the receptor, which then activates heterotrimeric G proteins ($G\alpha\beta\gamma$) by acting as a guanine nucleotide exchange factors (GEFs) to catalyze the exchange of GTP for GDP on the $G\alpha$ subunit. The activated $G\alpha$ -GTP dissociates from $G\beta\gamma$, and both subunits are free to interact with downstream effectors¹⁻⁴. RGS proteins recognize and directly bind to activated $G\alpha$ -GTP subunits through a conserved RGS domain and act as GAPs by stimulating the intrinsic GTPase activity of the $G\alpha$ subunit to hydrolyze GTP to GDP, thereby deactivating G protein signaling. Compelling evidence now indicates that GPCRs are platforms where specific sets of proteins assemble to execute receptor-specific signaling events. RGS proteins are central components of GPCR signaling complexes that fine-tune G protein signaling and serve as multifunctional integrators of these pathways⁵⁻⁹.

The RGS protein family consists of almost 40 members that share a conserved RGS domain, which selectively binds to activated $G\alpha$ -GTP subunits and, in nearly all cases, confers GAP activity. The RGS proteins are categorized into subfamilies based on sequence homology of the RGS domains and GAP function. The structures, functions, and regions flanking the RGS domains vary widely among the diverse members of this protein family ranging from simple polypeptides comprised of only an RGS domain with limited flanking regions to larger, more complex members with additional protein binding domains. The presence of binding domains for additional proteins allows these complex RGS proteins to serve as multifunctional integrators of G protein signaling pathways that regulate cell signaling and organ physiology^{6,10}. This review will highlight

the established signaling roles of RGS14, and how its capacity to bridge separate signaling networks could affect the acquisition of learning leading to episodic memory.

1.2 Molecular characteristics of Regulator of G protein Signaling 14 (RGS14)

1.2.1 RGS14 protein architecture

RGS14 is a 61 kDa protein classified in the D/R12 subfamily of RGS proteins along with its closest related RGS proteins, RGS10 and RGS12^{5,11,12}. RGS10 is a small protein (~20 kDa) that only shares high sequence identity with the RGS domain of RGS14. By contrast, RGS14 and RGS12 are more complex proteins with multi-domain structures^{12,13}. RGS14 contains an N-terminal RGS domain, which binds to and exerts GAP activity towards activated G α i/o-GTP subunits to limit the duration of heterotrimeric G protein signaling¹⁴. In addition, RGS14 also contains two tandem Ras/Rap-binding domains (RBDs) and a G protein regulatory (GPR, also referred to as a GoLoco motif) motif (Figure 1)¹³⁻¹⁵. RGS14 preferentially binds activated H-Ras-GTP through its first RBD¹⁶⁻¹⁸, and the tandem RBD region also mediates interactions with Rap2-GTP and Raf kinases^{13,17}. We recently have found that this region of RGS14 also can bind calmodulin (CaM) in a Ca²⁺-dependent manner¹⁹. RGS14 selectively binds inactive G α i1/3-GDP through the GPR motif to inhibit guanine nucleotide exchange (i.e. GDI activity) and localize to cellular plasma membranes²⁰⁻²³. The presence of these multiple protein binding domains indicates that RGS14 serves other important signaling functions in addition to the canonical GAP activity of RGS proteins. Of note, all of RGS14's identified binding partners have key roles in synaptic plasticity in the hippocampus making RGS14 well positioned to modulate neuronal physiology. We will first review the known signaling functions, localization, and regulation of RGS14 so as to

provide context for our subsequent discussion of RGS14's roles in brain, and our proposed model for how RGS14 integrates signaling in hippocampal CA2 neurons. We also will highlight recent findings about newly appreciated roles for hippocampal area CA2, the brain region where RGS14 is expressed.

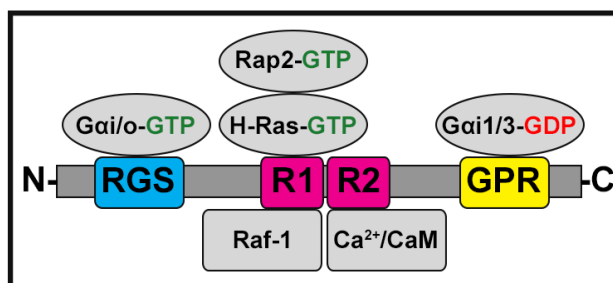


Figure 1.1 RGS14 domain structure and identified binding partners. RGS14 directly binds activated G α o and G α i subunits through its N-terminal RGS domain, and selectively interacts with inactive G α i1 and G α i3 at the GPR motif. RGS14 also contains tandem Ras/Rap-binding domains (R1 and R2) that directly bind activated H-Ras, Rap2, Ca²⁺/CaM, and Raf kinases.

RGS14 and RGS12 are the only RGS proteins that contain two G α binding domains, the GPR motif and the conserved RGS domain, allowing these members to interact with both active GTP-bound and inactive GDP-bound G α subunits^{14,20,24} RGS14 can clearly operate as a conventional GAP for members of the G α i/o subfamily^{14,15,24}, and we propose that RGS14 first engages G α i-GTP following activation of a GPCR. In support of this model, native RGS14 is located in both the cytosolic and membrane fractions of brain extracts¹⁴, and is visible in dendritic shafts and spine heads of hippocampal neurons by electron microscopy, but not at the plasma membrane²⁵. A small fraction of RGS14 may be recruited from the cytosol to act as a conventional GAP and

limit G α i-GTP signaling, and then become captured at the plasma membrane by the resulting G α i-GDP via its GPR motif. Once at the membrane, the RGS14:G α i1-GDP complex can serve as a signaling node to engage other signaling proteins/pathways. Curiously, truncated forms of RGS14 lacking the RGS domain can bind and engage other smaller RGS protein such as RGS2 and RGS4 to markedly enhance their GAP activity^{26,27} and this interaction is facilitated by the tandem Ras-binding domains (RBDs, R1 and R2)²⁶. The physiological significance of this unexpected interaction is unclear, but splice variants of RGS14 lacking the RGS domain have been reported that may operate in this manner²⁶.

The G α i-GDP-interacting GPR motif found in RGS14 is a defining feature shared by all members of the Group II activator of G protein signaling (AGS) proteins family²⁸. Recent evidence indicates these AGS proteins participate in “unconventional” G protein signaling that regulates cell and organ physiology^{29,30}. In contrast to traditional models of heterotrimeric G protein signaling initiated by GPCR activation, unconventional G protein signaling models^{24,28-31} posit that the G α protein exists in a resting state complex with a GPR protein, in place of G $\beta\gamma$, until activated by either a GPCR or a non-receptor GEF. The presence of these two G α binding sites uniquely positions RGS14 and RGS12 at the interface of these two protein (RGS and AGS) families to serve functions distinct from other conventional RGS proteins²⁴.

1.2.2 RGS14 bridges conventional, unconventional, and MAPK signaling

We and others have shown that RGS14 utilizes its complex protein architecture to integrate conventional and unconventional G protein signaling pathways^{23,32,33}. Cell imaging studies have shown that RGS14 localization in cells is heavily influenced by

interactions with G proteins. When expressed in cells alone, recombinant RGS14 predominantly localizes to the cytosol, but it rapidly moves between the cytosol and nucleus and associates with centrosomes in a cell cycle-dependent manner^{22,33}. Co-expression of G*ai*1/3 recruits RGS14 from the cytosol to the plasma membrane where they co-localize^{15,22,23}. Deletion or selective inactivation of a nuclear localization sequence (NLS) within the GPR motif eliminates the capacity of RGS14 to bind G*ai*1/3 at the GPR, recruit RGS14 to the plasma membrane, or localize to the nucleus, indicating G protein interactions with the GPR are necessary for proper subcellular localization of RGS14²⁰⁻²². Possible roles for RGS14 in the nucleus remain a mystery at this time. Native RGS14 has not yet been observed in the nuclei of hippocampal neurons²⁵, but this localization may be triggered by specific signaling events or may be relevant in B and T cell lymphocytes where RGS14 also is highly expressed. A role for RGS14 in the nuclei of hippocampal neurons cannot be ruled out, and remains a topic of exploration.

Evidence suggests that RGS14 functionally interacts with newly appreciated members of unconventional G protein pathways and participates in receptor-independent G protein signaling²³. Resistance to inhibitors of cholinesterase-8A (Ric-8A, also referred to as Synembryn) is a cytosolic guanine nucleotide exchange factor (GEF) that binds to and catalyzes nucleotide exchange on inactive G*ai*-GDP subunits³⁴ and regulates other GPR-containing proteins in complex with G*ai*1-GDP^{23,35,36}. When RGS14 and Ric-8A were transfected into cells, alone or together, both proteins co-localize in the cytosol. Co-expression of wild-type G*ai*1 causes both proteins to translocate to the plasma membrane suggesting they may form a functional signaling complex. Ric-8A interacts with RGS14 through the tandem RBD region to induce dissociation of the RGS14:G*ai*1-GDP complex

in cells and *in vitro* by competing with RGS14 for G α i1 to exert GEF activity. A role for RGS14 in unconventional G protein signaling could be physiologically relevant since RGS14 and Ric-8A natively co-localize in hippocampal CA2 neurons²³, but physiological roles for RGS14:G α i1 and Ric-8A interactions remain undefined.

The RGS14:G α i1 signaling complex can also functionally interact with a G α i-linked GPCR, thereby integrating conventional and unconventional G protein pathways³². Bioluminescence resonance energy transfer (BRET) studies in live cells validated that RGS14 binds G α i1/3 at the plasma membrane through the GPR motif, and showed that RGS14 selectively forms a complex with the Gi/o-linked α_{2A} -adrenergic receptor (α_{2A} -AR) in a G α i/o-dependent manner via the GPR motif. Interestingly, agonist stimulation of the α_{2A} -AR markedly decreased its interaction with RGS14 with no effect on the RGS14:G α i1 complex. Certain other Group II AGS proteins also interact with G α i1 and associate with G α i/o-linked GPCRs^{37,38}, but these proteins seem to dissociate from G α i1 following agonist stimulation, suggesting that the RGS14:G α i1-GDP complex may be regulated and function differently from other AGS:G α i1 complexes. Ric-8A induced dissociation of G α i1 from RGS14 and α_{2A} -AR, and even more so following agonist stimulation. These studies demonstrated that RGS14 functionally integrates conventional and unconventional G protein signaling pathways in live cells, and is regulated in a manner that is distinct from other RGS and GPR-containing proteins³².

Besides having two G α binding domains, RGS14 also contains tandem RBDs that position it to integrate G protein and MAPK cascades^{17,18}. RGS14 can suppress extracellular signal-regulated kinase (ERK) activation by a G α i1- and H-Ras/Raf-dependent mechanism¹⁷. RGS14 interacts selectively with activated H-Ras-GTP and Raf

kinases simultaneously to form a ternary complex, and these partners facilitate each other's interactions with RGS14. RGS14 binds activated H-Ras and Raf kinases in cells to inhibit platelet-derived growth factor (PDGF)-stimulated ERK 1/2 phosphorylation. When a targeted loss-of-function mutation that prevents H-Ras binding was introduced into the R1 domain of RGS14 (R333L), RGS14 could no longer suppress ERK phosphorylation indicating that RGS14 directly binds H-Ras-GTP to negatively regulate ERK signaling. Co-expression of G*ai*1 also prevented RGS14 from regulating ERK by disrupting its interactions with Raf kinases, but not H-Ras. Taken together, these data indicate that (1) RGS14 interactions with G*ai*1 and Raf kinases are mutually exclusive, and (2) RGS14 interactions with H-Ras and Raf kinases are necessary for RGS14 to inhibit ERK phosphorylation. These results suggest that RGS14 may serve as a G protein-regulated molecular switch to modulate H-Ras/ERK signaling depending upon the upstream signal and proteins in complex.

Following up on these findings, BRET studies examining G*ai*1:RGS14:H-Ras interactions in live cells support a model in which RGS14 toggles between G protein and MAPK signaling pathways¹⁸. These findings confirmed that RGS14 binds activated H-Ras-GTP through the first RBD^{16,17}, and binding of inactive G*ai*1-GDP enhances RGS14 interactions with H-Ras, likely promoting the assembly of a trimeric G*ai*1:RGS14:H-Ras complex¹⁸. Cell imaging data revealed that co-expression of G*ai*1 and/or constitutively active H-Ras(G12V) recruit RGS14 from the cytosol to plasma membrane where they co-localize. Consistent with this idea, activated H-Ras membrane localization is required for RGS14/H-Ras interactions.

In addition to G*ai*1-mediated regulation of H-Ras:RGS14 binding, specific GPCRs also can regulate the RGS14/H-Ras complex. As mentioned earlier, RGS14 associates with the Gi/o-linked α_{2A} -AR only in the presence of G*ai*/o proteins³². Co-expression of the α_{2A} -AR and G*ai*1 did not effect the basal interactions between RGS14 and active H-Ras, but agonist stimulation of the α_{2A} -AR resulted in a decreased RGS14/H-Ras BRET signal. The RGS14:G*ai*1 complex association with α_{2A} -AR was partially blocked in the presence of activated H-Ras, but H-Ras also reduced the agonist-induced dissociation of the RGS14/ α_{2A} -AR complex observed only in the presence of G*ai*1. These results demonstrate that H-Ras and the α_{2A} -AR reciprocally regulate one another's association with RGS14 in a G*ai*1-dependent manner. Regulation of the RGS14/H-Ras complex by α_{2A} -AR activation could induce a new conformation in RGS14 allowing it to engage downstream effectors. For example, the complex might rearrange to position RGS14 to GAP the G*ai*/o subunit activated by the α_{2A} -AR. Another possibility is that the G*ai*1:RGS14:H-Ras complex interacts with distinct effector(s) that specifically recognize the ternary complex. It remains to be determined whether this complex is subject to similar regulation by other GPCRs or non-receptor GEFs such as Ric-8A.

The structural basis for how RGS14 interacts with its partners to integrate these signaling pathways remains undefined at this time, but is an active area of research. The evidence discussed so far indicates that RGS14 undergoes significant intramolecular conformational rearrangements, depending on the binding partners, consistent with its role as a scaffolding protein. In particular, G*ai*1 interactions with RGS14 promotes association with activated H-Ras¹⁸ and/or the α_{2A} -AR³², whereas G protein binding

inhibits binding to Raf kinases¹⁷. Although the structures of individual domains contained in RGS14 have been elucidated, structural data of the full-length protein could yield great insight into the structural basis of the tightly regulated assembly of these signaling complexes. Ongoing experiments are examining whether RGS14 can bind multiple Gα proteins simultaneously through the RGS domain and the GPR motif, and how this affects the overall RGS14 structure and function.

1.2.3 Cellular regulation of RGS14

RGS14 is also subject to post-translational modifications that play an important role in modulating its functions. Kinases are prominent downstream targets of the cellular pathways linked to RGS14, and protein phosphorylation regulates the activity of many proteins, including RGS proteins³⁹. RGS14 negatively regulates Gαi/o-GTP signaling through the GAP activity of its RGS domain as well as GDI activity at the GPR motif, and Gαi/o activation canonically inhibits adenylyl cyclase, thereby reducing cellular levels of cAMP and, consequently, cAMP-dependent protein kinase A (PKA) activity. We have previously shown that RGS14 is phosphorylated at two sites (Ser 258 and Thr 494) by PKA *in vitro* and natively in B35 neuroblastoma cells⁴⁰. PKA-mediated phosphorylation of RGS14 at T494 increases its affinity for Gαi1-GDP binding at the GPR motif *in vitro*, suggesting this modification could promote and stabilize the assembly of a RGS14:Gαi1 signaling complex in cells. Though speculative, PKA-directed phosphorylation of RGS14 could serve as a feed-forward mechanism to potentiate PKA activity by facilitating interactions with Gαi1, which recruits RGS14 to the plasma membrane and is required for RGS14 to associate with a GPCR or cytosolic GEF. Once at the plasma membrane, RGS14's GAP activity could limit Gαi/o-GTP

signaling following GPCR activation (or receptor independent GEFs) to alleviate inhibition of adenylyl cyclase and elevate cAMP/PKA activity. PKA phosphorylation could also prolong the lifetime of G $\beta\gamma$ signaling events by stabilizing RGS14:Gai1-GDP complex formation. Implicit to this model is the idea that PKA phosphorylation promotes an RGS14:Gai1 complex at the plasma membrane to nucleate association with other binding partners in a multi-protein signaling complex (G protein, H-Ras-GTP, Ca²⁺/CaM) to regulate specific downstream effector pathways.

RGS14 also is phosphorylated by ERK at serine 52 *in vitro*³⁹. Whether this modification occurs in cells and the functional effects of this event are currently unknown, but remain a topic of interest. The fact that RGS14 directly engages the H-Ras/ERK signaling pathway suggests some feedback regulation. Proteomics studies have identified several additional phosphorylated residues on RGS14 from rodent and human tissues⁴¹. Therefore, it is likely that RGS14 is phosphorylated by many more kinases in its native environment. Identifying the kinases and cellular signals that trigger phosphorylation of RGS14 and the functional consequences of these modifications will provide great insight into the complex regulation of RGS14 *in vivo*. RGS14 may also be subject to other post-translational modifications (e.g. ubiquitination, lipid modifications, etc.) that could strongly influence its cellular functions.

In summary, RGS14 is a complex and highly unusual RGS protein that functionally integrates conventional G protein signaling with unconventional G protein pathways, MAPK signaling pathways, and possibly calcium signaling pathways. The signaling functions, subcellular localization, and binding partner interactions of RGS14 are tightly regulated by protein interactions and post translational modifications.

Therefore RGS14 uniquely sits at the interface between multiple signaling networks that have well-defined roles in physiology, and especially so in the regulation of synaptic plasticity within the hippocampal neurons where RGS14 is highly expressed.

1.3 RGS14 naturally limits learning and synaptic plasticity in hippocampal CA2

Previous studies characterizing the tissue distribution of RGS14 found that this signaling protein is present in brain, spleen, and B and T lymphocytes^{12-15,42}. Native RGS14 is found at high levels in brain of various species including mouse, rat, nonhuman primate, and human^{12,14,25,42-45}. In adult rodents, RGS14 is most highly expressed in brain, specifically in neurons^{14,25,42}. Most recently, we have shown that RGS14 mRNA/protein expression is upregulated during postnatal mouse brain development reaching its highest levels in adulthood⁴². Within the adult mouse brain, we demonstrated that RGS14 protein is highly enriched in spines and dendrites of pyramidal neurons in the CA2 subfield of the hippocampus^{25,42}. Although RGS14 likely has important functions in immune cells, this dissertation will focus on the defined role of RGS14 in episodic learning and memory and hippocampus function.

1.3.1 RGS14 suppresses LTP and spatial learning

RGS14 is highly expressed and restricted in its expression pattern to certain neurons of the hippocampus. The hippocampus has a critical role in forming new declarative memories, which includes memories for general facts as well as knowledge of personal experiences. The importance of the hippocampus in human memory encoding is best depicted by the case of patient H.M. (recently identified as Henry Molaison) who was unable to form new long-term declarative memories after his temporal lobes (including hippocampi) were surgically removed, despite intact motor learning and

intellectual abilities⁴⁶. Subsequent lesion studies in animal models experimentally demonstrated that intact hippocampal function is required for long-term memory formation across several species. Additional aspects/types of memory are non-hippocampal-dependent and are encoded by other brain regions, such as basal ganglia-dependent motor learning and amygdala-dependent auditory fear conditioning. It is now widely accepted that the hippocampus is responsible for many aspects of learning and memory including spatial, object recognition, social, and contextual memory.

Based on its high expression levels in hippocampus, we hypothesized that RGS14 likely serves a critical role in learning and memory. In studies designed to test this idea directly, we found that mice lacking RGS14 mRNA/protein (RGS14-KO) displayed enhanced performance in tests of hippocampal-dependent learning and memory compared with wild-type littermates²⁵. Spatial learning was assayed using the Morris Water Maze in which the mice use visual cues to navigate the water maze and locate a hidden escape platform. Over successive trial days both groups of mice learned the task, as indicated by decreased latency to find the submerged platform, but RGS14-KO mice exhibited a marked acceleration in their rate of spatial learning. RGS14-KO mice also exhibited an enhanced ability to recognize objects they had previously encountered in the novel object test when compared with wild-type littermates. Of note, RGS14-KO mice did not differ from wild-type littermates in non-hippocampal-dependent behaviors such as open-field locomotion, startle response, and anxiety. Taken together, these findings indicate that RGS14 naturally inhibits forms of learning and memory specific to the hippocampus.

1.3.2 LTP as a model of memory formation and typical mechanisms

The underlying mechanism(s) by which RGS14 regulates learning and memory are unclear, although the hippocampus in particular is known for the robust capacity of its resident neurons to express plasticity – i.e. the ability of neurons to modulate their responses to neuronal activity in a synapse-specific and activity-dependent manner. Several forms of synaptic plasticity have been reported in the mammalian brain, and these phenomena are differentially regulated across postnatal development and brain regions. Long-term potentiation (LTP), the stable increase in synaptic strength in response to brief periods of synaptic stimulation, is a prevalent form of plasticity observed in the hippocampus during learning in intact animals^{47,48}. Pharmacological and genetic manipulations that disrupt LTP similarly impair learning and memory formation leading to the widely accepted hypothesis that LTP is the cellular mechanism underlying memory formation and/or storage⁴⁹. Traditional views of the hippocampus have largely focused on the trisynaptic dentate gyrus (DG)-CA3-CA1 circuit as the primary route of information flow through the hippocampus⁵⁰. Neurons in entorhinal cortex layer II (ECII) provide excitatory input to DG granule cells, which in turn, form synapses on CA3 pyramidal neurons via mossy fiber projections. These pyramidal neurons within area CA3 synapse onto CA1 pyramidal neurons via Schaffer collateral (SC) projections. High-frequency synaptic stimulation of CA3 Schaffer collaterals readily induces LTP in CA1 pyramidal neurons, and the cellular mechanisms behind LTP have been extensively studied at these synapses⁵¹. Based on the key role that LTP plays in learning and memory, we postulated that RGS14 may play a pivotal role in modulating LTP in the hippocampus.

Long-term potentiation (LTP) is a complex process resulting from coordinated signaling events in postsynaptic spines, compartments protruding from dendrites where most excitatory synapses form, in response to neural activity⁵². In CA1 neurons, high-frequency stimulation of presynaptic SC inputs results in the activation of postsynaptic AMPA and NMDA-type glutamate receptors (AMPA and NMDARs, respectively). Calcium (Ca^{2+}) influx through NMDARs initiates various biochemical pathways that ultimately result in potentiation of the AMPA-mediated component of the excitatory postsynaptic current (EPSC), i.e. LTP. Of note, at least two reported RGS14 binding partners (e.g. CaM, H-Ras) are activated by postsynaptic Ca^{2+} and have critical functions in LTP induction and associated spine morphology changes⁵³⁻⁵⁶. Postsynaptic Ca^{2+} entry is required for LTP induction at CA3-CA1 synapses⁵⁷, and compelling evidence has demonstrated that postsynaptic Ca^{2+} entry activates these signaling events by activating the Ca^{2+} /calmodulin-dependent protein kinase II (CaMKII)⁵⁸. From there, the mechanisms are less clear, but one idea is that activated CaMKII phosphorylates postsynaptic AMPARs and in addition, initiates the activity of downstream kinase cascades leading to their enhanced trafficking to the postsynaptic membrane. Several lines of evidence demonstrate that CaMKII activation is both sufficient and necessary for LTP induction in CA1 neurons and some types of learning. One of the major downstream targets of CaMKII is the H-Ras-ERK pathway^{54,56}. Activity-dependent gene transcription, local protein synthesis at the stimulated synapse, and AMPAR exocytosis during LTP depend on H-Ras-ERK signaling^{55,59}. H-Ras-ERK activity is required, but unlike CaMKII, is not sufficient for LTP induction in CA1 neurons. Additional biochemical pathways also have defined roles in LTP induction at hippocampal CA1 synapses, but we

will only highlight cellular mechanisms relevant to RGS14 signaling and plasticity in hippocampal CA2 neurons.

The CA2 pyramidal neurons that express RGS14 also receive input from CA3 neurons, which form synapses onto the dendrites of CA2 neurons. However, this intervening area CA2 has been often overlooked and historically regarded as a “transition” zone between areas CA3 and CA1, despite early anatomical studies identifying CA2 as a separate subfield⁶⁰. Very recent evidence has shown that CA2 pyramidal neurons possess distinct anatomical, physiological, and genetic properties from pyramidal neurons in neighboring areas CA3 and CA1^{61,62}. In sharp contrast to CA1, SC synapses onto CA2 pyramidal neurons fail to support LTP following protocols that reliably induce LTP in CA1⁶³. Given the enhanced learning phenotype observed in RGS14-KO mice, we designed experiments to determine if loss of RGS14 affected LTP induction in CA2 pyramidal neurons. Much to our surprise, we found that RGS14-KO mice display a robust and nascent LTP in CA2 following SC stimulation but had no difference in LTP induction in CA1, where enhanced plasticity is traditionally associated with hippocampus-dependent learning²⁵. Consistent with previous reports that RGS14 negatively regulates ERK/MAPK activation, the nascent CA2 LTP observed in RGS14-KO mice could be blocked by a MEK/ERK inhibitor suggesting RGS14 may normally suppress ERK signaling to limit LTP in area CA2. These results demonstrate that RGS14 innately restricts activity-dependent plasticity in hippocampal area CA2, but not CA1. Taken together, these findings strongly suggest that the enhanced learning and memory observed with the loss of RGS14 is due to increased synaptic plasticity in CA2. This study was the first report to implicate hippocampal area CA2 and RGS14 in mediating

spatial learning and novel object recognition memory. Although the cellular mechanisms regulating atypical plasticity in area CA2 and its contributions to hippocampal function and behavior are not well understood, very recent findings have elucidated additional mechanisms governing CA2 physiology and associated behaviors⁶².

1.3.3 Possible mechanisms by which RGS14 suppresses plasticity in hippocampal CA2

Molecular mechanisms by which RGS14 suppresses LTP in CA2 neurons will now be considered. Our discussion will focus on signaling pathways that RGS14 engages and are operational in CA1 and CA2 neurons including Ca^{2+} , G protein, and H-Ras/ERK signaling pathways.

CA2 neurons are slightly less excitable than CA1 neurons, but Zhao et al. (2007) found that differences in the intrinsic electrophysiological properties relative to CA1 could not account for the plasticity resistant phenotype observed in CA2 pyramidal neurons⁶³. Therefore some molecular difference between CA2 and CA1 is likely the factor limiting synaptic plasticity in CA2. One peculiarity of CA2 neurons is their extracellular matrix, which contains a higher concentration of proteins believed to restrict plasticity that are not found in CA3/CA1⁶⁴⁻⁶⁶. In addition, a number of genes are highly expressed in CA2 besides RGS14, including Amigo2, STEP, calbindin, PCP4/Pep-19, TARP5, FGF5, neurotrophin-3, α -actinin 2, certain adenylyl cyclase isoforms (1,5,6), adenosine A1 receptor, vasopressin 1b receptor, and others^{62,67,68}. Of these genes, several are members of Ca^{2+} -activated signaling pathways (calbindin, PCP4/Pep-19, certain adenylyl cyclase isoforms, vasopressin 1b receptor), are known to influence synaptic plasticity, and are likely to contribute to the atypical plasticity observed in area CA2.

Germane to the discussion are our findings that RGS14 directly engages H-Ras/ERK signaling^{16–18,69}. As discussed, RGS14 binding of active H-Ras-GTP can inhibit ERK signaling. Within hippocampal neurons, ERK/MAPK signaling is essential for AMPA receptor trafficking to the post-synaptic density (PSD) and the enlargement of spines associated with LTP^{54–56,59}. Therefore, it is quite possible that RGS14 could inhibit LTP induction in CA2 neurons, at least in part, by inhibiting H-Ras/ERK signaling. Studies are ongoing to test this idea directly.

Also potentially relevant are our recent findings that RGS14 can engage Ca²⁺ signaling pathways by binding calmodulin (CaM) in a Ca²⁺-dependent manner¹⁹. At this time, we do not yet know if or how RGS14/CaM interactions affect LTP, though this mechanism is under active investigation. However, LTP induction as well as ERK-mediated AMPAR trafficking in spines are both Ca²⁺/CaM/CaMKII-dependent processes^{54,57–59}, and as noted, several Ca²⁺-binding proteins are highly expressed in CA2 pyramidal neurons^{68,70,71}. Earlier studies were designed to investigate if differences in Ca²⁺ handling could explain the synaptic stability of CA2 synapses. Cell imaging studies of Ca²⁺ dynamics in dendritic spines revealed that CA2 pyramidal neurons display smaller elevations in intracellular Ca²⁺ concentrations relative to CA1 or CA3 pyramidal neurons due to higher endogenous buffering capacity and rates of Ca²⁺ extrusion⁷². Raising intracellular Ca²⁺ transients in CA2 to levels comparable to CA3/CA1, either by elevating external Ca²⁺ concentration or inhibiting plasma membrane Ca²⁺ extrusion pumps, permits LTP induction. The synaptic potentiation due to high external Ca²⁺ was blocked by the NMDAR antagonist APV, indicating that Ca²⁺ influx through NMDAR is required, similar to canonical LTP observed in CA1. These findings indicate that CA2

neurons possess the cellular machinery to support LTP, but active Ca^{2+} regulation restricts the induction of activity-dependent plasticity in CA2. The robust Ca^{2+} extrusion rates and LTP-resistant phenotype can be explained, at least in part, by high expression levels of the CaM-binding protein Pep-19 in CA2 pyramidal neurons. Further, introducing camstatin, a functional peptide analog of Pep-19, into CA1 neurons resulted in much higher rates of Ca^{2+} extrusion similar to those observed in CA2 and blocked LTP induction following high-frequency stimulation of Schaffer collaterals. Simons et al. (2009) demonstrated that robust Ca^{2+} buffering and Ca^{2+} extrusion rates largely account for the limited expression of LTP in CA2 pyramidal neurons. Therefore, it was an unexpected finding that RGS14-KO mice displayed a robust capacity for LTP in CA2 at the time, because RGS14 had not yet been linked to Ca^{2+} -activated plasticity signaling. Our recent observations¹⁹ that RGS14 binds Ca^{2+} /CaM suggest there may be a functional link.

In summary, strong evidence suggests that the unique complement of genes enriched in RGS14-expressing CA2 pyramidal neurons gives rise to the atypical regulation of plasticity in this region. How RGS14 engages these signaling proteins and pathways to regulate LTP is an area of active investigation. While RGS14 has been shown to restrict the induction of activity-dependent LTP at SC inputs to hippocampal CA2 neurons, whether RGS14 also regulates A1R and/or Avpr1b/Oxtr-induced potentiation remains to be determined. RGS14 is well positioned to modulate these key signaling pathways required for CA2 plasticity through its known binding partners, and its capacity to functionally integrate certain components of these signaling pathways (Figure 4.1). RGS14 could heighten A1R-potentiation by its negative regulation of *Gai/o*

signaling at the RGS and GPR domains. Further, PKA activity underlying A1R-potentiation could utilize RGS14 phosphorylation to prolong this plasticity by increasing the affinity of RGS14 for $G\alpha i^{40}$, which could target RGS14 to inhibit subsequent A1R activation. Support for this idea is bolstered by our findings that RGS14 in complex with $G\alpha i1$ functionally associates with another $G\alpha i/o$ -linked GPCR³². No published reports have demonstrated a functional link between RGS14 and $G\alpha q$ implicated in Avpr1b/Oxtr-induced potentiation, but nonetheless, RGS14 may engage downstream partners such as CaM¹⁹ or other Ca^{2+} -activated signaling events that mediate this form of plasticity in CA2. However, these models are currently speculative, and the involvement of RGS14 in these forms of CA2 plasticity remains to be determined. The features of CA2 plasticity discussed thus far have been elucidated in the context of the synaptically stable SC synapses, but recent studies using refined genetic approaches have revealed previously unknown connections to area CA2 that provide far reaching implications for this region's function.

1.3.4 Connecting CA2 – redefining anatomical substrates of learning

Recent studies have thrust hippocampal area CA2, the region where RGS14 is expressed, out of the shadows and into the spotlight⁸¹. Kohara et al. (2014) used refined cell-type specific approaches to clarify functional circuitry linking the CA2 subfield to other brain areas. These studies extended current knowledge on CA2 circuitry by identifying a new CA2-centric circuit that operates in parallel with the classic DG-CA3-CA1 trisynaptic circuit (Figure 1.2). These studies revealed an alternative DG-CA2-CA1_{deep} trisynaptic circuit that may function to encode distinct aspects of learning and

memory from the traditional DG-CA3-CA1 trisynaptic circuit associated with hippocampus-dependent learning and memory.

Previous classical anatomical criteria define area CA2 as the region between subfields CA3 and CA1 containing large pyramidal cells similar in size and dendritic branching patterns to CA3, but lacking thorny excrescences indicative of innervation from the DG⁶⁰. The CA2 subfield is also anatomically distinguished by the selective targeting of CA2 pyramidal neurons by strong projections from the supramammillary nucleus of the hypothalamus (SuM)⁸². As previously discussed, CA3 pyramidal neurons send Schaffer collateral (SC) projections through the stratum radiatum (sr) to form synapses onto proximal dendrites of CA2 and CA1 neurons, and CA2 neurons dramatically differ from CA1 by the absence of activity-dependent plasticity at these synapses. In contrast to the synaptic stability of SC-CA2 synapses, the synapses at the distal dendrites of CA2 neurons formed by afferents from entorhinal cortex layers II and III (ECII and ECIII, respectively) projecting through the stratum lacunosum moleculare (slm)) form strong monosynaptic connections that are highly plastic and support LTP induction⁸³. More recent studies^{81,84} have confirmed a functional direct connection from ECII to CA2 but do not support the previous finding that ECIII projects to CA2. Of note, RGS14 appears to be expressed throughout the dendritic tree, and how it restricts LTP induction at the SC synapses but not the more distal synapses from the entorhinal cortex is unclear, but suggests differential distribution of signaling proteins along the proximal-distal axis of CA2 dendrites or differences in presynaptic signaling may underlie these differences in plasticity.

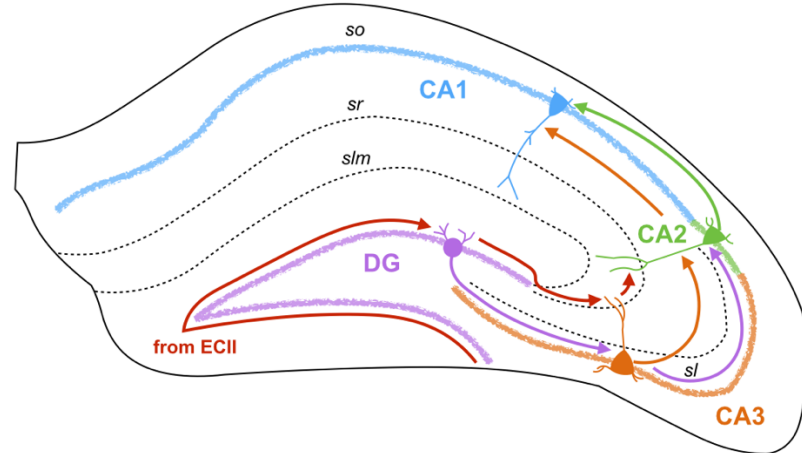


Figure 1.2. Area CA2 at the intersection of multiple hippocampal circuits. CA2 pyramidal neurons receive inputs from different brain regions along the proximal-distal axis of its dendrites (green). Hippocampal inputs from entorhinal cortex layer II (ECII, red) form synapses onto granule cells in the dentate gyrus (DG) and distal dendrites of CA3 and CA2 pyramidal neurons in the stratum lacunosum moleculare (slm). DG granule cells send mossy fiber synapses through the stratum lucidum (sl) that synapse onto the proximal dendrites of CA3 and CA2 pyramidal neurons (purple). CA3 pyramidal neurons form Schaffer collateral synapses (orange) onto CA2, which are usually LTP-resistant, as well as CA1 in the intermediate region of the dendrite in the stratum radiatum (sr). CA2 neurons form strong monosynaptic connections onto CA1 pyramidal neurons in the stratum oriens (so).

CA2 connectivity with other brain regions has also been studied to better understand its role in hippocampal circuitry, and provide insight into potential behaviors mediated by CA2. Within the hippocampus, RGS14-expressing CA2 neurons receive bilateral innervation from pyramidal neurons in ipsilateral and contralateral CA3 as well

as contralateral CA2⁸⁴. CA2 pyramidal neurons in turn send prominent projections to neurons in all CA fields (CA3, CA2, and CA1). Thus, CA2 forms reciprocal connections with CA3 while providing dense unilateral input into CA1 providing an anatomical substrate for unidirectional information flow through the hippocampus.

CA2 is also anatomically linked with brain regions outside the hippocampus. Several groups have confirmed the SUM afferent projections to CA2 satisfying one of the classical anatomical criteria for area CA2^{73,82,84-87}. A recent study identified a novel efferent projection from hippocampal CA2 to the SUM in the adult mouse brain, suggesting these two regions may reciprocally innervate each other to form a feedback loop⁸⁴. In addition to these inputs, independent studies have found reciprocal connections between area CA2 and the septal nuclei as well as the diagonal band of Broca. Neurons in area CA2 are also innervated by the median raphe nucleus and medial and lateral entorhinal cortex layer II. The paraventricular nucleus of the hypothalamus (PVN) was recently found to provide vasopressinergic input to CA2, demonstrating a likely source of the vasopressin to activate *Avpr1b* in CA2⁸⁴.

More recent studies employing genetic-based approaches have refined our understanding of CA2 circuitry. Using a modified rabies virus that could only be expressed in medial ECII (MECII) neurons to label monosynaptic inputs, Rowland et al. (2013) demonstrated a projection from CA2 pyramidal neurons indicating yet another reciprocal extra-hippocampal connection⁸⁸. Other recent studies using region-specific molecular markers found that CA2 pyramidal neurons surprisingly receive input from DG granule cells onto proximal dendrites in the stratum lucidum, despite lacking complex spines that are associated with mossy fiber synapses⁸¹. This study demonstrated

that in the mouse, DG granule cells directly synapse onto pyramidal neurons and interneurons in CA2, and that stimulation of these mossy fiber terminals results in a functional monosynaptic connection that is dominated by feed-forward inhibition similar to SC input^{81,83}. A subsequent study⁸⁹ further demonstrated that CA2 pyramidal neurons receive input from mature and immature granule cells. These immature granule cells are produced by neurogenesis in the dentate gyrus, which occurs throughout life and is intimately associated with hippocampus-dependent learning and memory. The mossy fiber terminals originating from newborn DG granule cells are smaller and take longer to develop in the CA2 subfield compared to CA3. While inflammation negatively regulates immature DG cell connections with CA2 and CA3, DG-CA2 projections arising from newborn neurons can be dramatically upregulated by exercise to a greater extent than those to neighboring CA3. Thus, environmental and developmental factors, in addition to the unique molecular composition, likely play a large role in shaping CA2 circuitry.

RGS14-expressing CA2 neurons also send dense projections through the stratum oriens to preferentially target CA1 pyramidal neurons located in the deep sublayer (CA1_{deep}), whereas CA3 innervates CA1 pyramidal neurons in the deep and superficial sublayers equally⁸¹. The preferential targeting of CA1_{deep} by CA2 makes sense of previous work where very few synaptically connected pairs of CA2-CA1 neurons could be identified⁸³. These findings were remarkable because they highlight a new trisynaptic circuit wherein ECII neurons project to DG, which send mossy fiber projections to CA2, which in turn synapse onto CA1 pyramidal neurons in the deep sublayer. The existence of several distinct circuits within the hippocampus might allow for separation of different input activity patterns to encode complementary/different aspects of memory within each

circuit. Moreover, the complex cortico-hippocampal circuitry demonstrated in these studies allows for several possible pathways for information flow through the hippocampus. For example, information could be routed through a disynaptic cortico-hippocampal circuit in which ECII directly stimulates CA2 that subsequently excites deep sublayer CA1 and/or reciprocally drives ECII. These reports consistently indicate that CA2 is positioned to serve as a central hub in the entorhinal-hippocampal network, and regulation of plasticity by RGS14 likely serves an important function in this network. For example, RGS14 in this context could prevent saturation/overlearning or preserve signal fidelity in this circuit.

The anatomical links described between CA2 and other regions provide clues into potential functions of area CA2 and RGS14 in mediating animal behavior. Reciprocal connectivity between CA2 and cholinergic projections (septal nuclei and diagonal band) may play an important role in attention and memory. Input from PVN demonstrates CA2 may integrate social information with other contextual information routed through the hippocampal circuit. Thus CA2 is poised to regulate theta rhythm in the hippocampus observed during exploratory behavior through connections with SUM. Consistent with our finding that robust CA2 plasticity in RGS14-KO mice correlates with enhanced spatial learning, CA2 connectivity to ECII could modulate “grid cells,” which help orient an animal’s sense of location in its environment. Stellate cells within MECII are putative grid cells that are responsible for forming a mental framework to navigate an environment^{90–92}; elimination of hippocampal excitatory input to grid cells abolishes the ability of these cells to form a grid pattern. RGS14-expressing neurons within area CA2 are the obvious candidates for providing excitatory drive to grid cells as the vast majority

of hippocampal inputs to MECII arise from CA2⁸⁸. The specific contribution of CA2 pyramidal neurons and the expression of RGS14 therein to grid cell function will provide great insight into the neural mechanisms underlying spatial learning and memory.

In summary, the relative stability at CA3-CA2 synapses and the pivotal role of RGS14 in this regard may provide a mechanism for tightly regulating plasticity at those synapses that can only be induced under specific circumstances⁶². We envision a circuit whereby CA3 inputs to CA2 may modulate rather than drive responses from CA2, thereby acting like a filter to preserve fidelity in the circuit and/or acting to differentially route information through the putative circuits within the hippocampus. Plasticity in CA2 may only occur when convergent input (e.g. vasopressin release from PVN during social interaction) allows selective encoding of some types of memory. RGS14 plays a central role in restricting plasticity at SC synapses onto CA2 neurons, and may therefore serve as a molecular regulator of memory storage at these specific synapses. Future studies are necessary to determine if RGS14 similarly regulates CA2 plasticity at its other synaptic inputs and modulates other forms of learning and memory linked to CA2.

1.4 Overall hypothesis and objective of this dissertation

Although much work has characterized the functions of RGS14 *in vitro* and as overexpressed protein in cells, substantially less is known about the cellular interactions of RGS14 in brain^{24,93}. Our lab has previously shown that RGS14 naturally inhibits synaptic potentiation in its host CA2 pyramidal neurons²⁵, but the mechanisms by which RGS14 restricts CA2 plasticity remained elusive. Like RGS14, a number of genes are selectively enriched in CA2 pyramidal neurons that contribute to the atypical plasticity of these neurons^{62,67,68,94}. Based on strong evidence that spine Ca²⁺ handling gates synaptic

plasticity in CA2, my thesis project investigated if RGS14 restricts LTP in CA2 by interacting with key Ca^{2+} signaling pathways.

The first aim of this project was to delineate the spatiotemporal expression pattern of RGS14 in mouse brain during postnatal development. We and others have shown that RGS14 protein is enriched in adult mouse brain^{14,44}, but these studies did not provide detailed anatomical analysis of localization during development. As a gene that seemingly only suppresses learning in mouse brain, it would be intriguing if RGS14 expression levels or localization were developmentally regulated, and these findings could provide insight into additional functions of RGS14. I first performed qRTPCR/immunoblot studies to compare RGS14 mRNA/protein expression levels in mouse brain across development and immunolabeling to determine the localization of RGS14 across brain regions. These results are discussed in Chapter 2.

The second aim of this project was to identify the cellular mechanism(s) RGS14 employs to block LTP induction in CA2 pyramidal neurons. The oft neglected CA2 subregion of the hippocampus has only recently become a subject of investigation, rendering the mechanisms underlying the unique plasticity enigmatic. I was also curious about which previously identified binding partners RGS14 might complex with in brain or if we would discover novel interactions with other CA2-enriched proteins linked to plasticity. I used a combined approach of biochemical techniques, electrophysiology, and two-photon imaging in CA2 neurons to define the mechanisms by which RGS14 restricts LTP. These findings are discussed in Chapter 3.

Overall, the goal of these studies was to investigate the signaling pathways RGS14 engages in neurons and identify the mechanisms critical for plasticity suppression

in hippocampal CA2 neurons. Determining these mechanisms will greatly advance our understanding of the biology underlying memory formation and provide new mechanistic insight into the regulation of plasticity in area CA2. Finally, this work could clarify why it is advantageous for the hippocampus to express genes to suppress learning and memory.

Chapter 2²:
Postnatal developmental expression of RGS14 in the mouse brain

² This chapter has been slightly modified from the published manuscript. Evans PR, Lee SE, Smith Y, and Hepler JR. Postnatal developmental expression of regulator of G protein signaling 14 (RGS14) in the mouse brain. (2014) *J. Comp. Neurol.* 522, 186–203.

2.1 Introduction

Regulator of G Protein Signaling 14 (RGS14) is a highly unusual signaling protein that integrates G protein and MAPkinase signaling pathways to regulate synaptic plasticity and hippocampal-based learning and memory^{17,25,95}. RGS14 was first identified as a complex scaffolding protein with an unconventional domain structure that allows it to interact with various protein binding partners^{13,96}. Like other RGS proteins⁶, RGS14 contains an RGS domain, which binds to and accelerates the intrinsic GTPase activity of activated *Gai/o*-GTP subunits to limit heterotrimeric G protein signaling. However, unlike most other RGS proteins, RGS14 also contains two tandem Ras/Rap-binding domains (RBDs), and a G protein regulatory (GPR) motif¹³⁻¹⁵. RGS14 preferentially binds activated H-Ras-GTP as well as Raf kinases through the first RBD (RBD1)^{16,17,95} and selectively binds inactive *Gai1/3*-GDP subunits through the GPR motif to inhibit guanine nucleotide exchange and localize to cellular membranes²⁰⁻²². RGS14 has been shown to suppress ERK1/2 activity through a *Gai1*- and H-Ras-dependent mechanism, indicating that RGS14 functionally integrates G protein and MAP kinase signaling pathways¹⁷.

Northern blot experiments⁹⁶, in situ hybridization studies⁴⁵, and quantitative PCR⁴³ have independently reported that RGS14 mRNA is present in rat and human brain tissue. Similarly, immunohistochemical studies⁴⁴ and immunoblot experiments¹⁴ have found that RGS14 protein is enriched in rat and monkey brain. In the adult mouse brain, RGS14 mRNA and protein are predominantly found in CA2 hippocampal neurons, specifically within spines and dendrites²⁵. CA2 neurons uniquely exhibit a marked resistance to long-term potentiation (LTP) of excitatory glutamatergic synaptic

transmission in response to stimulation of incoming CA3 Schaffer collaterals, which reliably induce LTP in neighboring CA1 neurons⁶³. However, we have found that RGS14 knockout (RGS14 KO) mice display nascent and robust LTP in CA2 neurons, indicating that RGS14 is a natural suppressor of CA2 synaptic plasticity²⁵. Consistent with our previous report of RGS14 as a suppressor of MAP kinase signaling¹⁷, CA2 LTP in RGS14 KO mice was blocked by a MEK/ERK inhibitor suggesting that RGS14 inhibits this pathway to limit synaptic plasticity in area CA2^{25,62}. Further, RGS14 KO mice have enhanced performance on tests of spatial and novel object memory, with no differences in nonhippocampal-dependent behaviors²⁵. Taken together, these data indicate that RGS14 is a natural suppressor of both synaptic plasticity and hippocampal-dependent learning and memory²⁴.

Although previous studies have examined the localization of RGS14 mRNA and protein in adult rat and monkey brain^{44,45}, a detailed anatomical analysis of RGS14 localization in mouse brain has not yet been reported. Further, no studies have examined the spatiotemporal expression pattern of RGS14 in the brain of any animal during postnatal development, a period in which hippocampal-dependent processes are required for adaptation and survival. Thus, to gain a better understanding of how RGS14 expression is regulated during postnatal mouse brain development, we examined total mRNA and protein levels using quantitative real-time PCR and immunoblotting. We also determined the localization and distribution of RGS14 protein during postnatal development by performing a detailed light microscopic immunohistochemical analysis of RGS14 localization in the mouse brain. We present the first comprehensive characterization of a recently described anti-RGS14 monoclonal antibody²⁵. Here we

report that RGS14 protein expression is absent from brain at birth, but is upregulated and differentially expressed across brain regions during postnatal development (P0-P21) into adulthood where expression is restricted to hippocampal regions CA2 and fasciola cinerea, anterior olfactory nucleus, and piriform cortex. These findings suggest new roles for RGS14 in regulating physiology and behavior during mouse brain development.

2.2 Experimental Procedures

Animals and tissue preparation

Male and female wild-type C57BL/6J and RGS14 knockout (RGS14-KO) mice were used in this study. All procedures were approved by the animal care and use committee of Emory University and conform to the U.S. National Institutes of Health guidelines. Adult (older than 2 months) wild-type and RGS14-KO mice were obtained from mouse colonies maintained at Emory University. RGS14-KO mice were created by insertion of a LacZ/Neo cassette that deletes exons 2-7 of the RGS14 gene, and these mice were backcrossed to the C57BL/6J background as previously described²⁵. Timed pregnant wild-type C57BL/6J female mice were purchased from Jackson Laboratories (Bar Harbor, Maine), and mice from these litters were collected at postnatal stages P0, P3, P5, P7, P10, P14, and P21. Mouse pups (P0, P3, and P5) were deeply anesthetized on ice in combination with isoflurane. At all other stages, mice were deeply anesthetized with isoflurane.

For immunohistochemical studies, P7 mice and older were deeply anesthetized with isoflurane and transcardially perfused with cold 0.9% saline solution, followed by 4% paraformaldehyde (PFA, w/v) in phosphate-buffered saline (PBS), pH 7.4. After perfusion, the brains were removed from the skull and immersion fixed in 4% PFA in

PBS, pH 7.4, for 24 hours at 4°C. P0, P3, and P5 mouse brains were fixed by immersion. Brains were embedded in paraffin and coronally sliced in 10 µm thick sections.

For immunoblotting studies, mice were deeply anesthetized and euthanized by decapitation. Brains were rapidly removed from the skull and homogenized on ice using a glass dounce homogenizer with 10 strokes in an ice-cold homogenization buffer containing 50 mM Tris, 150 mM NaCl, 1 mM EDTA, 2 mM DTT, 5 mM MgCl₂, phosphatase inhibitors (1:1,000, Sigma Aldrich), and one mini protease inhibitor cocktail tablet (Roche Applied Science, Basel, Switzerland), diluted with dH₂O to 10 mL, pH 7.4.

Antibody characterization

Antibodies, sources, and the concentrations at which they were used are listed in

Table 2.1.

TABLE 2.1: Primary Antibodies Used

Antibody	Immunizing Antigen	Host Species	Source/catalog number	Dilution
Beta actin	Synthetic peptide derived from residues 1-100 of human beta actin	Rabbit (polyclonal)	Abcam # ab8227	IB: 1:5,000
Flag M2-HRP	Flag peptide (DYKDDDDK) fused onto the N-terminus of interleukin 2 (IL-2)	Mouse (monoclonal)	Sigma Aldrich # A8592	IB: 1:25,000
Green Fluorescent Protein (GFP)	Recombinant GFP protein	Mouse (monoclonal)	MBL International # 5892	IB: 1:1,000
HA-Peroxidase, Clone HA-7	Synthetic peptide from residues 98-106 of human influenza virus hemagglutinin (HA) conjugated to KLH	Mouse (monoclonal)	Sigma Aldrich # H6533	IB: 1:1,000
Regulator of G Protein Signaling 14 (RGS14)	Full length rat RGS14	Mouse (monoclonal)	Neuromabs (Clone N133/21) # 75-170	IB: 1:1,000-5,000 IHC: 1:500

HEK293 cells (ATCC, Manassas, VA) were maintained in Dulbecco's modified eagle's medium (Mediatech) supplemented with 10% fetal bovine serum (Atlanta Biologicals, 5% after transfection), 2 mM L-glutamine (Invitrogen), 100 U/mL penicillin (Mediatech), and 100 mg/mL streptomycin (Mediatech) in a humidified environment at 37°C with 5% CO₂.

The rat RGS14 cDNA used in this study (Genbank accession number U92279) was acquired as described¹⁴. Flag-RGS14 truncation mutants containing residues 1-202, 205-490, 371-544, and 444-544 were created as described²². HA-RGS2, HA-RGS4, and HA-RGS16 were created in our laboratory as described⁹⁷. The Flag-RGS10 cDNA used in this study was kindly provided by Drs. Malu Tansey and Jae-Kyung Lee (Emory University School of Medicine). GFP-RGS12 TS was a kind gift of Dr. Rory Fisher (University of Iowa). Thioredoxin and hexa-histidine tagged RGS14 (TxH₆-RGS14) protein was purified as described¹⁴.

Transfections were performed using previously described protocols with polyethyleneimine³⁸ (PEI; Polysciences, Inc.). After 24 hours of expression, cells were washed with ice-cold PBS and harvested in a lysis buffer containing 50 mM Tris, 150 mM NaCl, 1 mM EDTA, 2 mM DTT, 5 mM MgCl₂, 1% Triton X-100 (v/v), phosphatase inhibitors (1:1,000, Sigma Aldrich), and one mini protease inhibitor cocktail tablet (Roche Applied Science, Basel, Switzerland), diluted with dH₂O to 10 mL, pH 7.4. Cells were lysed for one hour at 4°C rocking end-over-end, and subsequently centrifuged to pellet cell debris.

Immunoblotting

After preparing cell lysates and mouse brain homogenates, Bradford protein assays (Thermo Scientific) were performed to assess total protein content in order to normalize protein across samples. Samples were prepared for immunoblotting by diluting with 4X Laemmli sample buffer to a final 1X concentration and heating samples to 95°C in a heating block for 5 minutes. Mouse brain homogenates were subsequently sonicated on ice. Samples from the cell lysates and mouse brain homogenates were loaded onto 11% acrylamide gels and subjected to SDS-PAGE to separate proteins. Proteins were then transferred to nitrocellulose and subjected to immunoblotting to probe for RGS14 and to test the specificity of the anti-RGS14 antibody. After blocking nitrocellulose membranes for 1 hour at room temperature in blocking buffer containing 5% nonfat milk (w/v), 0.1% Tween-20, and 0.02% sodium azide, diluted in 20 mM Tris buffered saline, pH 7.6, membranes were incubated with primary antibodies diluted in the same buffer overnight at 4°C, except for anti-Flag and anti-HA primary antibodies. Membranes were washed in Tris buffered saline containing 0.1% Tween-20 (TBST) and subsequently incubated with either an anti-mouse, anti-rabbit, or anti-goat HRP-conjugated secondary antibody diluted in TBST (1:5,000, 1:25,000, or 1:3,000, respectively) for 1 hour at room temperature. Following block, anti-Flag-HRP and anti-HA-HRP primary antibodies were diluted in TBST and incubated with membranes for 1 hour at room temperature with no secondary antibody. Protein bands were visualized using enhanced chemiluminescence and exposing membranes to films.

Reverse transcription and real-time quantitative PCR

For real-time quantitative-PCR (qRT-PCR) studies, mice were deeply anesthetized and euthanized by decapitation. Brains were rapidly removed from the skull,

and total RNA was purified from whole brains using a PureLink RNA Mini Kit (Ambion). RNA yields were quantified using a Nanodrop 1000 (Thermo Scientific), and reverse transcription was performed using a SuperScript III First-Strand Synthesis SuperMix for qRT-PCR (Invitrogen) with 1 µg of total RNA from each brain. qPCR was performed using a DyNAmo HS SYBR Green qPCR kit (Thermo Scientific) on an iQ5 Multicolor Real-time PCR Detection System (Biorad). All samples were diluted 1:50 in nuclease-free water, and 8 µl of these dilutions were used for each SYBR Green PCR reaction containing 10 µl SYBR Green PCR Master Mix, 5 µM each primer, and dH₂O. The reactions were incubated for 30 seconds at 95°C, followed by 40 cycles with 30 seconds denaturation at 95°C, 30 seconds annealing at 60°C, and 30 seconds extension at 72°C. Following the amplification protocol, melt curves were generated for samples. RGS14 mRNA was amplified using the following oligonucleotide primers: forward primer, 5'-AAATCCCCGCTGTACCAAG-3'; reverse primer, 5'-GTGACTTCCCAGGCTTCAG-3'. The housekeeping gene glyceraldehyde 3-phosphate dehydrogenase (GAPDH, Genbank accession number M32599) was used as a standard to normalize levels of RGS14. GAPDH mRNA was amplified using the following oligonucleotide primers: forward primer, 5'-TGAAGCAGGCATCTGAGGG-3'; reverse primer, 5'-CGAAGGTGGAAGAGTGGGAG-3'.

qRT-PCR expression and analysis

Following qPCR amplification, the data were analyzed in Microsoft Excel. All qPCR reactions were performed on 96-well plates with all postnatal stages present and all samples tested in triplicate. For all qPCR analyses, RNA from two biological replicates was amplified in 5 separate qPCR reactions. Within each qPCR reaction, sample C(t)

values were averaged and RGS14 levels were normalized to GAPDH using the $\Delta\Delta C(t)$ method ($\Delta\Delta C(t) = 2^{-(RGS14-GAPDH)}$). $\Delta\Delta C(t)$ values from each experiment were averaged and expressed as percent of wild-type adult. Error bars represent the standard error of the mean.

Immunohistochemistry

Coronal sections of paraffin embedded mouse brains were manually dewaxed and dehydrated in a series of ethanol washes. Endogenous peroxidase tissue was quenched by incubating brain sections in 3% hydrogen peroxide diluted in methanol for 5 minutes at 40°C followed by 3 rinses in 0.075% Brij 35 solution Tris Brij pH 7.5 solution (0.1 M Tris-HCl pH 7.5, 0.1 M NaCl, 0.005 M MgCl₂, 0.075% Brij 35). Sections were then blocked for 1 hour and 45 minutes at 4°C with goat anti-mouse IgG AffiniPure fab fragment (Jackson Immunoresearch) at a dilution of 1:250 in blocking buffer (Vectastain standard ABC kit, Vector Laboratories). Sections were incubated with the RGS14 monoclonal antibody diluted in Tau Secret Formula (1:500) for 24 hours at 4°C. The following day, sections were rinsed three times in Tris Brij, pH 7.5 and incubated with 1:200 horse anti-mouse biotinylated secondary antibody diluted in Tris Brij containing 2% horse serum for 30 minutes at 37°C. Sections were then rinsed three times in Tris Brij and incubated for 80 minutes at 37°C in the avidin-biotin peroxidase complex (ABC) solution (Vectastain standard ABC kit, Vector Laboratories). For revelation, sections were first rinsed in Tris Brij solution, then incubated in a solution containing 0.096% 3,3'-diaminobenzidine tetrahydrochloride (DAB, Vector Laboratories) for 5 minutes. Finally, sections were counterstained with hematoxylin (Biomedica), and washed in Tris Brij followed by a rinse in distilled water containing 0.075% Brij 35 solution.

Light microscopy and photomicrograph production

Mouse brain sections mounted and coverslipped on glass slides were analyzed using an Olympus BX51 light microscope. Digital images of the slides were captured and analyzed using DP Controller software on a DP70 camera (Olympus). Brain regions were identified using the Allen Brain Atlas (<http://mouse.brain-map.org/>) coronal mouse brain reference atlas. Representative images were cropped for presentation and assembled into montages using Adobe Photoshop CS6 Extended.

2.3 Results

Antibody characterization

To validate the immunohistochemical findings of this study, we provide the first detailed characterization of an anti-RGS14 monoclonal antibody (clone N133/21) developed in collaboration between our laboratory and the NIH/NINDS-sponsored University of California-Davis/NeuroMab Facility (<http://neuromab.ucdavis.edu/catalog.cfm>). Our previous initial studies indicated that this antibody specifically recognizes native RGS14 in mouse brain²⁵. To identify the region on RGS14 containing the epitope recognized by the antibody, we performed a series of immunoblot experiments with this antibody probing cell lysates expressing different regions of RGS14 (Fig. 2.1). HEK293 cell lysates transfected with N-terminally Flag-tagged full-length rat RGS14, various N-terminally Flag-tagged RGS14 truncation mutants, or empty vector (pcDNA3.1) were immunoblotted for detection using the anti-RGS14 antibody (Fig. 2.1A). Rat RGS14 is 544 amino acids in length with a predicted molecular weight of 61 kDa. We detect a prominent band corresponding to full-length Flag-RGS14 at 62 kDa and also detect the presence of RGS14 truncation mutants

encoding residues 205-490 (32 kDa), 371-544 (21 kDa), and 444-544 (15 kDa). The anti-RGS14 antibody does not recognize any protein in HEK293 cell lysates transfected with the RGS14 truncation mutant encoding amino acids 1-202 or empty vector alone (Fig. 2.1B, left). Independently probing equal amounts of the cell lysates with an anti-Flag antibody reveals prominent bands for full-length RGS14 and all truncation mutants, but does not detect any protein cell lysates transfected with empty vector (Fig. 2.1B, right). The recognition of the RGS14 truncation mutants containing residues 205-490, 371-544, and 444-544, but not the mutant containing residues 1-202, indicates that the epitope recognized by this anti-RGS14 antibody is located between residues 444 and 490 of RGS14.

To demonstrate the specificity of the RGS14 antibody, we performed an immunoblot experiment probing mouse brain homogenate and cell lysates expressing various other epitope-tagged RGS proteins including RGS14's closest relatives, RGS12 and RGS10. Wild-type mouse brain homogenate and HEK293 cell lysates transfected with Flag-tagged rat RGS14, GFP-RGS12-TS, Flag-RGS10, RGS2-HA, RGS4-HA, RGS16-HA, or empty vector (pcDNA3.1) were immunoblotted for detection with the RGS14 antibody (Fig. 2.1C, left). Probing with the anti-RGS14 antibody only detects a prominent single band in wild-type mouse brain lysate at 61 kDa corresponding to native RGS14 and a slightly higher molecular weight band from cell lysate transfected with Flag-tagged full-length rat RGS14, but no bands are detected in cell lysates transfected with other RGS proteins or empty vector (Fig. 2.1C, right). The same cell lysates were also probed with an anti-GFP, anti-FLAG, or anti-HA antibody to confirm expression of transfected cDNAs (Fig. 2.1C top). These results demonstrate the specificity of the

RGS14 antibody as it does not detect any other RGS proteins, including RGS14's closest protein relatives RGS12 and RGS10^{6,98}. This antibody was also tested on human and monkey brain tissue, but does not detect any protein, either by immunoperoxidase labeling of brain sections or by immunoblot of brain tissue homogenates, suggesting that the specific epitope present in mouse and rat RGS14 recognized by this monoclonal antibody is not present in primate RGS14 (data not shown).

To determine the detection limit of this antibody, recombinant rat thioredoxin- and hexa-histidine-tagged RGS14 (TxH₆-RGS14) was purified to homogeneity, diluted in a range of decreasing concentrations, and immunoblotted with the RGS14 antibody. The antibody recognizes a prominent single band at 61 kDa and detects as little as 0.75 ng of pure TxH₆-RGS14 (Fig. 2.1D). The doublet observed with 100 ng and 50 ng of pure TxH₆-RGS14 reflects minor degradation products of the purified protein.

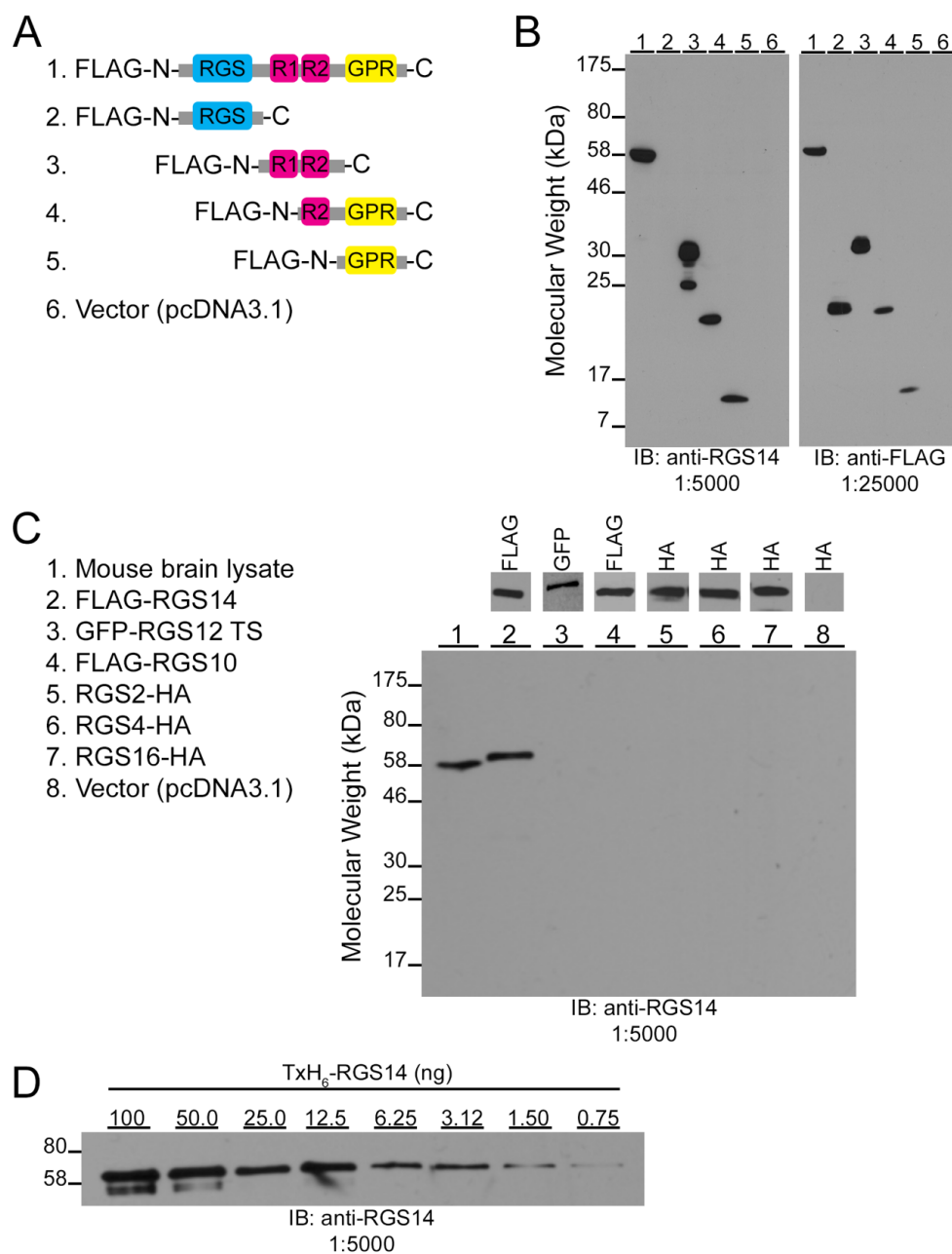


Figure 2.1 Characterization of the epitope, specificity, and sensitivity of the RGS14 mouse monoclonal antibody. **A:** Cartoons depicting the domain structure of Flag-tagged RGS14 truncation mutants used to map the region recognized by the antibody. *RGS*, Regulator of G protein signaling domain; *RBD*, Ras/Rap- binding domain; *GPR*, G protein regulatory motif. **B:** HEK293 cell lysates transfected with Flag-tagged RGS14 or

truncation mutant cDNAs were subjected to SDS-PAGE and immunoblotting with anti-RGS14 antibody (1:5,000). Equal amounts of these samples were separately subjected to SDS-PAGE and immunoblotting with an anti-Flag antibody (1:25,000) to verify cDNA expression. **C:** Wild-type mouse brain homogenate (Lane 1) and HEK293 cell lysates transfected with Flag-RGS14 (Lane 2), GFP-RGS12 TS (Lane 3), Flag-RGS10 (Lane 4), RGS2-HA (Lane 5), RGS4-HA (Lane 6), RGS16-HA (Lane 7), or empty vector (Lane 8, pCDNA3.1) were subjected to SDS-PAGE and immunoblotting with the anti-RGS14 antibody (1:5,000). Equal amounts of these samples were separately subjected to SDS-PAGE and immunoblotting with either an anti-Flag antibody (Lanes 2 and 4, 1:25,000), anti-GFP antibody (Lane 3, 1:1,000), or anti-HA antibody (Lanes 5-8, 1:1,000) to confirm protein expression. *GFP*, green fluorescent protein; *HA*, hemagglutinin. **D:** A serial dilution of purified thioredoxin- and hexa-histidine-tagged RGS14 (TxH₆-RGS14) at 100 ng, 50, 25, 12.5, 6.25, 3.12, 1.50, 0.75 ng was subjected to SDS-PAGE and immunoblotting with the anti-RGS14 antibody (1:5,000).

RGS14 mRNA and protein are upregulated during postnatal brain development

To quantify total levels of RGS14 mRNA throughout postnatal mouse brain development, mRNA was extracted from whole mouse brains at various postnatal stages and SYBR Green quantitative real-time PCR (qRT-PCR) reactions were performed. Quantitative analysis of mRNA levels reveals that RGS14 mRNA is found at very low levels in P0 brain and is gradually upregulated throughout postnatal development to reach the highest levels during adulthood (Fig. 2.2A). No RGS14 mRNA is amplified from adult RGS14-KO mouse brain, demonstrating the specificity of the oligonucleotide primers.

To analyze the expression levels of RGS14 protein throughout postnatal development, equal amounts of protein from mouse brain homogenates collected from different postnatal stages were subjected to SDS-PAGE, immunoblotting, and probed with the RGS14 antibody. In agreement with the observed increasing mRNA levels, RGS14 protein is first detected by immunoblot as a prominent 61 kDa band at P7 and is gradually upregulated during postnatal development until it reaches the highest levels in adult mouse brain (Fig. 2.2B, left). Of note, RGS14 protein levels do not change after reaching adulthood as similar amounts of RGS14 are observed in mice aged up to one year. Immunoblots loaded with equal amounts of protein from adult wild-type and RGS14-KO brain homogenates were probed with the RGS14 monoclonal antibody to demonstrate specificity. The antibody recognizes a single 61 kDa band in WT brain, but no signal is detected in RGS14-KO brain, indicating that this antibody specifically recognizes RGS14 (Fig 2.2B, right). The same blots were probed with an anti-beta actin antibody to demonstrate equal protein loading for all samples.

To validate RGS14 protein levels observed by immunoblot experiments, mouse brain sections from P0, P7, P14, P21, adult WT, and adult RGS14-KO mice containing hippocampus were immunoperoxidase-labeled with the anti-RGS14 antibody and analyzed by light microscopy (LM, Fig. 2.2C). Consistent with immunoblot experiments, no immunoperoxidase labeling is observed in P0 hippocampus indicating absence of significant RGS14 protein expression. However, immunoperoxidase staining results in a dark brown deposit, which intensely labels CA2 pyramidal dendritic arbors and fasciola cinerea (FC) neurons in P14, P21, and adult WT hippocampus. Low levels of DAB labeling are observed in P7 hippocampus compared to older mice, consistent with less

protein detected in immunoblot experiments at this age. Low-level background immunoreactivity is observed in the CA2 subfield of the adult RGS14-KO mouse brain. The nature of this staining is unclear, but may be non-specific background (see Discussion) as we find complete loss of the 61 kDa band corresponding full-length RGS14 protein by immunoblot with the same RGS14 antibody (Fig. 2.2B, right). Additionally, no RGS14 mRNA was detected in adult RGS14-KO mouse brain (Fig. 2.2A). Taken together, these studies demonstrate that RGS14 protein is not detectable until P7 after which time the protein is upregulated until adulthood where it continues to be expressed at the same level.

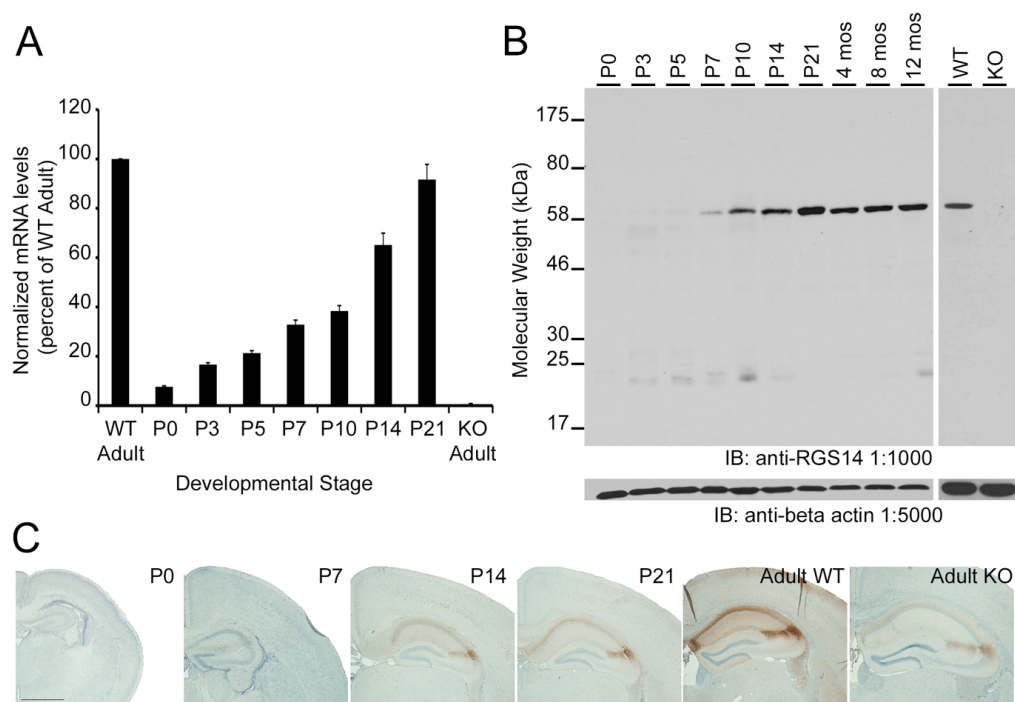


Figure 2.2 RGS14 mRNA and protein are upregulated in mouse brain during postnatal development. **A:** Quantification of RGS14 mRNA levels determined by quantitative real-time PCR (qRT-PCR). Within each qPCR reaction, sample C(t) values were averaged and RGS14 levels were normalized to GAPDH using the $\Delta\Delta C(t)$ method

($\Delta\Delta C(t) = 2^{-\Delta\Delta C(t)}$). $\Delta\Delta C(t)$ values from each experiment were averaged and expressed as percent of wild-type adult. Error bars represent the standard error of the mean. **B: Left**, Equal amounts of protein from wild-type mouse brain homogenates were subjected to SDS-PAGE and immunoblotting with an anti-RGS14 antibody (1:1,000). **Right**, Equal amounts of protein from adult RGS14 wild-type and knockout mouse brain homogenates were similarly subjected to SDS-PAGE and immunoblotting with an anti-RGS14 antibody (1:1,000). All samples were also probed with an anti-beta actin antibody (1:5,000) to demonstrate loading of equal protein amounts between samples. *WT*, wild-type; *KO*, RGS14 knockout. **C**: A series of low power micrographs of coronal mouse brain sections showing RGS14 immunoreactivity in hippocampus at different developmental stages. Scale bar = 1.0 mm.

Overall distribution of RGS14 immunoperoxidase labeling

Detailed anatomical analysis of coronal brain sections at the LM level reveals that RGS14 immunoperoxidase labeling is not detectable in any region of P0 mouse brain (data not shown). However, neuronal RGS14 immunoperoxidase labeling is observed as a dark brown deposit as early as P7, which continues to increase thereafter until adulthood (summarized in Table 2.2).

TABLE 2.2: Regional Brain Localization of RGS14

Region	Developmental Stage				
	P0	P7	P14	P21	Adult
Anterior Olfactory Nucleus (AON)	-	+	+	++	+++
Piriform Cortex (PIR)	-	+	+	++	+++
Orbital Cortex (ORB)	-	+	+++	+	+
Entorhinal Cortex (ENT)	-	+	+++	+++	+
Neocortex (Neo)	-	+	+++	+	-
Hippocampus - CA2	-	+	++	+++	++++
Hippocampus - CA1	-	-	++	+++	+
Fasciola cinerea (FC)	-	+	++	++	++++

RGS14 immunolabeling is detected in the anterior olfactory nucleus (AON) and piriform cortex known as primary cortical areas for olfactory processing. Labeling is also present during development in specific layers of orbital and entorhinal cortices, with transient immunoreactivity in neocortex. Finally, RGS14 immunoperoxidase labeling is most prominent in hippocampal CA2 and FC with immunoreactivity increasing with age. After detailed examination for RGS14 immunoreactivity throughout the entire mouse brain, these areas are the only regions displaying RGS14 immunoreactivity throughout development and in adulthood. No immunoreactivity is observed in RGS14-KO mice (except minimal labeling in CA2 subfield-see Discussion), indicating specificity of immunoperoxidase labeling (data not shown).

Anterior olfactory nucleus (AON) and piriform cortex

In the AON, RGS14 labeling is mainly concentrated in the soma and apical dendrites of neurons in P7, P14, P21 WT mice (Fig. 2.3A-I), while in the adult, strongly labeled neuronal cell bodies lay in a rich immunoreactive neuropil (Fig. 2.3J-L). The labeling is found throughout the whole extent of the AON in adolescent mice, but is particularly enriched in the dorsolateral portion of the structure in adult WT animals. At high magnification, some of the immunolabeled neurons display pyramidal morphology with a single, prominent apical dendrite extending from the soma (Fig 2.3I,L).

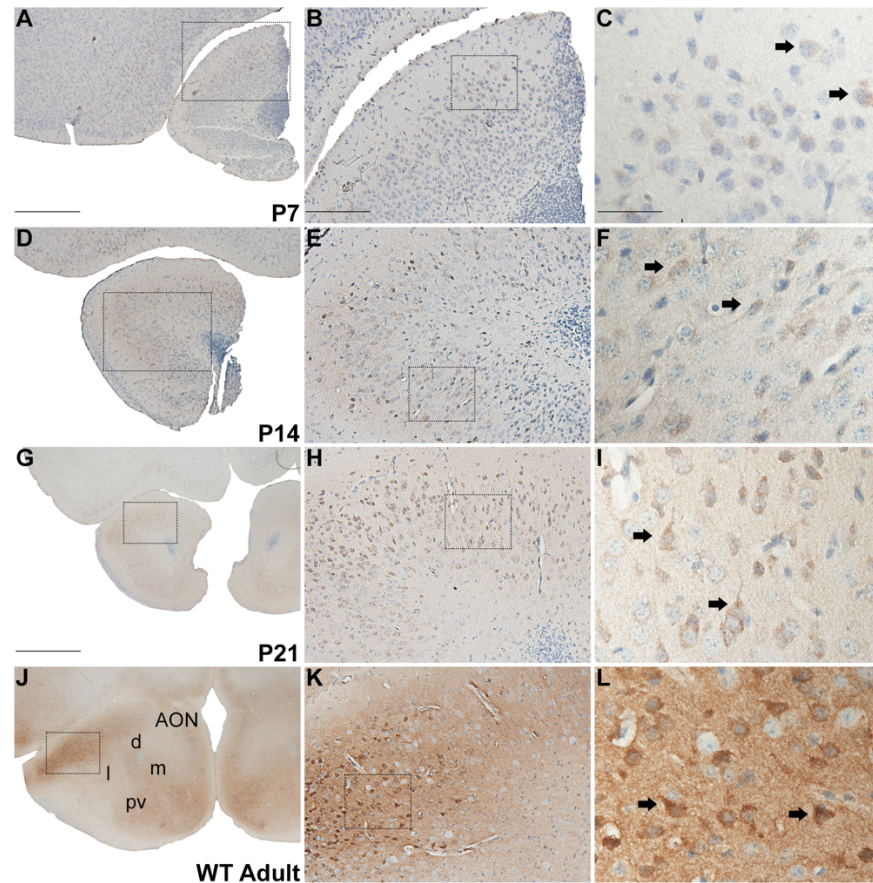


Figure 2.3 RGS14 immunolabeling in anterior olfactory nucleus (AON) of postnatal mouse brain. Low, medium, and high magnification views of coronal hemisections at P7, P14, P21, and adult wild-type mouse brain labeled with immunoperoxidase using an anti-RGS14 monoclonal antibody (A-L). RGS14 immunoreactivity increases in the AON during postnatal development, and staining is restricted to soma and proximal dendrites of neurons, some of which have a pyramidal shaped cell body until P21 (F,I). In adults, neuronal cell bodies are more heavily stained, and a significant neuropil immunostaining can be seen (J-L). Dashed boxes indicate region magnified in subsequent micrographs to the right. Arrows indicate immunolabeled neuronal perikarya. *AON*, anterior olfactory nucleus; *d*, dorsal; *m*, medial; *l*, lateral; *pv*,

posteroventral. Scale bars = 500 μm in A (applies to D); 1.0 mm in G (applies to J); 200 μm in B (applies to E,H,K); 50 μm in C (applies to F,I,L).

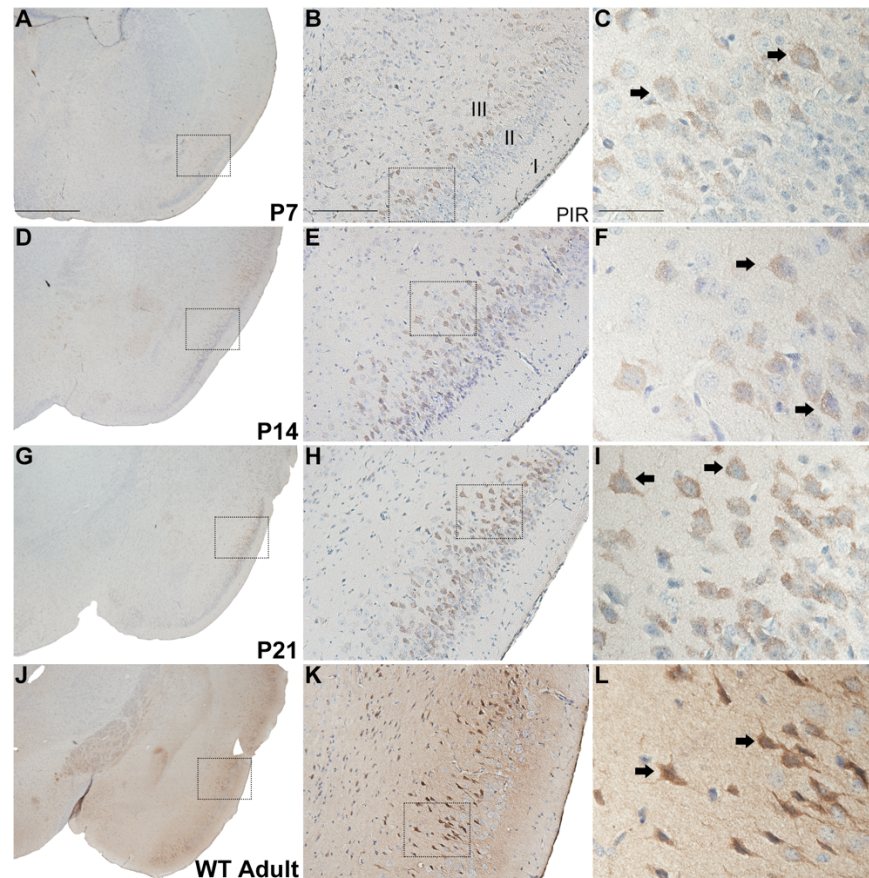


Figure 2.4 RGS14 immunoreactivity in postnatal mouse piriform cortex. Low, medium, and high magnification views of right coronal hemisections at P7, P14, P21, and adult wild-type mouse brain immunoperoxidase labeled with an anti-RGS14 antibody. RGS14 immunoreactivity increases in piriform cortex during postnatal development, and staining is localized to soma and proximal dendrites of neurons, some of which with a pyramidal shape (C,F,I,L). Dashed boxes indicate regions magnified in subsequent micrographs to the right. Arrows indicate immunolabeled neurons. *PIR*, piriform cortex. Scale bar = 1.0 mm in A (applies to D,G,J); 200 μm in B (applies to E,H,K); 50 μm in C (applies to F,I,L).

In the piriform cortex, RGS14 immunoreactivity is found mainly in layer II pyramidal neurons. Weak labeling is first observed at P7, but the immunolabeling intensity increases with age until reaching its highest level in adulthood (Fig. 2.4A-L). As found in AON, significant neuropil immunoreactivity and strong neuronal cell body and apical dendrite labeling are seen in the upper layers of the piriform cortex in adult animals (Fig. 2.4J-L).

Orbital and entorhinal cortices

At the level of the AON, RGS14 labeling is found from P7 onward in layers II/III and V of the orbital cortex with highest immunoreactivity detectable at P14 and in adults (Fig. 2.5). At high magnification, labeling is mostly concentrated in neuronal somata, some of which have a pyramidal shape, in the orbital cortex (Fig. 2.5F). In adults, light neuropil staining is also found throughout the orbital cortex (Fig. 2.5J-L).

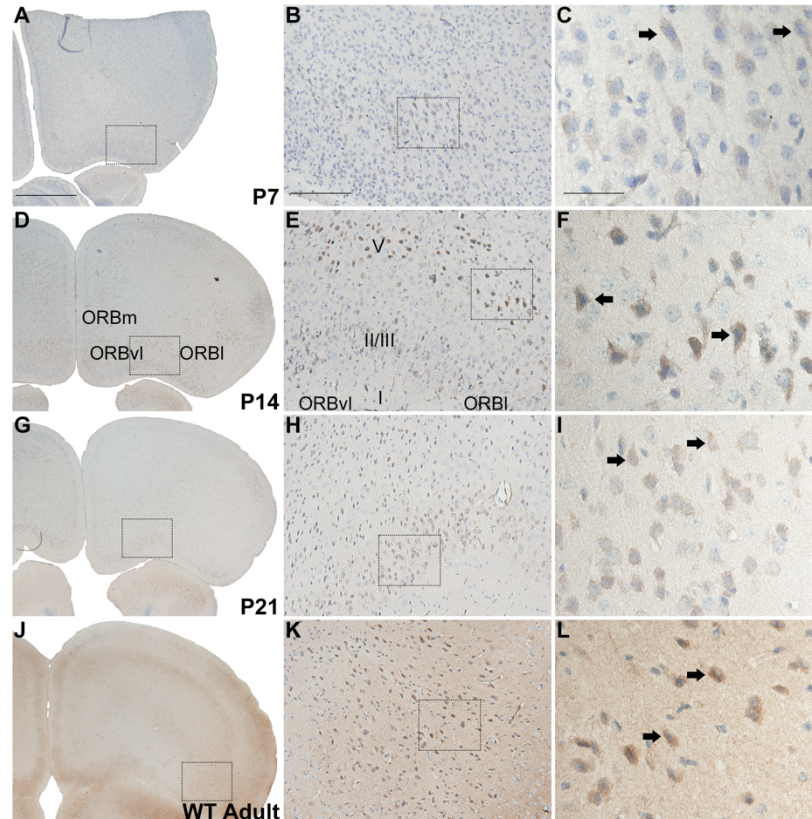


Figure 2.5 RGS14 immunoreactivity in postnatal mouse orbital cortex. Low, medium, and high magnification views of right coronal hemisections at P7, P14, P21, and adult wild-type mouse brain immunoperoxidase labeled with an anti-RGS14 antibody. RGS14 immunoreactivity in the orbital cortex is highest at P14 and in adults, and staining is localized to soma and proximal dendrites of neurons, some with a pyramidal shape (F,L). Dashed boxes indicate regions magnified in subsequent micrographs to the right. Arrows indicate immunolabeled neurons.; *ORB*, orbital cortex; *m*, medial; *vl*, ventrolateral; *l*, lateral. Scale bars = 1.0 mm in A (applies to D,G,J); 200 μ m in B (applies to E,H,K); 50 μ m in C (applies to F,I,L).

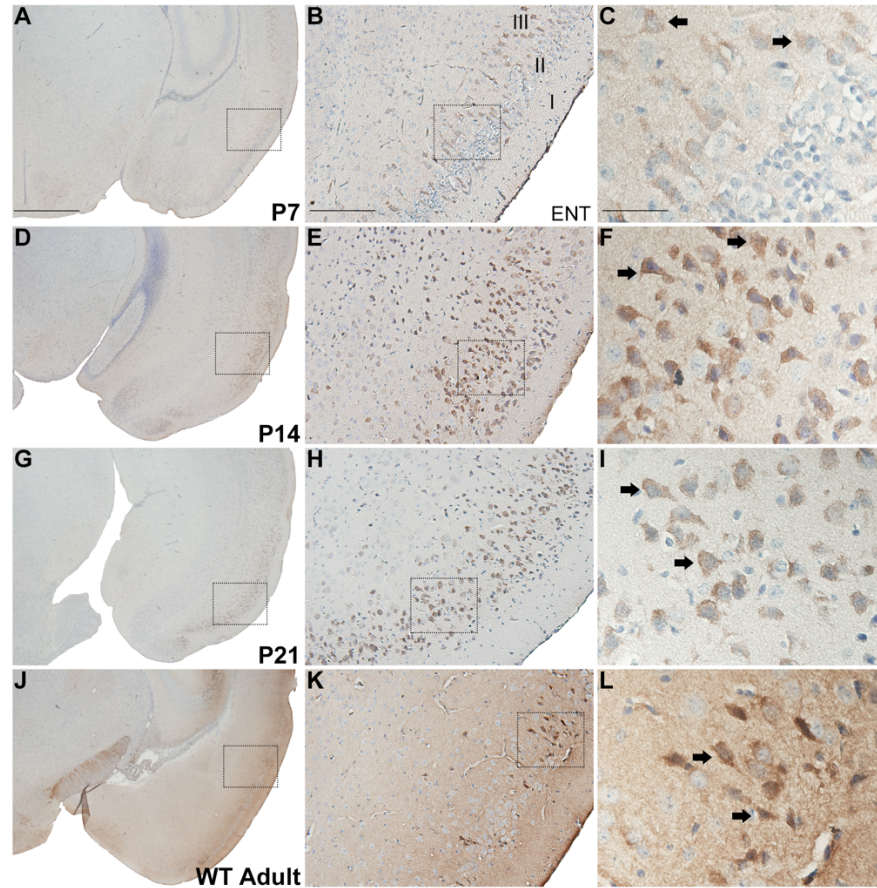


Figure 2.6 RGS14 immunoreactivity in postnatal mouse entorhinal cortex. Low, medium, and high magnification views of coronal hemisections from P7, P14, P21, and adult wild-type mouse brain immunoperoxidase labeled with an anti-RGS14 antibody. RGS14 immunoreactivity in the entorhinal cortex is highest at P14 and in adults, and the staining is localized to soma and apical dendrites of labeled neurons (F,I,L). In adults, a light immunoreactive neuropil can also be seen (J-L). Dashed boxes indicate regions magnified in subsequent micrographs to the right. Arrows indicate immunolabeled neurons. *ENT*, entorhinal cortex. Scale bars = 1.0 mm in A (applies to D,G,J); 200 μ m in B (applies to E,H,K); 50 μ m in C (applies to F,I,L).

Similarly, weak immunoreactivity is first detected at P7 in layer II/III neurons of the entorhinal cortex (Fig. 2.6A-C). Immunolabeling is most prominent at P14 and in adults, with a slight decline in immunoreactivity at P21, (Fig. 2.6D-L). As in other cortical regions, some of the labeled cell bodies display a pyramidal shape appearance, and the neuropil labeling is most intense in adults (Fig. 2.6J-L).

Transient expression of RGS14 in neocortex

Throughout the rostral-caudal axis of the adolescent mouse brain, light to moderate immunoreactivity for RGS14 is observed in layers II/III and V of pyramidal-shaped neocortical neurons between P7 and P21, while it is undetectable in adults (Fig. 2.7A-L). A similar pattern of Immunolabeling is found across several regions of neocortex including orbital, somatomotor, somatosensory, auditory, and visual areas.

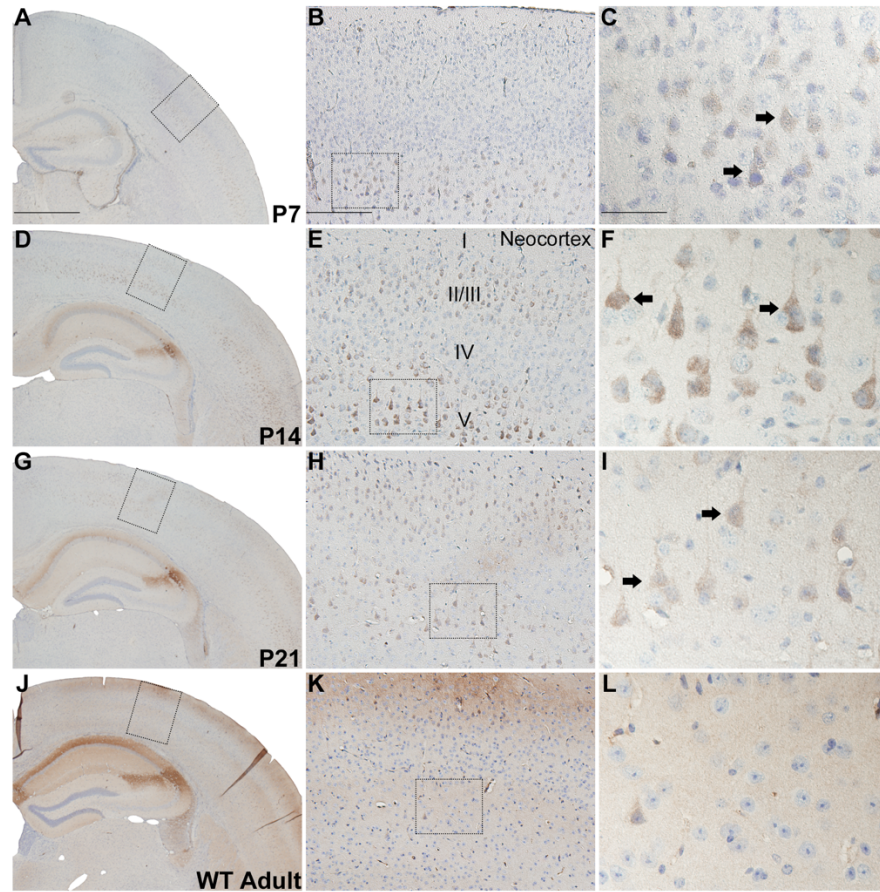


Figure 2.7 RGS14 immunolabeling is transiently expressed in postnatal mouse neocortex. Low, medium, and high magnification views of coronal hemisections from P7, P14, P21, and adult wild-type mouse brain immunoperoxidase labeled with an anti-RGS14 antibody. RGS14 immunoreactivity is highest at P14 in neocortical layers II/III and V, and staining is localized to soma and apical dendrites of pyramidal neurons (F). Immunostaining is less intense at P21 (G-I) and is undetectable in adults (J-L). Dashed boxes indicate regions magnified in subsequent micrographs to the right. Arrows indicate immunolabeled neurons. Scale bars = 1.0 mm in A (applies to D,G,J); 200 μ m in B (applies to E,H,K); 50 μ m in C (applies to F,I,L).

Hippocampal RGS14 immunoreactivity increases throughout development

In the hippocampus, weak RGS14 immunoperoxidase labeling, first observable at P7 in hippocampal CA2, is significantly upregulated until it reaches its highest levels in adult WT mouse brain (Fig. 2.8A-P). Staining is most prominent at the soma and dendritic arbors of CA2 pyramidal neurons as well as in fasciola cinerea (FC). Labeling is also occasionally observed in the soma and proximal dendrites of a very sparse population of CA1 neurons at P14 and P21 (Fig. 2.8G,K), while in adults the stratum lacunosum moleculare and stratum radiatum in CA1 region harbored significant neuropil immunoreactivity (Fig. 2.8O). Of note, the CA1 neuropil immunoreactivity in adults is due to immunoperoxidase labeling of CA2 neurites, which extend through this plane of area CA1.

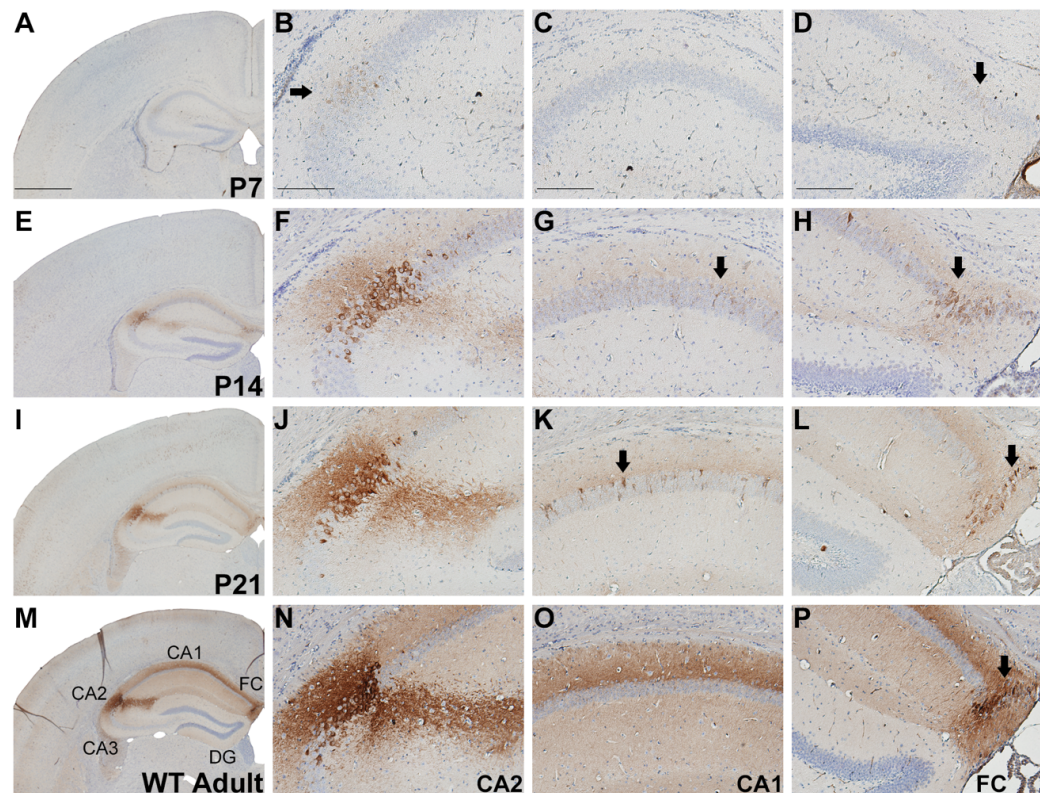


Figure 2.8 RGS14 immunolabeling in postnatal mouse hippocampus. Low and medium magnification views of hemisections from P7, P14, P21, and adult wild-type mouse

brains immunoperoxidase labeled with an anti-RGS14 antibody. RGS14 immunoreactivity increases in hippocampal CA2 during development, which results in an extensive labeling of the dendritic arbors of CA2 pyramidal neurons (F,J,N). RGS14 immunoreactivity in fasciola cinerea (FC) also increases with age, reaching its highest levels in the adult mouse brain (arrows in D,H,L,P). At P14 and P21, the cell bodies and proximal dendrites of a small population of CA1 pyramidal neurons display immunoreactivity, while in adults, a significant neuropil immunostaining of CA1 region can be seen (M,O). Arrows indicate immunolabeled neurons. *FC*, fasciola cinerea; *DG*, dentate gyrus. Scale bars = 1.0 mm in A (applies to E, I, M); 200 μ m in B-D (applies to F-H, J-L, N-P).

2.4 Discussion

Our results provide the first detailed anatomical analysis of the expression of RGS14 in the developing and adult mouse brain. In doing so, we also provide the first comprehensive characterization of a newly described anti-RGS14 monoclonal antibody, confirming its specificity and sensitivity for detecting RGS14 protein in mice. We show that both mRNA and protein levels are gradually upregulated throughout postnatal development, reaching their highest levels in the adult mouse brain, except for the neocortex, which displayed a lower level of immunostaining in adults than at earlier time points (i.e. P7-P21). As a complement to our previous report of RGS14 as a hippocampal CA2 and FC enriched gene²⁵, the current findings demonstrate that RGS14 protein is also significantly expressed in the anterior olfactory nucleus, piriform cortex, orbital cortex, entorhinal cortex, and neocortex in mice.

Contrary to previous immunohistochemical studies in monkey and rat brain⁴⁴ which reported broad RGS14 protein expression in both neurons and glia, our results show a much more restricted distribution of RGS14 protein expression limited to neuronal cell bodies in fewer brain regions. The differences in localization profiles between our study and these previous results could be due to species differences in RGS14 distribution or, more likely, from antibody specificity. In that regard, it is worthy noting that our findings are entirely consistent with independently reported adult mouse brain *in situ* hybridization data from the Allen Mouse Brain Atlas (<http://mouse.brain-map.org>) examining RGS14 mRNA expression and distribution patterns in the adult mouse brain.

Our findings are also consistent with independent microarray studies on adult human (<http://human.brain-map.org/>) and non-human primate (<http://www.blueprintnhpatlas.org/>) brain tissue, both reporting that RGS14 mRNA is most highly expressed in hippocampal CA2 and moderately expressed in CA1. Contrary to our findings in mice, these data also show high levels of RGS14 mRNA expression in the striatum (caudate nucleus and putamen), which could suggest a unique striatal function for RGS14 in primates relative to rodents. Germane to this, mRNA and protein variants of RGS14 have been reported in primates (see below), and it is possible that RGS14 variants could be differentially expressed in CA2 versus striatum in primates. However, this idea is speculative since the sequence(s) of the RGS14 transcript(s) detected in these microarray data sets are unknown. Further immunoperoxidase staining and *in situ* hybridization studies are required to characterize the localization of RGS14 protein and mRNA in the primate brain. A detailed characterization of the RGS14

mRNA/protein species found in primate brain and a comprehensive analysis of their distribution and subcellular localization could provide great insight into the roles of RGS14 in human physiology and disease.

Antibody characterization and specificity

Previous studies have shown that RGS14 protein is enriched in brain^{14,44}, but the lack of a fully characterized, specific anti-RGS14 antibody has limited immunohistochemical analysis of protein distribution in brain. Here we show that the anti-RGS14 mouse monoclonal antibody (Clone N133/21, NeuroMabs) used in our study is very specific and sensitive for RGS14, and that this antibody recognizes an epitope in the C-terminal region of the mouse and rat RGS14 protein. Furthermore, this antibody recognizes a single 61 kDa protein band in mouse brain corresponding to native, full-length RGS14 protein. Although whole-genome shotgun sequencing⁹⁹ has predicted lower molecular weight variants of RGS14 including the region of the protein containing the antibody epitope, this antibody did not detect these proteins by immunoblot. However, we cannot rule out the possibilities that these variants may be expressed at an undetectable level for immunoblot, or perhaps expressed outside of mouse brain.

We observed very light immunoperoxidase labeling with this antibody in the hippocampal CA2 subfield, but not in other regions of adult RGS14 KO mice (Figure 2.2C). While we cannot conclude that this staining necessarily represents non-specific background labeling, several lines of evidence suggest that this is the case. Previous studies showed that hippocampal CA2 exhibits background immunoreactivity to antibodies against proteins not present in this region¹⁰⁰ as well as a unique extracellular milieu surrounding these neurons that may be non-specifically labeled⁶⁵. Because this

light background staining is not present in P0-P14 mice, it suggests that the CA2-specific antigen protein(s) the antibody cross-reacts with is also developmentally upregulated. Another possible explanation is that the low level of background labeling is caused by the general anti-mouse IgG secondary antibody, rather than the use of a IgG subclass-specific secondary antibody¹⁰¹. However, no immunolabeling was observed in control experiments in which primary antibody was omitted. Alternatively, we cannot definitively exclude the possibility that the RGS14 KO mice used are not complete knock-outs. These mice were generated by deleting exons 2-7 of the RGS14 gene that may result in a low production of a smaller molecular weight variant from exons 8-11, which would contain the epitope recognized by the anti-RGS14 monoclonal antibody. Arguing against this possibility, however, are our findings (Figure 2.2A-B) showing that we could not detect either the full-length RGS14 protein or any lower molecular weight variants by immunoblot, or RGS14 mRNA by qRT-PCR. Taken together, our hypothesis is that this staining represents low-level non-specific staining as has been reported for other proteins¹⁰⁰.

Upregulation of RGS14 during postnatal development: implications for early learning and synaptic plasticity

We recently reported that RGS14 suppresses synaptic plasticity in CA2 neurons as well as hippocampal-based spatial and novel object recognition memory in adult mice²⁵. Other studies strongly suggest that CA2 plays a significant role in social behavior and temporal order for memories¹⁰², and initial experiments have shown that the social neuropeptides oxytocin and vasopressin induce synaptic potentiation in CA2 pyramidal neurons⁶². Therefore, the upregulation of RGS14 protein beginning at P7 may allow for a

period of regionally enhanced plasticity and learning during early postnatal development to allow newborn pups to adapt to their environment and form strong social bonds, i.e. maternal attachment. For example, the increase in RGS14 protein after P7 may serve as a filter to allow hippocampal CA2 to encode episodic memories only under specific conditions. This may coincide with new synapse formation and/or pruning during early postnatal development, shaped by environmental inputs such as maternal bonding and other social interactions.

Olfaction plays a major role in guiding rodent behaviors including social recognition. In mammals, odorants are first processed by the olfactory bulb, which targets specific structures collectively referred to as primary olfactory cortex, including the anterior olfactory nucleus (AON) and piriform cortex¹⁰³. The olfactory cortex is responsible for processing and associating odorants with specific events¹⁰⁴. The expression of RGS14 in pyramidal neurons in both the AON and piriform cortex makes it well positioned to modulate primary olfactory inputs and thus guide olfactory and social learning. RGS14 is also expressed in orbital and entorhinal cortical neurons, which receives substantial input from primary olfactory cortical areas. This distribution pattern, therefore, suggests that RGS14 could play a pivotal role in modulating olfactory processing in different brain regions. Further studies are required to determine if RGS14 regulates olfaction in mice.

RGS14: a suppressor of plasticity in multiple neuronal populations?

Although we have found that RGS14 restricts CA2 synaptic plasticity, its role in the other brain areas remains to be determined. Of note, the subcellular immunoperoxidase labeling for RGS14 is distinct in CA2 compared with other regions.

In hippocampal CA2, RGS14 staining is much more heavily concentrated in the apical and basal dendrites of pyramidal neurons while than in other areas where the labeling is lighter and often restricted to the soma and apical dendrites of pyramidal neurons, such as in CA1. Of note, RGS14 immunoreactivity in CA1 did not colocalize with any known markers of CA1 interneurons (Chris McBain, personal communication), and we therefore deduce that RGS14 is likely expressed in a very small, sporadic subset of CA1 pyramidal neurons. This difference in localization suggests that RGS14 may play a distinct role in plasticity suppression for area CA2 rather than in other neuronal populations outside of the hippocampus. One possibility is that RGS14 modulates synaptogenesis and dendrite development as its expression is dramatically upregulated during the first two postnatal weeks, a time of extensive synapse formation and pruning in rodent brain¹⁰⁵. We have recently shown that RGS14 coordinates G α i1 and H-Ras signaling to modulate neurite outgrowth in PC12 cells⁹⁵. The transient expression of RGS14 in neocortex, which peaks at P14, suggests that it must have a distinct purpose at this time in early development.

Implications for RGS14 and area CA2 in human cognition and behavior

Humans and primates also express a roughly equivalent long isoform (approximately 63 kDa) of RGS14 as well as shorter splice variants that lack the N-terminal RGS domain⁴⁴. Our findings indicate that, at least in mouse brain, RGS14 is expressed as the full length 61 kDa isoform and that expression is largely limited to hippocampal area CA2 in adulthood. Hippocampal long-term potentiation (LTP) is believed to underlie certain key aspects of human learning, memory, and cognition, most notably spatial and contextual learning. While hippocampal LTP has been thoroughly characterized in the dentate gyrus (DG)-CA3-CA1 trisynaptic pathway, significantly less

is known about the role of LTP-resistant area CA2 in overall hippocampal functions or behaviors^{63,106}. It has recently been shown that, in contrast to Schaffer collateral inputs, entorhinal cortex inputs to CA2 are capable of producing LTP, but the cellular mechanisms underlying this plasticity remain to be demonstrated⁸³. Moreover, a number of genes, including RGS14, are highly expressed in CA2, but not CA1^{67,68}, suggesting that the cellular mechanisms regulating plasticity in CA2 may differ from the well-known pathways in CA1 neurons. Further experiments are required to understand the unique cellular machinery governing CA2 plasticity, and the role of CA2 in mediating overall hippocampal function. Our findings are consistent with the hypothesis of Caruana et al. (2012), suggesting that the relative synaptic stability of CA2 is designed to allow encoding of memories only under specific circumstances, such as in early postnatal development when RGS14 protein is not expressed.

The contribution of area CA2 to putatively linked behaviors is in the early stages of exploration, but initial experiments strongly suggest that CA2 plays a significant role in several forms of learning/memory including social, spatial, object recognition, and temporal order⁶². Area CA2, in particular, is associated with human pathologies including Alzheimer's disease, schizophrenia, autism and bipolar spectrum disorders, as well as ischemia/epilepsy^{102,107-110}. RGS14 has also recently been identified as a candidate gene in a study of fear learning in mice¹¹¹, which could suggest a role for RGS14 in human post-traumatic stress disorder (PTSD). Thus, RGS14 could function to selectively allow encoding of CA2 under certain conditions, e.g. maternal attachment in the neonate, while filtering storage of memories that could be maladaptive, e.g. traumatic life events. Microarray studies reporting high levels of RGS14 expression in adult human and non-

human primate CA2 suggest that RGS14's role as a suppressor of plasticity and hippocampal-dependent learning in mice may also extend to primates. The unique expression of RGS14 in the primate striatum indicates that it could serve yet unknown functions specific to primates. Further studies are needed to elucidate roles for RGS14 and hippocampal region CA2 in human behavior and disease.

Chapter 3³:
RGS14 limits postsynaptic calcium to block CA2 synaptic plasticity

³ This chapter has been slightly modified from the manuscript submitted for publication. Evans PR, Parra-Bueno P, Smirnov MS, Lustberg DJ, Yang JJ, Seyfried NT, Griffin PR, Dudek SM, Yasuda R, and Hepler JR. (*Submitted*) RGS14 limits postsynaptic calcium to block CA2 synaptic plasticity.

3.1 Introduction

Pyramidal neurons in hippocampal area CA2 differ dramatically from neighboring CA3/CA1 pyramidal neurons in that synaptic long-term potentiation (LTP) is not as readily induced⁶³. A number of genes are selectively expressed in CA2 pyramidal neurons^{67,68}, and a few of these proteins have been shown to contribute to the atypical plasticity features of CA2^{25,62,72,74,79,112,94}. We previously identified Regulator of G Protein Signaling 14 (RGS14) as a critical factor restricting CA2 synaptic plasticity and learning and memory²⁵. RGS14 knockout (RGS14 KO) mice display a robust and nascent capacity for LTP in CA2 pyramidal neurons, which is absent in wild-type (WT) mice, and exhibit enhanced spatial memory in the Morris Water Maze. However, the cellular mechanism(s) by which RGS14 suppresses LTP in CA2 remain unknown.

RGS14 is a complex scaffolding protein with an unconventional protein architecture that allows it to integrate G protein signaling and ERK/MAPK signaling^{24,93}. The lack of plasticity in CA2 has been attributed to robust calcium (Ca^{2+}) buffering and extrusion mechanisms relative to CA3/CA1⁷², and synaptic potentiation of CA2 synapses by Ca^{2+} -dependent mechanism but no evidence has linked RGS14 to Ca^{2+} -activated signaling pathways required for LTP induction. Therefore, we investigated whether RGS14 restricts plasticity in hippocampal CA2 by modulating Ca^{2+} -stimulated pathways.

3.2 Experimental Procedures

Plasmids and proteins

RGS14¹¹³ and CaM¹¹⁴ were expressed and proteins purified as previously described. The rat RGS14 cDNA used in this study (GenBank accession number U92279) was acquired as described¹⁴. FLAG-RGS14 truncation mutants containing

residues 1-202, 205-490, 371-544, and 444-544 were created as described²². The RGS14-Luciferase construct used in these studies was created as described¹¹⁵. The FLAG-CaMKII α plasmid was a generous gift from Chris Yun (Emory University School of Medicine). pCAG-GFP, pCMV-GcAMP6S, and pCAG-mCherry constructs were generously provided by Ryohei Yasuda (MPFI).

Dansyl-CaM fluorescence measurements

Steady-state fluorescence spectra were recorded using a QM1 fluorescence spectrophotometer (Photon Technology International) with a xenon short arc lamp at 25°C as previously described¹¹⁴. For dansyl-CaM fluorescence measurement, 1 mL solution containing 0.5-1 μ M dansyl-CaM in 50 mM Tris-HCl, 100 mM KCl, pH 7.5 with 2 mM Ca²⁺ or 5 mM EGTA was titrated with 5–10 μ L aliquots of the RGS14 peptide stock solution (1–5 μ M) in the same buffer. The fluorescence spectra were recorded between 400 and 600 nm with an excitation wavelength at 335 nm and the slit width set at 4–8 nm.

Cell culture and transfection

HeLa cells (ATCC) were maintained in Dulbecco's modified Eagle's medium (Mediatech) supplemented with 10% fetal bovine serum (Atlanta Biologicals, 5% after transfection), 2 mM L-glutamine (Invitrogen), 100 U/mL penicillin (Mediatech), and 100 mg/mL streptomycin (Mediatech) in a humidified environment at 37°C with 95%O₂/5% CO₂. Transfections were performed using previously described protocols with polyethyleneimine (PEI; Polysciences)³⁸. After 24 hours of expression, cells were washed with PBS and harvested in an ice-cold lysis buffer containing 50 mM Tris, 150 mM NaCl, 2 mM DTT, 5 mM MgCl₂, 1% Triton X-100 (v/v), phosphatase inhibitors

(1:1,000; Sigma Aldrich), and one mini protease inhibitor cocktail tablet (Roche Applied Science), pH 7.4. Lysis buffer was supplemented with 2 mM CaCl₂ or 5 mM EDTA (“+ Ca²⁺” and “- Ca²⁺”, respectively). Cells were lysed for 1h at 4°C rotating end-over-end, and subsequently centrifuged to pellet cell debris. Cleared cell lysates were then subjected to CaM-Agarose pull-down assays or co-immunoprecipitation prior to immunoblotting.

CaM-Agarose pull-down assays

For CaM-Agarose pull-down assays with purified RGS14 protein, 25 µl of CaM-Agarose beds (Sigma) were washed twice with a binding buffer composed of 20 mM HEPES, 150 mM NaCl, 0.1% Tween-20 (v/v), pH 7.5 supplemented with either 0.1 mM CaCl₂ (“+ Ca²⁺”) or 5mM EDTA (“- Ca²⁺”). 0.25 µg of purified RGS14 protein was diluted in each binding buffer, and 10% of these samples were removed as input samples for immunoblotting. The remaining RGS14 protein was incubated with pre-washed CaM-Agarose beads for 2h at 4°C, and beads were then thoroughly washed in the appropriate binding buffer. Proteins were eluted with Laemmli buffer, heated at 95°C in a heating block, and subjected to SDS-PAGE and immunoblotting.

For CaM-Agarose pull-down assays with recombinant FLAG-RGS14 expressed in HeLa cells, cell lysates were prepared as described above. 50 µl of CaM-Agarose beads washed twice with a binding buffer composed of 20 mM HEPES, 100 mM NaCl, pH 7.5 supplemented with either 2 mM CaCl₂ (“+ Ca²⁺”) or 5mM EDTA (“- Ca²⁺”). 10% of the initial cell lysates was removed as input samples for immunoblotting. The remaining RGS14 protein was incubated with pre-washed CaM-Agarose beads for 2h at 4°C, and beads were then thoroughly washed in the appropriate binding buffer. Proteins

were eluted with Laemmli buffer, heated at 95°C for 5 mins, and subjected to SDS-PAGE and immunoblotting.

HeLa cell co-immunoprecipitation (co-IP)

RGS14-Luciferase and FLAG-CaMKII α were co-transfected into HeLa cells and lysed in the presence/absence of Ca²⁺ as described above. 50 μ l of anti-FLAG M2 agarose affinity gel (Sigma) or Protein G sepharose beads (GE, negative control) were pre-blocked with 3% BSA and then incubated with cell lysates for 3h at 4°C. Beads were washed thoroughly in ice cold tris-buffered saline (TBS), and proteins were eluted with an equal volume of Laemmli buffer, heated at 95°C for 5 mins, and subjected to SDS-PAGE and immunoblotting.

Mouse brain co-immunoprecipitation (co-IP)

Adult RGS14 WT and KO mice were deeply anesthetized by isoflurane inhalation and euthanized by decapitation. Brains were rapidly removed from the skull and homogenized on ice using a glass dounce homogenizer with 10 strokes in an ice-cold buffer containing 50 mM Tris, 150 mM NaCl, 5 mM EDTA, 5 mM MgCl₂, phosphatase inhibitors (1:1,000, Sigma Aldrich, St. Louis, MO), and one mini protease inhibitor cocktail tablet (Roche Applied Science), pH 7.4. Membranes were solubilized by the addition of 1% NP-40 for 1h at 4°C and subsequently centrifuged to pellet debris. Cleared brain homogenates were incubated with an anti-RGS14 mouse monoclonal antibody (20 μ g, Neuromabs) overnight at 4°C. The following day, 100 μ l of Protein G Dynabeads (ThermoFisher) were added to homogenates for 1h to precipitate antibody-bound protein complexes. Protein G Dynabeads were washed thoroughly with ice-cold TBS and immediately digested for mass spectrometry.

Mass spectrometry and peptide analysis

The resulting peptides were analyzed independently by reverse-phase liquid chromatography coupled with tandem mass spectrometry (LC-MS/MS) as previously described¹¹⁶. Briefly, peptide mixtures were loaded onto a C₁₈ column (100 μm i.d., 10 cm long, 5 μm resin from Michrom Bioresources, Inc.) and eluted over a 5–30% gradient (Buffer A: 0.4% acetic acid, 0.005% heptafluorobutyric acid, and 5% AcN; Buffer B: 0.4% acetic acid, 0.005% heptafluorobutyric acid, and 95% AcN). Eluates were monitored in a MS survey scan followed by nine data-dependent MS/MS scans on an LTQ-Orbitrap ion trap mass spectrometer (Thermo Finnigan). The LTQ was used to acquire MS/MS spectra (2 *m/z* isolation width, 35% collision energy, 5,000 AGC target, 150 ms maximum ion time). The Orbitrap was used to collect MS scans (300–1600 *m/z*, 1,000,000 AGC target, 750 ms maximum ion time, resolution 60,000). All data were converted from raw files to the .dta format using ExtractMS version 2.0 (Thermo Finnigan). The resulting peptides were filtered using the mouse brain proteome as a background and sorted into functional groups using DAVID Functional Annotation Bioinformatics Database^{117,118}.

***In vitro* CaMKII phosphorylation assays**

Purified CaMKII (NEB) was first pre-activated for 10 mins at 30°C in NEBuffer for protein kinases containing 50mM Tris-HCl, 10mM MgCl₂, 0.1 mM EDTA, 2mM DTT, 0.01% Brij 35, pH 7.5, supplemented with 2mM CaCl₂, 1.2 μM CaM, and 200 μM ATP. 50 U pre-activated CaMKII α was then incubated for 20 mins at 30°C with 4x10⁶ cpm of [Y -³²P]-ATP (Perkin Elmer) and 2 μg of purified RGS14 or H6-Gai1. A small amount of purified proteins (2.5%) were set aside as input samples for immunoblotting.

Reactions were quenched by the addition of Laemmli sample buffer and heating at 95°C for 5 mins. Proteins were then separated by SDS-PAGE, and acrylamide gels were dried and exposed to film to detect phosphorylation by autoradiography.

Immunoblotting

Samples were loaded onto 11% acrylamide gels and subjected to sodium dodecyl sulfate-polyacrylamide gel electrophoresis (SDS-PAGE) to separate proteins. Proteins were then transferred to nitrocellulose and subjected to immunoblotting to probe for proteins of interest. After blocking nitrocellulose membranes for 1 hour at room temperature in blocking buffer containing 5% nonfat milk (w/v), 0.1% Tween-20, and 0.02% sodium azide, diluted in 20 mM TBS, pH 7.6, membranes were incubated with primary antibodies diluted in the same buffer overnight at 4°C, except for anti-FLAG primary antibody. An anti-RGS14 mouse monoclonal antibody (Neuromabs) was used at a 1:1,000 or 1:5,000 dilution to detect recombinant or purified proteins, respectively. An anti-His mouse monoclonal antibody (Qiagen) was used at a dilution of 1:500 to detect purified hexa-histidine-tagged G α i1 (H₆-G α i1). Membranes were washed in TBS containing 0.1% Tween-20 (TBST) and subsequently incubated with an anti-mouse (1:5,000) horseradish peroxidase (HRP)-conjugated secondary antibody diluted in TBST for 1 hour at room temperature. Following block, anti-FLAG-HRP (1:35,000, Sigma) primary antibody was diluted in TBST and incubated with membranes for 1 hour at room temperature with no secondary antibody. Protein bands were visualized using enhanced chemiluminescence and exposing membranes to films.

Hydrogen/deuterium exchange (HDX) mass spectrometry

Solution phase amide HDX was carried out with a fully automated system as described previously¹¹⁹. Briefly, 4 μl of 10 μM RGS14 was diluted to 25 μl with D_2O -containing HDX buffer and incubated at 4°C for 10, 30, 60, 900, or 3,600 s. Following on exchange, back-exchange was minimized, and the protein was denatured by dilution to 50 μl in a low pH and low temperature buffer containing 0.1% (v/v) TFA in 3 M urea (held at 1°C). Samples were then passed across an immobilized pepsin column (prepared in house) at 50 $\mu\text{l min}^{-1}$ (0.1% (v/v) TFA, 15°C); the resulting peptides were trapped on a C8 trap cartridge (Hypersil Gold, Thermo Fisher). Peptides were then gradient eluted from 4% (w/v) CH_3CN to 40% (w/v) CH_3CN , 0.3% (w/v) formic acid over 5 min at 2°C across a 1 X 50-mm C18 HPLC column (Hypersil Gold, Thermo Fisher) and electrosprayed directly into an Orbitrap mass spectrometer (LTQ Orbitrap with ETD, Thermo Fisher). Peptide ion signals were confirmed if they had a MASCOT score of 20 or greater and had no ambiguous hits using a decoy (reverse) sequence in a separate experiment using a 60-min gradient. The intensity-weighted average m/z value (centroid) of each peptide's isotopic envelope was calculated with software developed in house¹²⁰ and corrected for back-exchange on an estimated 70% recovery and accounting for the known deuterium content of the on-exchange buffer. To measure the difference in exchange rates, we calculated the average percentage of deuterium uptake for RGS14 following 10, 30, 60, 900, and 3,600 s of on exchange. From this value, we subtracted the average percentage of deuterium uptake measured for the Ca^{2+} /CaM:RGS14 complex (2:1 molar ratio).

Animals

Animals in all experiments were housed under a 12h:12h light/dark cycle with access to food and water *ad libitum*. All experimental procedures conform to US NIH guidelines and were approved by the animal care and use committees of Emory University, Max Planck Florida Institute for Neuroscience, and the National Institute of Environmental Health Sciences. RGS14 KO mice were generated and maintained as previously described²⁵. Both male and female RGS14 WT/KO animals were used in all experiments. Reporter mice expressing enhanced green fluorescent protein (eGFP) in CA2 pyramidal neurons (Amigo2-eGFP; Tg(Amigo2-EGFP)LW244Gsat) were crossed with RGS14 WT/KO mice to label CA2 dendrites for field recordings.

Acute slice preparation

Adult RGS14 WT or KO;Amigo2-eGFP+ mice (P20-P50) were sedated by isoflurane inhalation, and perfused intracardially with a chilled choline chloride solution. Brain was removed and placed in the same choline chloride solution composed of 124 mM choline chloride, 2.5 mM KCl, 26 mM NaHCO₃, 3.3 mM MgCl₂, 1.2 mM NaH₂PO₄, 10 mM glucose and 0.5 mM CaCl₂, pH 7.4 equilibrated with 95% O₂/5% CO₂. Coronal slices (400 μm) were prepared, and slices were maintained in a submerged chamber at 32°C for 1h and then at room temperature in oxygenated ACSF.

Extracellular Recordings and LTP protocol

Experiments were performed at room temperature (~21°C), and slices were perfused with oxygenated ACSF containing 2 mM CaCl₂, 2 mM MgCl₂ and 100 μM picrotoxin. One or two glass electrodes (resistance ~4 MΩ) containing the same ACSF solution was placed in the *stratum radiatum* of CA2 or CA1

respectively (~100–200 μm away from the soma) while stimulating Schaffer Collateral fibers with current square pulses (0.1 ms) using a concentric bipolar stimulation electrode (FHC). CA2 region was detected by Amigo2-eGFP fluorescence. The initial slope of the EPSP was monitored with custom software. The stimulation strength was set to ~50% saturation. LTP was induced by applying 3 sets of high frequency stimuli (100 Hz, 1 s) with 20 s intervals. All data was analyzed with an in-house program written in MATLAB (MathWorks). Data are presented as mean \pm SEM. Statistical comparisons were performed using two-way ANOVA, and Sidak's multiple comparisons test was used to compare the same CA region between RGS14 WT and KO animals. Differences between datasets were judged to be significant at $p \leq 0.05$. Statistical analyses were performed in GraphPad Prism 7.

For pharmacological LTP experiments, slices from RGS14 KO/Amigo2-eGFP+ animals were perfused with either ACSF for controls or ACSF supplemented with either APV (50 μM , Sigma), KN62 (10 μM , Tocris), or PKI (14-22) amide myristoylated (1 μM , Enzo Life Sciences). For KN62 experiments, RGS14 KO control slices were perfused with ACSF containing 0.01% DMSO as a vehicle control. Electrophysiological recordings and LTP induction protocol were performed as described above. All data was analyzed with an in-house program written in MATLAB (MathWorks). Data are presented as mean \pm SEM. Statistical comparisons were performed using Student's t test to compare each inhibitor with respective KO control, and differences between datasets were judged to be significant at $p \leq 0.05$. Statistical analyses were performed in GraphPad Prism 7.

Tissue preparation and histology

Adult Amigo2-eGFP mice were anesthetized by isoflurane inhalation and transcardially perfused with 4% paraformaldehyde in PBS. Brains were postfixed for 24h, submerged in 30% sucrose in PBS, and sectioned coronally at 40 μ m on a cryostat. Sections were washed in PBS, blocked for at least 1h in 5% normal goat serum (NGS, Vector Labs) diluted in 0.1% PBS-X (0.1% Triton X-100 in PBS) at room temperature, and incubated in primary antibodies diluted in the same buffer overnight. A chicken polyclonal anti-GFP antibody (Abcam) was used at a 1:2,000 dilution to enhance Amigo2-eGFP fluorescence with either a rabbit polyclonal anti-PCP4 antibody (Santa Cruz) or a rabbit polyclonal anti-Wfs1 antibody (ProteinTech). Sections were thoroughly washed in 0.1% PBS-X and incubated in secondary antibodies (Alexa goat anti-chicken 488 and Alexa goat anti-rabbit 568, Invitrogen) diluted at 1:500 for 2h at room temperature. Finally, sections were washed in 0.1% PBS-X and mounted under ProLong Gold Antifade fluorescence media with DAPI (Invitrogen). Sections were then imaged on a Zeiss 710 meta confocal microscope using a 40X oil-immersion lens.

Organotypic slice preparation

Hippocampal slice cultures were prepared from postnatal day 6-8 RGS14 WT/KO mice as described previously¹²¹. In brief, hippocampi were dissected and sliced at 320 μ m thickness using a tissue chopper. The slices were plated on a membrane filter (Millicell-CM PICMORG50, Millipore). These cultures were maintained at 37 °C in an environment of humidified 95% O₂ and 5% CO₂. The culture medium was exchanged with fresh medium every three days. After 7-10 days in culture, neurons were sparsely transfected with ballistic gene transfer¹²² using gold beads (9-11 mg) coated with either

plasmids containing cDNA for GFP (10 μ g) for sLTP experiments or plasmids for GcAMP6S (10 μ g) and mCherry (25 μ g) for Ca^{2+} imaging experiments. Slices were imaged after 3-12 days following transfection. CA2/CA1 neurons were identified by somatic location and branching morphology of the apical dendrites.

Two-photon fluorescence microscopy and two-photon glutamate uncaging

Glutamate uncaging and imaging of live neurons were performed under a custom-built two-photon microscope with two Ti:Sapphire lasers (Chameleon, Coherent) as previously described¹²³. In brief, the lasers were tuned at the wavelength of 920 nm and 720 nm for imaging and uncaging, respectively. The intensity of each laser was independently controlled with electro-optical modulators (Conoptics). The fluorescence was collected with an objective (60x, 1.0 numerical aperture, Olympus), divided with a dichroic mirror (565dcxr) and detected with photoelectron multiplier tubes (PMTs) placed after wavelength filters (ET520/60M-2P for green, ET620/60M-2p for red, Chroma). MNI-caged L-glutamate (4-methoxy-7-nitroindoliny-yl-caged L-glutamate, Tocris) was uncaged with a train of 4-8 ms laser pulses (2.7-3.0 mW under the objective, 30 times at 0.5 Hz) near a spine of interest. Experiments were performed at room temperature in ACSF solution containing (in mM): 127 NaCl, 2.5 KCl, 25 NaHCO₃, 1.25 NaH₂PO₄, 4 CaCl₂, 25 glucose, 0.001 tetrodotoxin (Tocris) and 4 MNI-caged L-glutamate, bubbled with 95% O₂ and 5% CO₂. We examined secondary/tertiary branches of apical dendrites of CA1 and CA2 pyramidal neurons in organotypic cultured hippocampus slices at 10-22 days *in vitro*.

For spine Ca^{2+} imaging, neurons were co-transfected with GcAMP6S to detect Ca^{2+} transients (green) and mCherry as a volume marker (red) to control for spine growth

during the sLTP induction protocol. Images were acquired using fast-framing two-photon fluorescence microscopy (15.63 Hz frame rate) over a 10s baseline before inducing structural plasticity by glutamate uncaging with a train of 4-8 ms laser pulses (2.7-3.0 mW under the objective, 30 times at 0.5 Hz) near a spine of interest. Samples were imaged for approx. 30 seconds after the final pulse to ensure attenuation of GcAMP6S Ca^{2+} transients. Images were analyzed with MATLAB (MathWorks) and ImageJ. Data are presented as the change in fluorescence intensity ratio (G/R) from baseline \pm SEM.

Imaging automation

For sLTP experiments images were acquired as a z stack of five slices with 1 μm separation, averaging 5 frames/slice. Using multi-position imaging of spines with high-throughput automation (MISHA), dendritic spines at 4 positions on separate secondary/tertiary dendrites were imaged simultaneously employing algorithms for autofocusing¹²⁴ and drift correction¹²⁵ to maintain position and optimal focus during long imaging experiments (see Fig S3). Baseline images were acquired over 5 mins prior to uncaging (1 min, 30 pulses at 0.5 Hz) followed by 30 mins of imaging post-uncaging. A 5 min baseline stagger was incorporated to avoid data loss during uncaging events.

Post hoc immunostaining

Immediately following two-photon imaging experiments, organotypic hippocampal slices were fixed in 4% paraformaldehyde for 30 mins at room temperature. Slices were then washed thoroughly in 0.01M PBS, permeabilized for 15 mins in 0.3% PBS-X (0.3% Triton X-100 in PBS), and washed again in PBS. Slices were blocked for at least one hour at room temperature in a blocking solution containing 10% NGS (Vector Labs) diluted in 0.1% PBS-X prior to incubation in primary antibodies diluted in the

same blocking solution for 42 hours at room temperature. A rabbit polyclonal anti-PCP4 antibody (Santa Cruz) was used at a 1:500 dilution to delineate area CA2 in all experiments. For sLTP experiments with GFP-expressing neurons, a chicken polyclonal anti-GFP antibody (Abcam) was used at a dilution of 1:1,000 to visualize imaged neurons. For GcAMP6S experiments, co-transfected mCherry (cell fill) fluorescence was used to identify imaged neurons. Sections were thoroughly washed in 0.1% PBS-X and incubated in secondary antibodies (Alexa goat anti-chicken 488 and Alexa goat anti-rabbit 568, Invitrogen) diluted at 1:500 for 2h at room temperature. After rinsing samples thoroughly in 0.1% PBS-X, slices were optically cleared by incubating in a 60% 2,2'-Thiodiethanol solution (v/v, Sigma) for 30 mins at room temperature¹²⁶. Intact organotypic slices were imaged in the same clearing solution in glass bottom dishes (Willco) on a Zeiss 880 laser-scanning confocal microscope.

Image and Data Processing

Confocal laser scanning microscope images were processed using FIJI software (NIH v2.0.0). Images were only adjusted for brightness/contrast and cropped for presentation.

Statistical Analyses

All statistical analyses were performed in GraphPad Prism 7.

3.3 Results

Novel interactions between RGS14 and calcium signaling proteins

While many studies have examined RGS14's binding partners and signaling functions in recombinant systems^{24,93}, substantially fewer have investigated these interactions in brain where RGS14 is enriched^{14,25,42}. To identify candidate signaling

pathways through which RGS14 natively inhibits LTP in CA2, we first co-immunoprecipitated (co-IP) RGS14 protein complexes from WT and KO mouse brain and performed differential mass spectrometry. Functional annotation of candidate proteins revealed RGS14 previously unknown associations with LTP/calcium signaling, actin capping/binding, and cytoskeleton pathways in mouse brain (Table 3.1). RGS14 also interacts with G Protein/signal transduction pathways including previously identified binding partners G α o and G α i (Fig S1A). In addition, several proteins identified in this proteomics screen are also calmodulin-(CaM-) binding proteins, and CaM also co-immunoprecipitated with RGS14 from mouse brain. We therefore hypothesized that RGS14 might directly interact with CaM to mediate interactions with the other candidate proteins.

Functional Group	Gene Symbol	Description	Diff IP Spectral Counts	RGS14 WT IP Spectral Counts	RGS14 KO IP Spectral Counts
	<i>RGS14</i>	regulator of G-protein signaling 14 [Mus musculus]	98	138	40
G Protein/Signal Transduction	<i>Gnai1</i>	guanine nucleotide-binding protein G(i) subunit alpha-1 [Mus musculus]	11	21	10
	<i>Gnai3</i>	guanine nucleotide-binding protein G(k) subunit alpha [Mus musculus]	4	4	0
	<i>Gnao1</i>	guanine nucleotide-binding protein G(o) subunit alpha isoform B [Mus musculus]	3	4	1
	<i>Gnb1</i>	guanine nucleotide-binding protein G(I)/G(S)/G(T) subunit beta-1 [Mus musculus]	6	6	0
	<i>Opal</i>	dynamamin-like 120 kDa	28	28	0

		protein, mitochondrial isoform 2 precursor [Mus musculus]			
	<i>Tufm</i>	elongation factor Tu, mitochondrial isoform 1 [Mus musculus]	8	8	0
LTP/calcium signaling	<i>Calm2</i>	calmodulin [Mus musculus]	3	5	2
	<i>Camk2a*</i>	calcium/calmodulin-dependent protein kinase type II subunit alpha isoform 1 precursor [Mus musculus]	4	8	4
	<i>Camk2b*</i>	calcium/calmodulin-dependent protein kinase type II subunit beta isoform 3 [Mus musculus]	14	15	1
	<i>Ppp1cb*</i>	serine/threonine-protein phosphatase PP1-beta catalytic subunit [Mus musculus]	3	3	0
	<i>Ppp3ca*</i>	serine/threonine-protein phosphatase 2B catalytic subunit alpha isoform [Mus musculus]	10	12	2
	<i>Ppp3r1*</i>	calcineurin subunit B type 1 [Mus musculus]	3	3	0
	<i>Atp1a2*</i>	sodium/potassium-transporting ATPase subunit alpha-2 precursor [Mus musculus]	6	7	1
	<i>Atp2a2*</i>	sarcoplasmic/endoplasmic reticulum calcium ATPase 2 isoform b [Mus musculus]	5	5	0
	<i>Atp2b1*</i>	plasma membrane calcium ATPase 1 [Mus musculus]	2	3	1
	<i>Atp2b2*</i>	plasma membrane calcium-transporting ATPase 2 [Mus musculus]	2	2	0
	<i>Itpka*</i>	inositol-trisphosphate 3-kinase A [Mus musculus]	2	2	0
	<i>Slc1a3</i>	excitatory amino acid	3	5	2

		transporter 1 [Mus musculus]			
	<i>Slc25a5*</i>	ADP/ATP translocase 2 [Mus musculus]	2	3	1
	<i>Stx1b</i>	syntaxin-1B [Mus musculus]	2	4	2
	<i>Stxbp1</i>	syntaxin-binding protein 1 isoform b [Mus musculus]	3	3	0
	<i>Sv2a</i>	synaptic vesicle glycoprotein 2A [Mus musculus]	5	7	2
Actin remodeling	<i>Actb</i>	actin, cytoplasmic 1 [Mus musculus]	36	92	56
	<i>Add1*</i>	alpha-adducin isoform 1 [Mus musculus]	5	5	0
	<i>Capza1</i>	F-actin-capping protein subunit alpha-1 [Mus musculus]	5	6	1
	<i>Capza2</i>	F-actin-capping protein subunit alpha-2 [Mus musculus]	9	13	4
	<i>Capzb</i>	F-actin-capping protein subunit beta isoform b [Mus musculus]	9	13	4
	<i>Cfl1</i>	cofilin-1 [Mus musculus]	2	3	1
	<i>Coro1c</i>	coronin-1C [Mus musculus]	3	3	0
	<i>Coro2b</i>	coronin-2B [Mus musculus]	9	10	1
	<i>Dbn1</i>	drebrin isoform 1 [Mus musculus]	21	29	8
	<i>Fscn1</i>	fascin [Mus musculus]	2	2	0
	<i>Flii</i>	protein flightless-1 homolog [Mus musculus]	2	2	0
	<i>Gsn*</i>	gelsolin isoform 2 [Mus musculus]	6	6	0
	<i>Myo5a*</i>	unconventional myosin-Va [Mus musculus]	21	23	2
	<i>Myo5c*</i>	myosin-Vc [Mus musculus]	3	4	1
	<i>Myo6*</i>	unconventional myosin-VI [Mus musculus]	15	16	1

	<i>Myo18a*</i>	unconventional myosin-XVIIIa [Mus musculus]	34	40	6
	<i>Myl6b</i>	myosin light chain 6B [Mus musculus]	4	4	0
	<i>Myl9*</i>	myosin regulatory light polypeptide 9 [Mus musculus]	3	3	0
	<i>Myl12b*</i>	myosin regulatory light chain 12B [Mus musculus]	11	27	16
	<i>Sptan1*</i>	spectrin alpha chain, non-erythrocytic 1 isoform 2 [Mus musculus]	85	137	52
	<i>Sptbn1*</i>	spectrin beta chain, non-erythrocytic 1 isoform 1 [Mus musculus]	80	116	36
	<i>Sptbn2</i>	spectrin beta chain, brain 2 [Mus musculus]	29	32	3
	<i>Tmod2</i>	tropomodulin-2 [Mus musculus]	10	10	0
	<i>Tpm1*</i>	tropomyosin alpha-1 chain isoform 2 [Mus musculus]	3	3	0
	<i>Tpm2*</i>	tropomyosin beta chain isoform 3 [Mus musculus]	3	3	0
	<i>Tpm3*</i>	tropomyosin alpha-3 chain isoform 5 [Mus musculus]	2	4	2
Cytoskeleton (non-actin)	<i>Ank2</i>	ankyrin-2 isoform 3 [Mus musculus]	5	5	0
	<i>Ank3</i>	ankyrin-3 isoform c [Mus musculus]	5	5	0
	<i>Baspl</i>	brain acid soluble protein 1 [Mus musculus]	8	12	4
	<i>Dpysl2</i>	dihydropyrimidinase-related protein 2 [Mus musculus]	10	12	2
	<i>Dynll2</i>	dynein light chain 2, cytoplasmic [Mus musculus]	2	2	0
	<i>GM5620</i>	PREDICTED: tubulin alpha-1C chain isoform 4 [Mus musculus]	10	29	19
	<i>Map1a</i>	microtubule-associated	5	11	6

		protein 1A isoform 1 [Mus musculus]			
	<i>Map1b</i>	microtubule-associated protein 1B [Mus musculus]	11	11	0
	<i>Map2*</i>	microtubule-associated protein 2 isoform 1 [Mus musculus]	2	5	3
	<i>Map6*</i>	microtubule-associated protein 6 isoform 1 [Mus musculus]	11	11	0
	<i>Myh9*</i>	myosin-9 [Mus musculus]	49	74	25
	<i>Myh10*</i>	myosin-10 [Mus musculus]	81	190	109
	<i>Myh11*</i>	myosin-11 isoform 1 [Mus musculus]	60	75	15
	<i>Myh14*</i>	myosin-14 isoform 2 [Mus musculus]	27	27	0
	<i>Sept7</i>	septin-7 isoform 1 [Mus musculus]	2	2	0
	<i>Tuba1a</i>	tubulin alpha-1A chain [Mus musculus]	2	3	1
	<i>Tubb2b</i>	tubulin beta-2B chain [Mus musculus]	43	94	51
	<i>Tubb3</i>	tubulin beta-3 chain [Mus musculus]	15	33	18
	<i>Ywhag</i>	14-3-3 protein gamma [Mus musculus]	9	10	1
	<i>Ywhaz</i>	14-3-3 protein zeta/delta isoform 1 [Mus musculus]	4	11	7

Table 3.1 RGS14 natively interacts with G protein, calcium-activated plasticity

signaling, and actin cytoskeleton pathways in mouse brain. List of candidate RGS14 interacting proteins identified by LC-MS/MS analyses of RGS14 co-immunoprecipitation from brain. Red font indicates previously reported RGS14 binding partner, and an asterisk indicates calmodulin-binding proteins within each functional group. Differential IP spectral counts were calculated by subtracting peptide spectral counts detected in KO mouse brain IP from spectral counts in WT mouse brain IP.

Using the CaM target database¹²⁷, two putative CaM-binding domains with high predictive scores were identified in the Ras Binding Domain (RBD) region of RGS14 (Figure 3.1C, Figure 3.2B). We found RGS14 directly interacts only with Ca²⁺/CaM by performing CaM-Agarose pull-down assays with purified RGS14 protein in the presence or absence of Ca²⁺ (Figure 3.1A). We validated this direct, Ca²⁺-dependent interaction with fluorescence spectroscopy measurements of purified dansyl-CaM and RGS14 observing an increase in fluorescence (indicative of binding) only in the presence of Ca²⁺ (Figure 3.1B). This assay also revealed a 1:1 binding stoichiometry between Ca²⁺/CaM and RGS14. To identify region on RGS14 containing the CaM-binding site, we performed CaM-Agarose pull-downs with cell lysates expressing different regions of RGS14 and immunoblotting for FLAG-tags on the truncation mutants. These experiments confirmed that Ca²⁺/CaM binds RGS14 in the tandem RBD region containing the predicted CaM-binding sites, as only full-length RGS14 and the RBD construct containing the putative sites (3) pulled down with Ca²⁺/CaM (Figure 1C). Using differential hydrogen/deuterium exchange (HDX) mass spectrometry we found that Ca²⁺/CaM binding to RGS14 causes increased deuterium incorporation in the tandem RBD region flanking the predicted CaM-binding domains (Figure 3.1D), and the destabilization of the secondary structure of these peptides become significant over time (Figure 3.2C). We hypothesized this unique conformational change may poise RGS14 to interact with a downstream CaM effector. CaMKII was a promising target because it was identified in our co-IP proteomics screen and has a prominent role in plasticity⁵⁸. Co-IP experiments with recombinant RGS14 and CaMKII co-expressed in HeLa cells revealed that RGS14 binds to CaMKII in a Ca²⁺-independent manner (Figure 3.1E). Further, *in*

vitro radiolabeling assays demonstrated that RGS14 is directly phosphorylated by CaMKII (Figure 1F). These results show that RGS14 interacts with Ca²⁺/CaM and CaMKII, confirming two candidate binding partners identified in our proteomics study and providing evidence for a new role for RGS14 in Ca²⁺ signaling regulation.

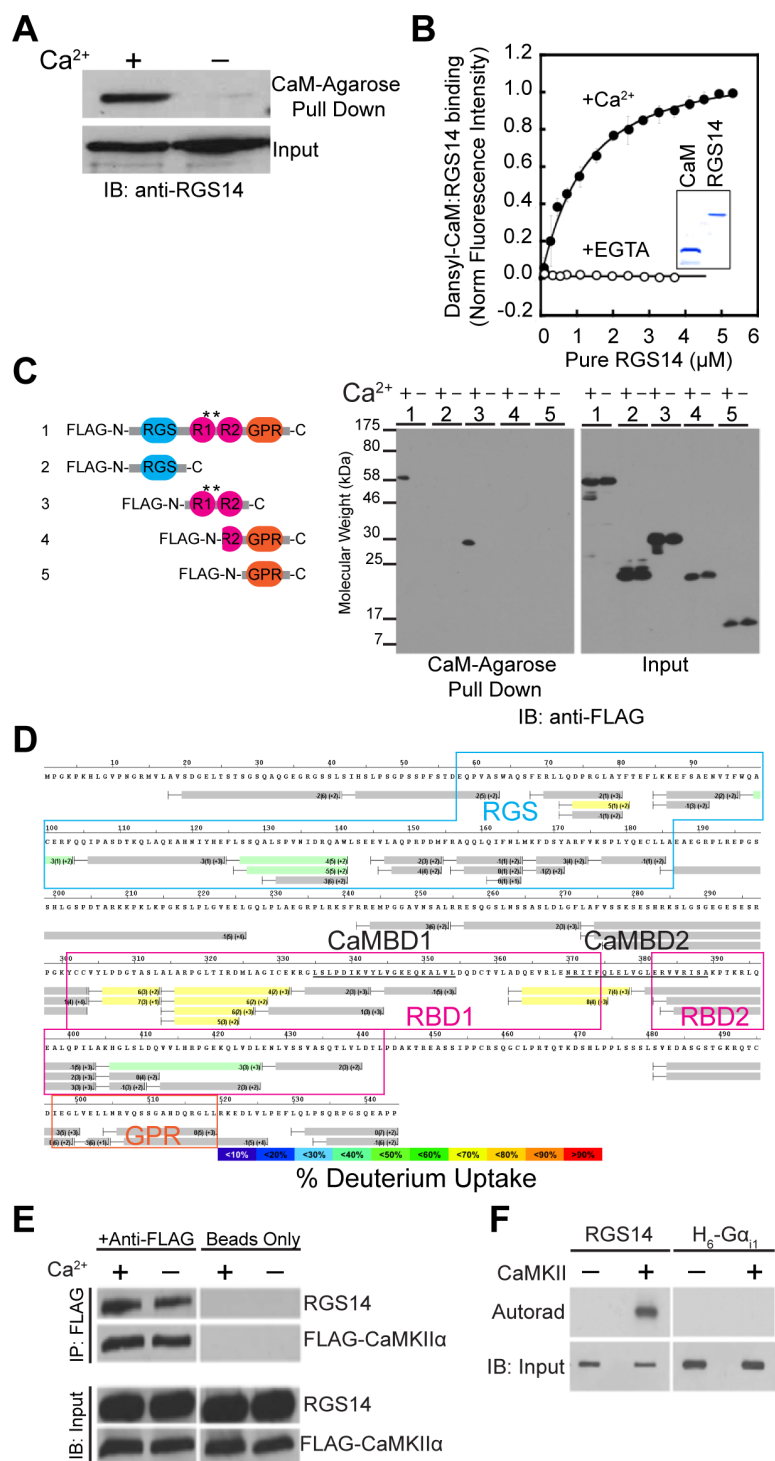


Figure 3.1. RGS14 directly interacts with Ca²⁺/CaM and CaMKII. (A) Purified RGS14 pulls down with CaM-Agarose beads specifically in the presence of Ca²⁺. (B) Dansyl-CaM fluorescence binding assays also show RGS14 directly interacts with

Ca²⁺/CaM, but not apo-CaM. Inset: Coomassie stain of purified Dansyl-CaM and RGS14 proteins. Data are represented as mean normalized fluorescence intensity \pm SEM. (C) Left: schematic representation of the domain structure of FLAG-tagged RGS14 truncation mutants used to map the interacting region with Ca²⁺/CaM. Asterisks indicate the location of the predicted CaMBDs. Right: RGS14 interacts with Ca²⁺/CaM through its tandem RBD region. Full-length FLAG-tagged RGS14 or truncation mutant cDNAs expressed in HeLa cells were pulled down by CaM-Agarose beads in the presence or absence of Ca²⁺. Recovered proteins were then subjected to SDS-PAGE and immunoblotting with an anti-FLAG antibody (right). Immunoblotting of input cell lysates with an anti-FLAG antibody verifies expression of all constructs (right). (D) A differential HDX heat map for the RGS14•Ca²⁺/CaM complex. Each bar represents an individual peptide with the color corresponding to the average percentage change in deuterium exchange between apo-RGS14 and RGS14•Ca²⁺/CaM over six time points (10, 30, 60, 300, 900, and 3600 s). The numbers in the first parentheses indicate the S.D. for three replicates. The numbers in the second parentheses indicate the charge of the peptide. Boxed regions indicate residues corresponding to the RGS (blue), RBDs (magenta), and GPR motif (orange); black bars underline the two predicted CaMBDs. Changes in deuterium exchange are indicated by the colored scale bar. (E) HeLa cells co-transfected with RGS14-Luciferase and FLAG-CaMKII α cDNAs were lysed, and protein complexes were immunoprecipitated with anti-FLAG agarose beads (+Anti-FLAG) or Protein G Sepharose beads (Beads Only) as a negative control. Immunoblotting of input cell lysates verifies expression of both cDNAs. (F) Purified RGS14 is directly phosphorylated by CaMKII α *in vitro*. Purified RGS14 or H₆-G α_{i1} (negative control)

percent deuterium exchange at six time points (10, 30, 60, 300, 900, and 3600 s) \pm SEM. Unpaired t tests were used to compare deuterium exchange between apo-RGS14 and RGS14•Ca²⁺/CaM at each time point.

CA2 LTP in RGS14 KO mice requires NMDAR, CaMKII, and PKA activity

We next asked if RGS14 modulates these Ca²⁺ signaling pathways to block LTP at Schaffer collateral synapses onto CA2 pyramidal neurons. To overcome technical barriers in localizing dendrites of CA2 pyramidal neurons in hippocampal slices, we crossed RGS14 KO mice with an Amigo2-eGFP reporter mouse line. We validated this mouse line selectively labels CA2 pyramidal neurons by immunolabeling for the DG- and CA2-enriched protein PCP4 and the CA1 molecular marker Wfs1. We found that Amigo2-eGFP fluorescence colocalizes with PCP4 immunoreactivity (Figure 3.3A,3.4A) but does not overlap with immunostaining for the CA1 marker Wfs1 (Figure 3.3B, 3.4B). We first performed field recordings in brain slices from adult RGS14 WT and KO; Amigo2-eGFP⁺ mice and replicated previous findings that high-frequency stimulation (3 x 100 Hz) induces robust synaptic potentiation in CA2 neurons of RGS14 KO mice, which is absent in WT mice, and similar to CA1 controls (Figure 3.3C; Lee et al., 2010). As previously reported, there were no differences in baseline synaptic responses between RGS14 WT and KO mice (Figure 3.4C) Comparing the mean field excitatory postsynaptic potential (fEPSP) slope averaged from 40-60 minutes after LTP induction, we found that the KO CA2 fEPSP slope was significantly larger than WT CA2 while CA1 controls were not significantly different (Figure 3.3D, two-way ANOVA results for genotype were $F(1,55)=6.64$, $p=0.0127$; results for CA region were $F(1,55)=2.478$,

$p=0.1212$; results for interaction were $F(1,55)=3.992$, $p=0.0507$. Sidak's *post hoc* comparison WT CA2–KO CA2 $p=0.0036$, WT CA1–KO CA1 $p=0.9028$).

To determine if the nascent LTP present in CA2 neurons of RGS14 KO mice requires Ca^{2+} signaling, we performed the same LTP induction protocol in brain slices prepared from RGS14 KO;Amigo2-eGFP+ mice in the presence of pharmacological inhibitors of these pathways (Figure 3.3I). The CA2 LTP in RGS14 KO mice was effectively blocked by bath application of the NMDAR antagonist APV (50 μ M, blue) as well as inhibitors of CaMKII (KN-62, 10 μ M) or PKA (PKI, 1 μ M; Figure 3.3E-G). Comparing the mean fEPSP slope 40-60 minutes following LTP induction, we found a significant reduction in each inhibitor relative to KO controls (unpaired t-tests: APV $p=0.0104$; KN-62 $p=0.0102$; PKI $p=0.0454$). Together these findings indicate that the nascent LTP in CA2 neurons of RGS14 KO mice requires NMDAR, CaMKII, and PKA activity and elucidating similar underlying mechanisms as plasticity described in CA1.

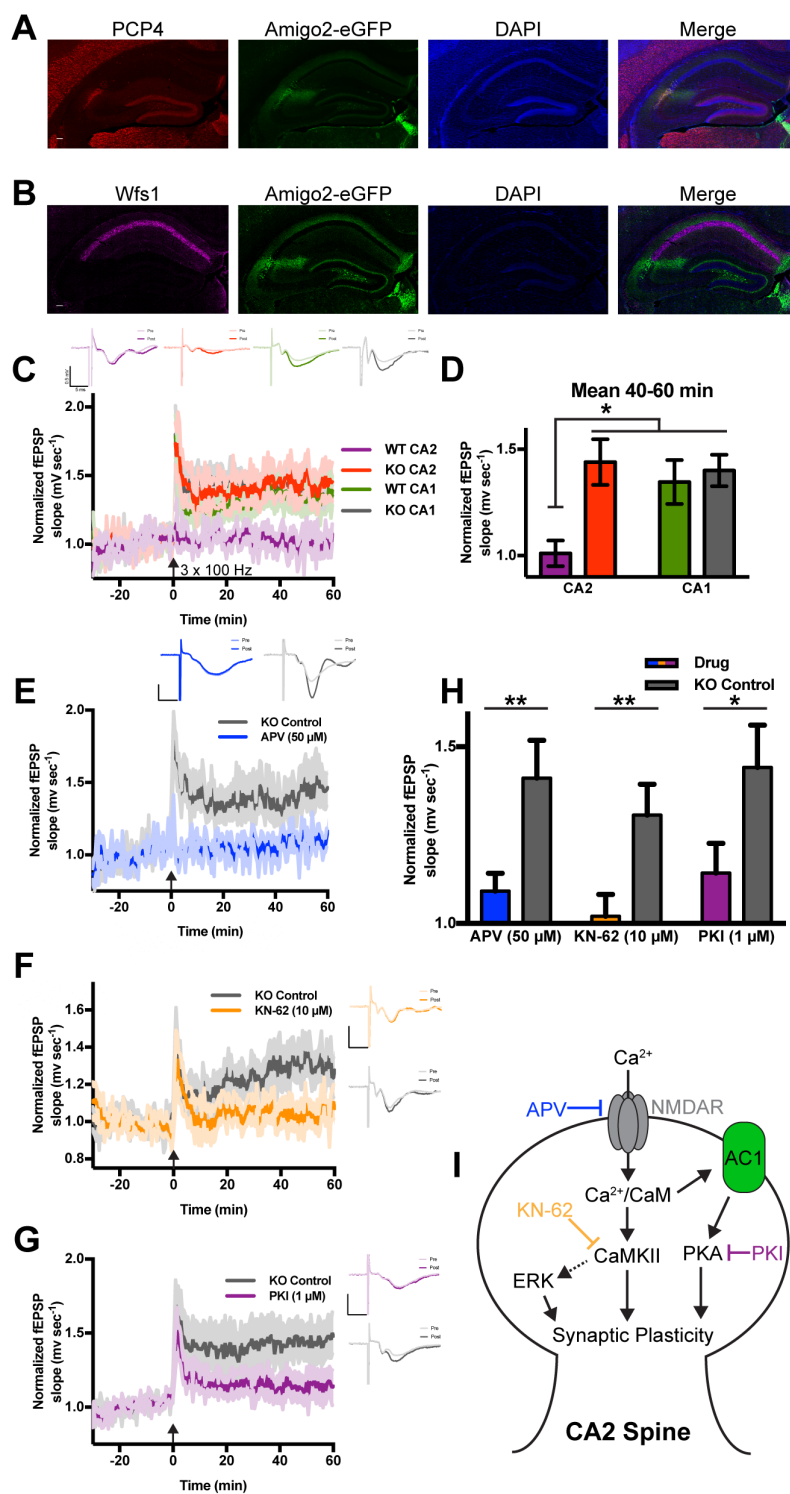


Figure 3.3 Nascent CA2 LTP in RGS14 KO mice follows similar mechanisms to CA1. (A) Amigo2-eGFP (green) labels CA2 pyramidal neurons and overlaps with the CA2 molecular marker PCP4 (red). Scale bar = 100 μ m. (B) Amigo2-eGFP fluorescence

(green) does not colocalize with immunoreactivity for the CA1 pyramidal neuron marker Wfs1 (magenta). Scale bar = 100 μm . (C) Summary graph of field recordings from adult Amigo2-eGFP+;RGS14 WT/KO mice validate RGS14 KO mice possess a capacity for LTP in CA2 (red), which is absent in WT mice (purple), with no differences in CA1 plasticity (green, gray). LTP was induced by HFS (3 x 100 Hz) at time 0 (arrow). Data are represented as mean (line) normalized fEPSP slope \pm SEM (shading). WT CA2 n = 14; KO CA2 n = 16; WT CA1 n = 17; KO CA1 n = 12. Insets (top) are representative traces of field potentials recorded from CA2 and CA1 neurons of RGS14 WT/KO mice before (light font) and after (dark font) LTP induction. (D) Loss of RGS14 unleashes CA2 plasticity. Quantification of the mean normalized fEPSP slope from 40-60 mins following LTP induction (C) with error shading representing SEM. There is a significant difference in LTP induction between WT and KO CA2, whereas there is no difference between WT and KO CA1 controls (** $p \leq 0.01$, Sidak's multiple comparison testing). (E-G) Summary graphs of LTP induction experiments performed in area CA2 of RGS14 KO mice either in the presence (color) or absence (gray) of drug. LTP was induced by HFS (3 x 100 Hz) at time 0 (arrow). Data are represented as mean (line) normalized fEPSP slope \pm SEM (shading). Insets (top) are representative traces of field potentials recorded from CA2 neurons of RGS14 KO mice before (light font) and after (dark font) LTP induction. Bath application of APV (50 μM , blue) to antagonize NMDARs, KN-62 (10 μM , orange) to inhibit CaMKII, or PKI (1 μM , purple) to inhibit PKA all block LTP induction in KO CA2 neurons. (H) Nascent LTP in KO CA2 neurons requires NMDAR, CaMKII, and PKA. Bar graph displaying the mean normalized field potential slope (mV sec^{-1}) from 40-60 mins following LTP induction (E-G) with error bars representing SEM. Each inhibitor

was compared with paired KO CA2 controls by unpaired t-test (** $p \leq 0.01$, * $p \leq 0.05$). For APV, drug $n = 14$, KO control $n = 13$. For KN-62, drug $n = 19$, KO control $n = 16$. For PKI, drug $n = 18$, KO control $n = 16$. (I) Working model of plasticity signaling in a CA2 spine. Activation of postsynaptic NMDARs allows Ca^{2+} influx, which binds CaM to initiate signaling to promote synaptic plasticity. Inhibitors used in these experiments are displayed in the associated color.

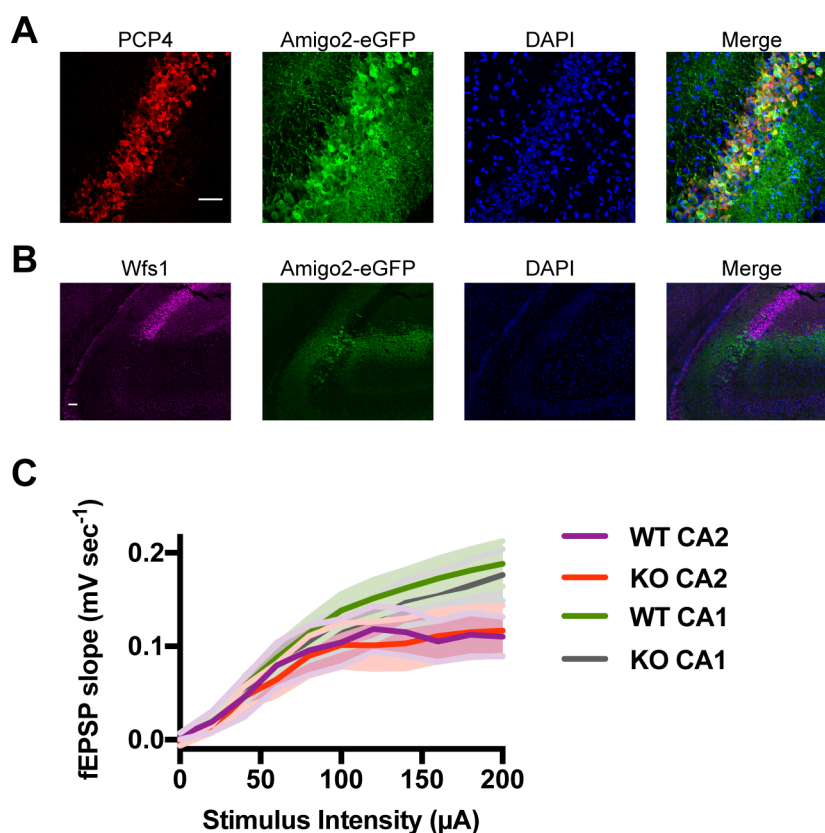


Fig 3.4. Supplemental immunostaining and input/output curves. (A) Higher magnification images of Amigo2-eGFP labeling (green) showing colocalization with PCP4 immunoreactivity (red), a molecular marker enriched in CA2 pyramidal neurons. Scale bar = 50 μm . (B) Higher magnification images of Amigo2-eGFP labeling (green) highlighting the distinct, non-overlapping signal with immunoreactivity for the CA1 marker Wfs1 (magenta). Scale bar = 50 μm . (C) Basal synaptic transmission at Schaffer

collateral synapses onto CA2/CA1 pyramidal neurons is not altered in RGS14 KO mice. Summary graphs of input-output curves for fEPSP slope in response to CA3 Schaffer collateral stimulation intensity.

RGS14 inhibits spine structural plasticity in CA2 neurons

With our new finding that CA2 neurons of RGS14 KO utilize similar mechanisms as CA1 neurons to support synaptic potentiation, we wondered if RGS14 might play a role in activity-dependent spine structural plasticity (sLTP) since it is often associated with LTP in CA1 and relies on similar mechanisms^{128,129}. In addition, actin/cytoskeleton signaling proteins associated with RGS14 in our proteomics screen (Table 3.1) and RGS14 is enriched in CA2 spines and dendrites²⁵. To determine if RGS14 modulates spine sLTP, we cultured hippocampal slices from RGS14 WT and KO mice and performed two-photon fluorescence microscopy and two-photon glutamate uncaging to induce spine structural plasticity in *stratum radiatum* of CA2 and CA1 (Figure 3.5). In order to collect more data from each neuron during long experiments, we developed an automated imaging method to image multiple dendritic spine positions simultaneously. This technique, multiposition imaging of spines with high-throughput automation (MISHA) tracks coordinates of multiple dendritic segments on the same neuron and uses autofocus¹²⁴ and drift correction¹²⁵ algorithms during the experiment (Figure 3.6).

We found that stimulated spines of WT CA2 neurons exhibit reduced volume change compared to KO CA2 neurons or CA1 controls (Figure 3.5A-C). When comparing the mean sLTP between samples, there was a significant interaction effect of genotype and CA region during the sustained phase of sLTP (21-25 mins, $p=0.0482$) but

not during the transient phase ($p=0.0583$, 1-3 mins). To validate the cellular location of all neurons imaged in these studies, slices were fixed immediately following two-photon imaging, and PCP4 immunostaining was performed to delineate the boundaries of hippocampal area CA2 (Figure 3.5, red). These results indicate that RGS14 also naturally restricts sLTP of CA2 spines.

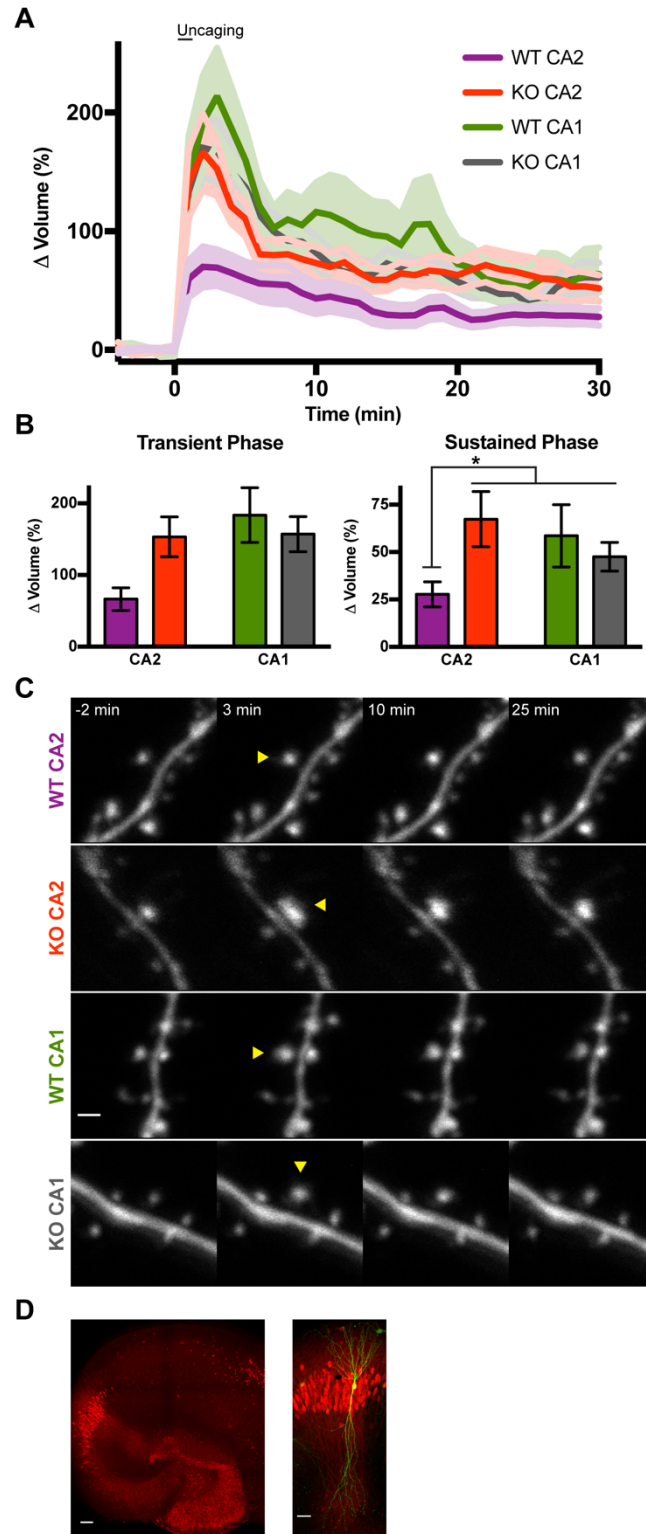


Figure 3.5 RGS14 impairs spine structural plasticity. (A) Averaged time course of spine volume change during the induction of spine structural plasticity by two-photon

glutamate uncaging in the absence of extracellular Mg^{2+} . The number of samples (spines/neurons) for stimulated spines are 20/6 for WT CA2, 17/7 for KO CA2, 24/7 for WT CA1, and 20/7 for KO CA1. Error bars denote SEM. (B) Quantification of the transient (1-3 mins) and sustained (21-25 mins) phases of sLTP after spine stimulation. (C) Representative two-photon fluorescence images of spine sLTP induction in GFP-expressing hippocampal pyramidal neurons. Arrowhead indicates the stimulated spine. Scale bar = 1 μm . (D) Representative post-hoc immunostaining to delineate hippocampal CA region of imaged neurons. Left: Organotypic hippocampus slice culture stained for the DG- and CA2-enriched gene PCP4 (red). Scale bar = 100 μm . Right: Magnified view of area CA2 in PCP4 immunostained (red) hippocampus on left with a biolistically labeled CA2 pyramidal neuron expressing GFP (green). Scale bar = 50 μm .

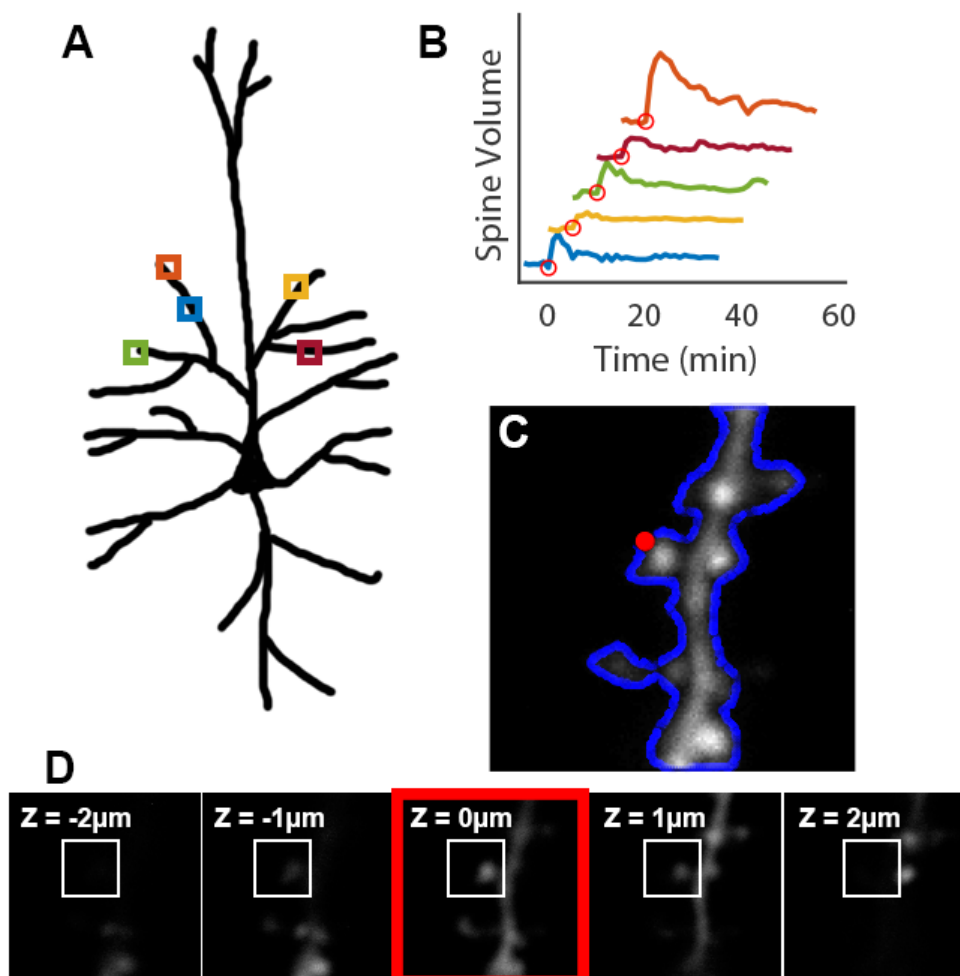


Fig 3.6 Multiposition Imaging of Spines with High Throughput Automation (MISHA). (A) Spines with varying X,Y,Z coordinates are identified on separate secondary/tertiary dendritic branches. (B) Uncaging (red circles) of spines is staggered to avoid important data loss during one-minute uncaging events. (C) Lateral drift correction is achieved by comparing a maximum intensity projection image to a reference image (not shown) and thresholding fluorescence to determine cell perimeter (blue). The uncaging ROI (red circle) is shifted to the nearest point on the spine perimeter (blue) immediately prior to uncaging. (D) Representative Z stack used for focus correction. The optimal Z position (red square) is found by comparing relative focus values of the image immediately surrounding the uncaging ROI (white square).

RGS14 attenuates spine Ca^{2+} transients during structural plasticity induction

Spine Ca^{2+} is critical for the induction of synaptic plasticity⁵⁶, and we found that the synaptic potentiation observed in CA2 neurons of RGS14 KO mice requires Ca^{2+} -dependent signaling (Figure 3.3). We next asked if the attenuated spine structural plasticity observed in WT CA2 neurons containing RGS14 was due to reduced spine Ca^{2+} during glutamate uncaging. Performing fast framing two-photon fluorescence microscopy (15.63 Hz frame rate), we monitored Ca^{2+} -dependent fluorescence changes in neurons expressing the genetically encoded calcium indicator GcAMP6S (green) elicited during sLTP induction. Neurons were also transfected with mCherry (red) to control for spine enlargement during the experiment, and Ca^{2+} transients were analyzed in the ratiometric change in fluorescence intensity from baseline (Figure 3.7; $\Delta\text{G}/\text{R}$). Glutamate uncaging pulses elicited much larger spine Ca^{2+} transients in CA2 neurons of RGS14 KO mice compared to WT littermates. Both RGS14 WT and KO CA1 controls displayed similar changes in spine Ca^{2+} during sLTP induction. We generated pulse triggered averages for the Ca^{2+} responses to all 30 glutamate uncaging pulses delivered during the experiment to analyze changes in spine Ca^{2+} (Figure 3.7C). Normalizing the baseline value to analyze uncaging evoked Ca^{2+} , we found that WT CA2 spines display similar spine Ca^{2+} transients to CA1 controls, while KO CA2 neurons display significantly larger fluctuations. Normalizing maximum values for Ca^{2+} responses did not reveal any apparent differences in kinetics. Moreover, we did not notice any difference in Ca^{2+} -dependent fluorescent changes evoked by glutamate uncaging in dendrites between any groups (Figure 3.8). Together, these data indicate that the presence of RGS14 limits

uncaging evoked spine Ca^{2+} transients in CA2 neurons and increased spine Ca^{2+} provides a mechanism to explain the nascent plasticity observed in KO CA2 neurons.

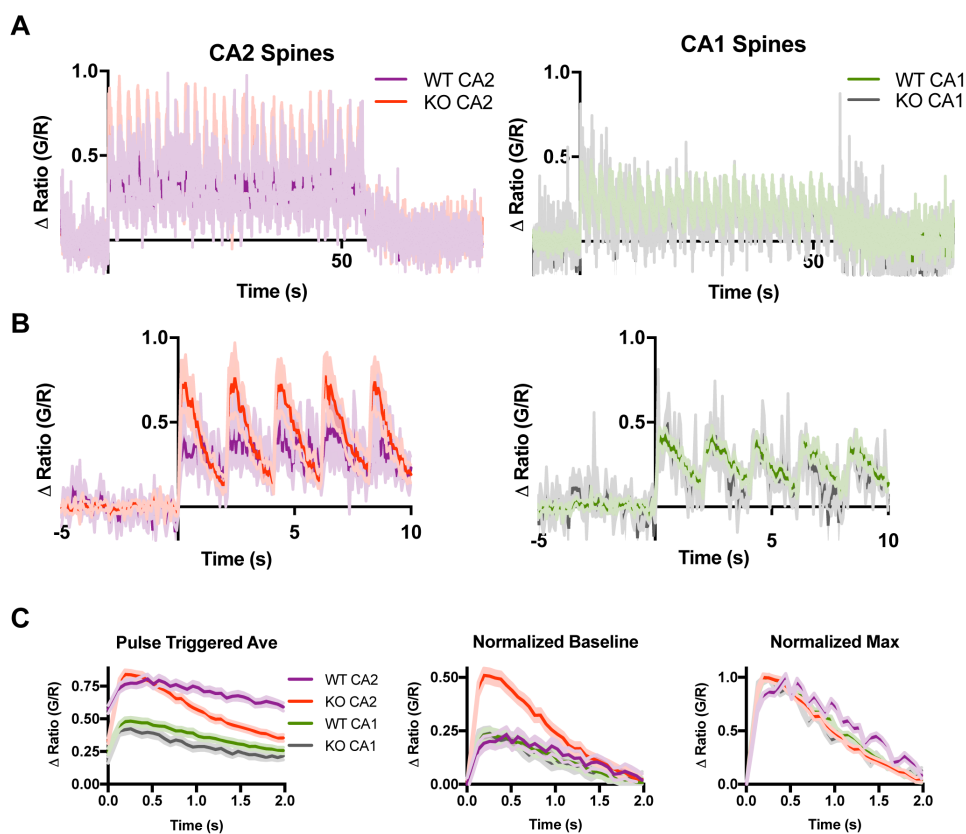


Figure 3.7 RGS14 restricts CA2 spine Ca^{2+} levels. (A) Averaged time course of GcAMP6S Ca^{2+} transients in spines during the induction of spine structural plasticity by two-photon glutamate uncaging in the absence of extracellular Mg^{2+} . The number of samples (spines/neurons) for stimulated spines are 6/2 for WT CA2, 15/3 for KO CA2, 28/4 for WT CA1, and 7/2 for KO CA1. Data are displayed as mean ratiometric change in fluorescence intensity (green/red). Error bars (shading) denote SEM. (B) Expanded view of averaged time course of GcAMP6S Ca^{2+} transients in spines during the first 10 sec (5 pulses) of the two-photon glutamate uncaging protocol shown in panel A. (C) Pulse triggered averages for all spine GcAMP6S Ca^{2+} transients evoked during the induction of spine structural plasticity (left). Normalizing the pulse triggered averages

baseline to zero (middle) to visualize Ca^{2+} transients reveals KO CA2 spines have much larger spine Ca^{2+} entry than WT CA2 or CA1 controls. Normalizing the maximum change (right) in spine Ca^{2+} shows similar kinetics between all cell types. Data are displayed as mean ratiometric change in fluorescence intensity (green/red). Error bars (shading) denote SEM.

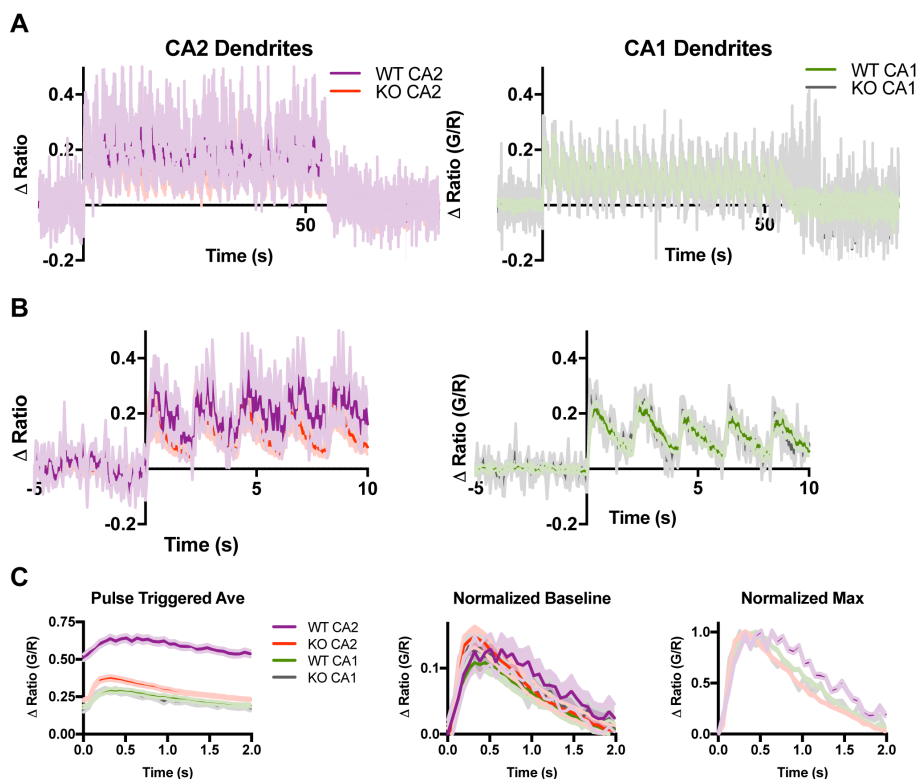


Fig 3.8 Similar changes in dendritic Ca^{2+} levels during spine structural plasticity.

(A) Averaged time course of GcAMP6S Ca^{2+} transients in dendrites during the induction of spine structural plasticity by two-photon glutamate uncaging in the absence of extracellular Mg^{2+} . The number of samples (dendrites/neurons) for stimulated spines are 6/2 for WT CA2, 15/3 for KO CA2, 28/4 for WT CA1, and 7/2 for KO CA1. Data are displayed as mean ratiometric change in fluorescence intensity (green/red). Error bars (shading) denote SEM. (B) Expanded view of averaged time course of GcAMP6S Ca^{2+}

transients in dendrites during the first 10 sec (5 pulses) of the two-photon glutamate uncaging protocol shown in panel A. (C) Pulse triggered averages for all dendritic GcAMP6S Ca^{2+} transients evoked during the induction of spine structural plasticity (left). Normalizing the pulse triggered averages baseline to zero (middle) to reveals similar changes in dendrite Ca^{2+} levels between all cell types during glutamate uncaging. Normalizing the maximum change (right) in dendritic Ca^{2+} shows similar kinetics between all cell types. Data are displayed as mean ratiometric change in fluorescence intensity (green/red). Error bars (shading) denote SEM.

3.4 Discussion

In this study we have identified and characterized a previously unknown role for RGS14 in the regulation of Ca^{2+} signaling, providing new insight into the Ca^{2+} -dependent mechanisms RGS14 uses to block plasticity in hippocampal area CA2. Specifically, a proteomics based approach shows that native RGS14 naturally engages key members of Ca^{2+} signaling pathways required for plasticity, and we identify Ca^{2+} /CaM and CaMKII as RGS14 binding partners. Moreover, we find that synaptic potentiation present in CA2 neurons lacking RGS14 requires NMDAR, CaMKII, and PKA activity (also Ca^{2+} activated), revealing a striking similarity to mechanisms underlying LTP in CA1^{125,126}. We further demonstrate with two-photon glutamate uncaging that RGS14 restricts sLTP since stimulated spines of RGS14 KO CA2 neurons exhibit long-lasting spine growth lacking in RGS14 WT CA2 neurons. Finally, we show that spine Ca^{2+} transients are greatly enhanced during the induction of spine structural plasticity, indicating that RGS14 naturally limits spine Ca^{2+} elevations during synaptic stimulation.

Novel RGS14 binding partners identified in mouse brain

Our initial proteomics screen significantly extends previous knowledge on the signaling functions of native RGS14 in mouse brain by identifying several novel candidate binding partners (Table 3.1). Ontology sorting of the protein complexes that co-immunoprecipitated with RGS14 provides the first evidence of roles for RGS14 in Ca^{2+} -activated LTP signaling, actin regulation, and cytoskeleton signaling. Further, we validated that RGS14 functionally regulates Ca^{2+} -stimulated mechanisms to block long-lasting synaptic potentiation and spine Ca^{2+} transients to impair spine structural plasticity. Of note, we also found that native RGS14 associates with known binding partners $\text{G}\alpha\text{i}$ and $\text{G}\alpha\text{o}$ in mouse brain indicating RGS14 regulates G protein signaling in neurons as well as cell lines.

While this mass spectrometry approach greatly advances our understanding of the signaling functions of native RGS14 in brain, these data also provoke new questions about RGS14 and plasticity suppression in CA2. For example, it remains to be demonstrated whether RGS14 suppresses actin remodeling or cytoskeleton pathways to block CA2 plasticity in addition to limiting Ca^{2+} signaling. The possibility exists that RGS14 associates with actin/cytoskeleton pathways simply to transport the protein from the nucleus to dendrites/spines following transcription. Another question emerging from these studies is whether RGS14 functionally integrates these diverse pathways in CA2 neurons or if subpopulations of RGS14 exist in brain that selectively engage different key members of these pathways. Evidence exists for multiple biochemical populations of RGS14 in rodent brain¹⁴, and associations between RGS14 and its various binding partners influence the dynamic subcellular localization²² and ability to interact other proteins^{17,18,108} providing support for this multiple pools of RGS14 that could serve

distinct signaling functions. Lastly, future studies investigating the importance of other central Ca^{2+} signaling proteins identified here with the regard to synaptic plasticity will extend our understanding of the complex regulation RGS14 exerts to block LTP.

RGS14 Interactions with CaM/CaMKII: implications for CA2 plasticity and beyond

From our initial list of candidate proteins, we identified and characterized Ca^{2+} /CaM and CaMKII as novel binding partners of native RGS14. We found that RGS14 directly interacts with Ca^{2+} /CaM only in the presence of Ca^{2+} with a 1:1 binding stoichiometry. While our results demonstrated that Ca^{2+} /CaM binds RGS14 in the tandem RBD region, it remains to be demonstrated which of the two putative CaM binding domains mediates this interaction. Despite intensive mutagenesis efforts of both CaM binding sites, we were unable to create a mutant of RGS14 that cannot bind Ca^{2+} /CaM (data not shown). One possibility is that RGS14 can bind Ca^{2+} /CaM at either site, but the interaction at one site may occlude the other CaM binding site to produce a 1:1 stoichiometry. Ca^{2+} /CaM may also bind RGS14 at residues distinct from the predicted sites, but we find this possibility unlikely as differential HDX revealed conformational changes in residues flanking the putative CaM binding domains. It also remains to be demonstrated whether Ca^{2+} /CaM interactions link RGS14 to the downstream Ca^{2+} -activated signaling proteins identified in our mass spectrometry studies.

We have also shown that RGS14 interacts with and is directly phosphorylated by CaMKII (Figure 4.1). In contrast to the RGS14: Ca^{2+} /CaM complex, we find that RGS14 binds to CaMKII in a Ca^{2+} -independent manner. This finding suggests that Ca^{2+} /CaM binding may not be necessary for RGS14 to associate with CaMKII. Future experiments to identify the site(s) on RGS14 phosphorylated by CaMKII in cells and how CaMKII

phosphorylation affects RGS14's known functions will be central to refining our model. One potential model of plasticity regulation is that RGS14 exists in a pre-complex with CaMKII to prevent Ca^{2+} /CaM from activating CaMKII following Ca^{2+} influx during synaptic activity. Further experiments are also necessary to determine the precise roles of Ca^{2+} /CaM binding and CaMKII phosphorylation in RGS14's ability to suppress plasticity in CA2 pyramidal neurons.

Is RGS14 the defining plasticity factor between CA2 and CA1?

One particularly interesting finding from these experiments is that loss of RGS14 unleashes plasticity in CA2 pyramidal neurons that is strikingly similar to CA1 pyramidal neurons. Specifically, we found the synaptic potentiation in CA2 neurons of RGS14 KO mice required activation of postsynaptic NMDARs as well as CaMKII and PKA activity. Along with our previous results that the LTP in RGS14 KO CA2 neurons is MEK/ERK-dependent²⁵, these data demonstrate that the cellular mechanisms governing plasticity in CA1 neurons underlie nascent plasticity in RGS14 KO CA2 neurons^{125,126}. Additionally, we found that loss of RGS14 restores spine structural plasticity to CA2 pyramidal neurons, another prominent plasticity feature of CA1. Finally, preliminary studies show that viral expression of RGS14 in CA1 pyramidal neurons effectively blocks LTP induction (data not shown). Together these data indicate that RGS14 naturally inhibits plasticity in CA2 pyramidal neurons by cellular pathways common to both CA2 and CA1. Despite expressing several genes implicated in limiting plasticity^{72,87,107}, loss of RGS14 alone is sufficient to endow CA2 pyramidal neurons with robust plasticity²⁵. This finding suggests that the other molecular factors suppressing plasticity in CA2 converge

on RGS14, underscoring RGS14's role as an unusual, multi-functional scaffolding protein.

RGS14 impairs spine structural plasticity and limits spine Ca²⁺ elevations

Our finding showing that spine Ca²⁺ transients in WT CA2 neurons and CA1 controls are similar during sLTP induction, but that CA2 spines lack plasticity, is consistent with previous evidence that robust Ca²⁺ handling mechanisms suppress plasticity in CA2 spines⁷². Here, we show that RGS14 plays a key role in this process by restricting the elevation of spine Ca²⁺, though the mechanisms by which RGS14 does this remain unclear. Ca²⁺ and CaM modulating proteins (plasma membrane Ca²⁺ pumps (PMCA) and PCP4/Pep-19, respectively) are reported to contribute to the suppression LTP in CA2 neurons⁷², and RGS14 could coordinate its actions with these protein/pathways to suppress plasticity. Furthermore, the induction of elevated Ca²⁺ in CA2 spines (here) and in CA1 spines under nearly identical conditions¹²⁷ are both largely NMDAR-dependent, so RGS14 may limit NMDAR Ca²⁺ influx. Consistent with this idea, we find that the nascent LTP in CA2 neurons due to the loss of RGS14 is fully blocked by NMDAR antagonism. In addition, RGS14 could also influence Ca²⁺ extrusion through its interactions with Ca²⁺/CaM and/or the PMCA isoforms identified in our proteomics screen. Future studies will determine if RGS14 affects influx, buffering, and/or extrusion of Ca²⁺ in order to alter Ca²⁺ levels in CA2 spines.

Also of interest will be identifying the downstream signaling pathways that are unleashed by the amplified Ca²⁺ levels in CA2 spines of RGS14 KO mice. We have demonstrated a requirement for Ca²⁺-driven activation of CaMKII, PKA, and Ras/ERK cascades in the nascent CA2 LTP, but RGS14 may also suppress other pathways to gate

LTP in CA2 neurons. Finally, ongoing experiments are examining if RGS14 functionally integrates Ca^{2+} signaling with G protein and/or ERK pathways in CA2 neurons to exert complex regulation over plasticity therein. In summary, our findings here provide the first evidence that RGS14 is a critical player regulating postsynaptic Ca^{2+} and downstream signaling in CA2 neurons, and define the novel cellular mechanisms by which RGS14 gates synaptic plasticity.

Chapter 4⁴:
Discussion

⁴ A portion of this chapter has been published. Evans PR, Dudek SM, and Hepler JR (2015) Regulator of G Protein Signaling 14 (RGS14): A Molecular Break on Synaptic Plasticity Linked to Learning and Memory. *Prog Mol Biol Transl Sci.* 133:169-206.

4.1 RGS14 expression during early postnatal development: the aging conspiracy against plasticity in CA2

Heightened synaptic plasticity is prevalent during critical periods of postnatal brain development when sensory experience influences the maturation of neural circuitry. Early life events have profound impacts on the hippocampus that can persist into adulthood, and hippocampal-dependent processing of spatial and social information is required for adaptation and survival in early development. Given that RGS14 suppresses hippocampus-dependent learning and memory, we investigated if RGS14 expression is regulated during postnatal mouse brain development⁴². We found that RGS14 protein is undetectable at birth (P0) with very low levels of mRNA present in brain. RGS14 mRNA and protein expression levels are dramatically upregulated in brain during postnatal mouse brain development, with protein first detected at P7, and both increasing over time until reaching highest sustained levels in adulthood. This expression pattern was mirrored by upregulated immunoreactivity for RGS14 protein observed in hippocampal CA2. Taken together with behaviors mediated by area CA2, these data suggest that the absence of RGS14 protein may permit enhanced (or unfiltered?) hippocampus-dependent learning during the first weeks of life, such as maternal bonding and acquiring spatial memory of the environment. Subsequent upregulated expression of RGS14 beginning at P7 could serve to selectively filter episodic learning and memory storage driven by experience.

The presence of RGS14 expression coincides with the most prevalent period of synapse formation and pruning¹⁰⁵ suggesting that the appearance of RGS14 and other CA2-enriched signaling proteins could possibly shape the maturation of hippocampal CA2 circuitry. The CaM-binding PCP4/Pep-19 is essential for synaptic plasticity in area

CA2⁷², and its expression pattern in CA2 is strikingly similar to that of RGS14¹³⁰. The enrichment of PCP4 in area CA2 underlies, at least in part, the robust Ca²⁺ buffering and extrusion properties⁷². The development expression pattern of A1R in rodent hippocampal CA2 also resembles the trends for RGS14 and PCP4⁷³. Further, perineuronal nets (PNNs) that surrounding CA2 neurons have been shown to increase during development and restrict plasticity in other brain regions^{65,107,129}. A recent study demonstrated that PNNs in surround spines of CA2 pyramidal neurons in stratum radiatum, and degradation of the PNNs restore LTP to CA2 pyramidal neurons¹⁰⁷. However, the cellular mechanisms by which PNNs restrict plasticity induction in area CA2 remain unknown. The coincident appearance and the expression patterns of these genes in area CA2 suggests that plasticity is developmentally regulated in this region to influence hippocampal circuitry and learning. Another possible interpretation of the concerted expression of these proteins serves a neuroprotective function to stabilize and preserve hippocampal CA2 throughout life. While these findings offer developmental insight into CA2, these studies also revealed RGS14 expression in brain regions outside of hippocampal CA2.

4.2 RGS14 regulation of Ca²⁺ signaling in CA2 spines

Our findings provide the first evidence linking RGS14 to the regulation of Ca²⁺ signaling relevant to synaptic plasticity, and we identify Ca²⁺-activated signaling is critical for LTP in CA2 neurons of RGS14 KO mice. RGS14 was also found to inhibit CA2 spine structural plasticity (sLTP), and KO CA2 spines displayed significantly larger transients compared to WT CA2 or CA1 controls during sLTP induction. These results indicate that RGS14 limits NMDAR-mediated Ca²⁺ elevations in spines as glutamate

uncaging under these conditions almost exclusively engages NMDAR to elevate Ca^{2+} ¹³². It further suggests that additional Ca^{2+} -regulating mechanisms besides RGS14 are present in CA2 spines as similar Ca^{2+} elevations in WT CA2, which are very similar to CA1, are insufficient to produce structural plasticity.

The finding that WT CA2 neurons displayed similar spine Ca^{2+} changes to CA1 controls was initially perplexing, as CA2 neurons were previously reported to have attenuated spine Ca^{2+} transients relative to CA1⁷². However, those experiments used somatic action potentials to evoke spine Ca^{2+} transients⁷², which likely engaged different Ca^{2+} sources including voltage-sensitive calcium channels, than in our conditions which isolated NMDAR Ca^{2+} . Our results that WT CA2 spine Ca^{2+} transients, which are similar to CA1, are insufficient to drive plasticity suggests that additional calcium handling machinery is present in CA2 spines to inhibit plasticity. Our data showing that plasticity occurs in KO CA2 spines when greatly enhanced Ca^{2+} elevations is consistent with this hypothesis that factors negatively regulating Ca^{2+} in CA2 spines must be overpowered to permit plasticity. Similarly, brief application of high extracellular Ca^{2+} to brain slices from WT animals also restores synaptic potentiation to CA2⁷².

4.3 Working model of CA2 plasticity regulation by RGS14

Here we have defined the cellular mechanisms by which RGS14 naturally suppresses plasticity in its host CA2 pyramidal neurons, providing the first evidence that RGS14 restricts spine Ca^{2+} levels and downstream signaling. Specifically, the nascent LTP found in CA2 neurons of mice lacking RGS14 requires NMDAR, CaMKII, and PKA activity. Together with our finding that NMDAR-dependent spine Ca^{2+} transients evoked by glutamate uncaging are much larger in CA2 neurons of RGS14 KO mice, we

reason that RGS14 naturally inhibits Ca^{2+} influx through NMDARs. We further speculate the enhanced Ca^{2+} elevations are sufficient to overpower the robust Ca^{2+} buffering and extrusion mechanisms present in CA2 spines to induce plasticity. The molecular mechanisms by which RGS14 inhibits NMDAR function remains an area of active interest. Additionally, it is unclear whether the attenuation of spine Ca^{2+} influx by RGS14 is sufficient to restrict activation of downstream cascades to promote synaptic plasticity or if RGS14 employs additional mechanisms downstream to limit plasticity signaling (e.g. inhibiting ERK binding activated HRas, altering CaMKII activity by CaM or CaMKII interactions, etc.). Finally, RGS14 is well poised to influence Ca^{2+} extrusion from CA2 spines through its direct interaction with Ca^{2+} /CaM or association with PMCAs although additional experiments are necessary to determine if RGS14 serves a role in this process.

Another area of future investigation is to determine if RGS14 modulates CA2-specific forms of potentiation. CA2 neurons also express $\text{G}\alpha\text{q}$ -linked vasopressin 1b receptor (Avpr1b) and oxytocin (Oxtr) receptors^{130,131}, and stimulation of these receptors also modulates synaptic responses in area CA2¹⁰⁶. The Avpr1b receptor is highly restricted in its expression to CA2 pyramidal neurons¹³⁰. Application of specific Avpr1b agonists to rat and mouse brain slices induced synaptic potentiation of excitatory currents selectively in CA2, but not in CA1¹⁰⁶. These “social” neuropeptides vasopressin and oxytocin both enhance social cognition¹³². Consistent with reports of Oxtr expression in areas CA2 and CA3 of the hippocampus, a specific oxytocin receptor agonist also enhanced excitatory synaptic responses in CA2 and CA3, but not in CA1^{106,131}. Agonist stimulation of $\text{G}\alpha\text{q}$ -linked GPCRs such as Avpr1b and Oxtr increase intracellular Ca^{2+}

levels. In line with known roles for Ca^{2+} signaling in CA2 LTP (see above), Avpr1b and Oxtr agonists potentiate synaptic responses in CA2 through a Ca^{2+} -dependent mechanism similar to activity-dependent LTP in CA2 neurons of RGS14 KO mice as the effects of both agonists required synaptic stimulation during agonist treatment, NMDAR activation, postsynaptic Ca^{2+} entry, and CaMKII activity¹⁰⁶. Unlike the A1R-potentiation of LTP in CA2, these increases in synaptic strength were not mediated by PKA, suggesting that either Ca^{2+} or cAMP signaling events can modulate synaptic plasticity in CA2. Previous evidence and findings presented here indicate that RGS14 may modulate this form of potentiation^{19,40,62}.

In addition to regulating Ca^{2+} -dependent LTP signaling, RGS14 engages active G α i/o-GTP and inactive G α i1-GDP or G α i3-GDP. At least one G α i/o-coupled GPCR, specifically the A1 adenosine receptor (A1R), is highly expressed in CA2 neurons⁷⁹. Recent studies show that antagonizing A1R is the primary mechanism by which caffeine enhances cognition¹⁰⁵. A1R antagonists including caffeine have been shown to enhance LTP in hippocampal CA1 neurons^{133,134}, and Simons et al. (2012) demonstrated that oral administration of caffeine to rats potentiates synaptic transmission in CA2 neurons, but not those in area CA1¹⁰⁵. Brief application of caffeine or other, more selective A1R antagonists directly to hippocampal slices also produced long-lasting synaptic potentiation postsynaptically in CA2, indicating that caffeine enhances synaptic efficacy in CA2 through blockade of A1Rs. Similar effects on synaptic strength were only observed in CA1 at substantially higher concentrations indicating that caffeine likely enhances cognition by inducing plasticity in area CA2. The A1R-potentiation at CA2 synapses was not dependent on Ca^{2+} -activated pathways required for canonical LTP

induced high-frequency stimulation as it was unaffected by NMDAR antagonism, Ca^{2+} chelation, or inhibition of CaMKII. Rather the enhancement of synaptic responses in CA2 by A1R antagonists is mediated by cAMP-dependent activation of PKA, consistent with relieving G*ai*/o inhibitory effects on adenylyl cyclase by blockade of the linked GPCR. The RGS14:G*ai*1 signaling complex can couple to at least one Gi/o-linked receptor (α_{2A} -AR) in exogenous expression systems^{18,32}. Whether RGS14 engages A1Rs or other G*ai*/o-linked GPCRs in CA2 neurons to modulate synaptic plasticity is unknown, but is a current topic of investigation.

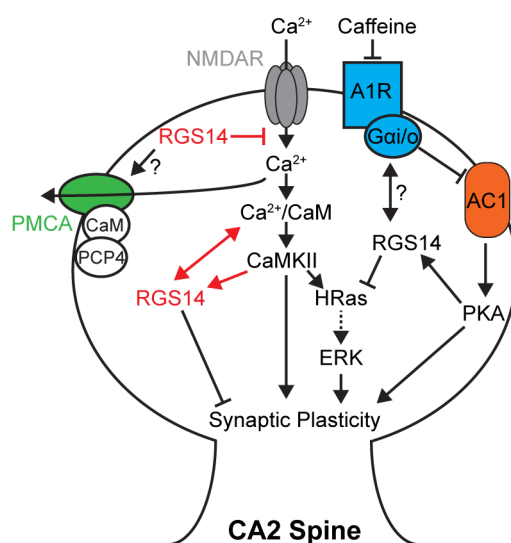


Figure 4.1 Postsynaptic signaling regulating plasticity in hippocampal CA2 pyramidal neurons. RGS14 is well positioned to modulate CA2 plasticity through its interactions with multiple binding partners. During synaptic activity sufficient to induce plasticity, Ca^{2+} enters the spine through postsynaptic NMDARs (top) where it binds CaM. Here, we have provided the first evidence that RGS14 limits NMDAR-mediated Ca^{2+} influx (Left). RGS14 also binds $\text{Ca}^{2+}/\text{CaM}$, and the functional consequences of this interaction on CA2 plasticity are currently under investigation (Left). $\text{Ca}^{2+}/\text{CaM}$ directly

activates CaMKII, which initiates downstream kinase signaling cascades (including HRas/ERK) to enhance glutamate sensitivity. We also found that RGS14 binds to and is phosphorylated by CaMKII, although the consequences of these interactions remain elusive (left). Not shown is the Ca^{2+} /CaM-mediated activation of adenylyl cyclase 1 (AC1), a Ca^{2+} -responsive cyclase enriched in CA2 pyramidal neurons. Ca^{2+} is roughly extruded from CA2 pyramidal neurons by plasma membrane Ca^{2+} ATPases (PMCA) that are regulated by PCP4 and perhaps by RGS14 (Left). RGS14, at least in part, restricts plasticity in CA2 pyramidal neurons by suppressing MAPK/ERK activity. RGS14 binds H-Ras and Raf kinases to inhibit MAPK/ERK signaling (right) While interactions with Gai strongly influence HRas/Raf binding it is unknown if RGS14 regulates G protein signaling in CA2 spines. Adenosine A1R antagonists potentiate synaptic responses in CA2 by relieving Gai/o inhibition on adenylyl cyclase and downstream PKA activation, but this form of plasticity does not require Ca^{2+} activated pathways. It is currently unknown if RGS14 modulates A1R signaling or associates with other Gai/o-linked GPCRs in area CA2. PKA phosphorylates RGS14 at two residues, but how this modification affects signaling events in hippocampal CA2 remain to be determined. (Right).

4.4 Defining mnemonic functions for CA2 and RGS14

Although the often overlooked area CA2 has only recently become a topic of investigation, strong evidence supports critical roles for CA2 in processing social^{95,106,135–137}, spatial^{25,137–140}, and temporal aspects^{95,139} of memory formation. In rodents, hippocampal CA2 neurons highly express two GPCRs closely linked to social behavior, vasopressin 1b receptors (Avpr1b) and the oxytocin receptor (Oxtr)^{130,131}. Similar to loss

of RGS14²⁵, stimulation of Avpr1b induces long-lasting potentiation specifically in CA2 pyramidal neurons¹⁰⁶. Given that the Avpr1b is largely restricted in its expression to CA2 pyramidal neurons, behavioral studies of mice lacking Avpr1b (Avpr1b KO) provide valuable insight into the function of CA2 in other behaviors. Avpr1b KO mice display normal sensorimotor function, olfactory discrimination, exploratory behavior, and spatial memory. However, Avpr1b KO mice are deficient in measures of sociability and social novelty⁹⁵, showing a lack of interest in social interaction or motivation. In tests of social novelty Avpr1b KO mice fail to distinguish between novel and familiar mice, indicating they either do not prefer the novel animal or do not remember the familiar conspecific. These studies demonstrate that Avpr1b is required for normal social interactions and memory, consistent with the role of vasopressin as a social neuropeptide.

Devito et al. (2009) investigated whether hippocampus-dependent contextual learning and memory were perturbed in Avpr1b KO mice⁹⁵. These experiments revealed that Avpr1b KO mice had a specific impairment in the temporal order of events. In the “what-where-when” memory task, Avpr1b KO mice exhibited normal performance for where in the arena they explored the objects, validating previous studies demonstrating intact spatial memory in these animals. However, Avpr1b KO mice were impaired in recognizing previously encountered objects and failed to remember the temporal order in which the objects were presented relative to wild-type littermates. In the object-trace-odor assay, Avpr1b KO mice could associate odors with objects and demonstrated intact relational memory, but they failed to discriminate an odor associated with a previously encountered object over a temporal delay. Taken together, these studies suggest that the Avpr1b, likely in CA2, is required for the proper temporal association of episodic events.

In addition to social recognition, the appropriate expression of aggression is another key component of mammalian social behavior. Male and female Avpr1b KO mice display reduced territorial and maternal aggression, and specific pharmacological antagonism of the Avpr1b mirrors this behavior¹⁴¹. Reintroduction of Avpr1b by lentiviral injection into CA2 pyramidal neurons of Avpr1b KO mice partially rescued Avpr1b expression and restored male aggression in response to intruder attacks¹⁰⁶. Additional control behavioral studies proved this effect was specific to aggression and not, for example, anxiety-like behavior. These findings demonstrate that expression of Avpr1b in CA2 underlies the proper expression of aggressive behaviors in rodents. Additional behavioral analyses will be required to discern additional facets of behavior mediated by Avpr1b in CA2 and if RGS14 contributes to these behaviors.

In further support of a key role for CA2 in social behaviors, a recent study found that CA2 is necessary for social memory¹³⁶. Silencing of CA2 pyramidal neurons by expression of tetanus neurotoxin (TeNT) resulted in profound deficits in social memory. Although sociability remained intact, silencing CA2 resulted in animals that failed to display a preference for novel mouse over a familiar littermate indicating lack of social novelty and further that CA2 activity is required to encode social memory. The effects of CA2 silencing were specific to social recognition/memory as there were no differences in a battery of other hippocampal and non-hippocampal behaviors. Among these behaviors not affected by CA2 silencing were novel object recognition and spatial learning and memory assayed by Morris water maze, despite a trend for these mice to learn the task slower. Because loss of RGS14 in CA2 neurons results in robust plasticity correlating with enhanced performance in these tasks²⁵, we hypothesized that area CA2 functions in

spatial learning and that silencing CA2 synaptic transmission would conversely cause impairments in spatial learning and object recognition. Thus it is possible that spatial information is routed through alternative circuits when CA2 is silenced. Alternatively, the lack of effect on spatial memory function could be due to an incomplete silencing of CA2 over the entire length of the hippocampus.

Consistent with our observation of enhanced spatial learning in RGS14 KO mice²⁵, *in vivo* electrophysiology recordings in behaving rodents have shown that CA2 pyramidal neurons function as place cells^{137–140}, neurons which support a cognitive map of space by preferentially firing in distinct areas of a spatial environment referred to as a place field. In contrast to place cells in CA3/CA1, CA2 place cell ensembles display differences in population coding and remap to a greater extent over time than between spatial contexts¹³⁹. This finding is consistent with previous reports that area CA2 plays an important role in the temporal order of events⁹⁵. Using *in vivo* recordings from single neurons, a recent study has shown that CA2 place fields globally remap in response to the introduction of another animal (either familiar or novel) or a novel object¹³⁷. Therefore, CA2 neurons are able to update spatial representations based on social or contextual alterations as well as over time. Most recently, Kay et al. (2016) have shown that a specific population of CA2 neurons encode spatial location during immobility and sleep¹⁴⁰. Further, this signal for space is part of a hippocampus-wide network activity newly identified in this study. Together, these studies indicate that CA2 plays a critical role in processing spatial information but does so in a manner distinct from those observed in CA3/CA1.

In summary, these initial findings suggest that RGS14-expressing neurons of hippocampal area CA2 encode social^{95,106,135–137}, spatial^{25,137–140}, and temporal aspects^{95,139} of episodic memory. Future studies are necessary to determine the precise mnemonic functions of hippocampal CA2 and assess the contribution of RGS14 (and other genes enriched in CA2) to these processes. The distinct molecular makeup of CA2 pyramidal neurons provides promising avenues to study CA2 function using genetic-based targeting approaches. Selective deletion of genes in CA2 and manipulation of CA2 activity *in vivo*, e.g. employing optogenetic stimulation or DREADDs, in combination with *in vivo* recordings during behavior, will offer great insight into the type(s) of information processed by this region and its function in learning and memory. Understanding the normal functions of CA2 will also provide insight into the contribution of CA2 dysfunction in human neurological disorders.

4.5 Roles for RGS14 and CA2 in human behavior and disease

In humans and non-human primates, RGS14 is expressed abundantly in CA2 hippocampal neurons much like in rodents^{133,134}, and hippocampal dysfunction characterized by cognitive impairments is a central feature of numerous human neuropsychiatric diseases. Early evidence demonstrating that hippocampal CA2 is a distinct hippocampal subfield, rather than an intermingling of CA3 and CA1, originated from reports that CA2 neurons display unique pathology in some human neurological conditions and are resistant to neuronal injury in others^{62,107–109,135}. In the normal aged human and Alzheimer's disease (AD) patient brain, area CA2 is resistant to tau neurofibrillary tangle formation, a hallmark of AD¹³⁶. Conversely, neurofibrillary pathology is selectively observed in the CA2 subfield in rare cases of specific human

tauopathies. Within the hippocampus, autopsy tissue from human schizophrenic patients feature a prominent and selective loss of parvalbumin immunoreactivity¹⁰⁷ (a molecular marker for a subtype of inhibitory interneurons), decreased size of pyramidal cells¹³⁷, and reduced AMPA receptor binding in the CA2 subregion of the hippocampus¹³⁸. The age-dependent loss of parvalbumin immunoreactivity in human schizophrenic patients was recently shown to occur in the Df(16)A+/- mouse model of the 22q11.2 microdeletion¹⁴⁸, a genetic risk factor for developing several neuropsychiatric disorders, namely schizophrenia, in humans. As would be predicted by the loss of interneurons, CA2 pyramidal neurons displayed age-dependent reduction in feedforward inhibition as well as intrinsic neuron properties that greatly diminish the ability of CA2 to fire action potentials. Finally, these mice displayed impaired social memory, and the authors hypothesized this was due to decreased CA2 synaptic output¹⁴⁸. How these CA2 specific alterations contribute to the symptoms of schizophrenia are currently unknown, but further study of the mnemonic functions of CA2 could provide great insight into its role in the disease etiology.

Hippocampal CA2 also displays resilience in response to neuronal insults. Unlike surrounding hippocampal subfields, CA2 survives in several models of hypoxia/ischemia^{108,109}, and CA2 differs from CA1/3 in that no detectable neuronal loss is observed in human subjects following blunt head injury¹³⁹. Perhaps the strongest evidence of CA2's resilience comes from studies demonstrating the diminished susceptibility to seizure-induced cell loss in human epileptic patients and experimental models of temporal lobe epilepsy^{135,140}.

What properties bestow this robust neuroprotective phenotype and what is the significance of selectively sparing CA2? As discussed above, the unique molecular composition of area CA2 and its resistance to LTP induction, due to RGS14 and robust calcium handling properties, are proposed to underlie the distinctive pathology and resistance to cell death. Aberrant hyperphosphorylation of tau protein is a central mechanism in neurofibrillary tangle degeneration, and the lack of tau pathology in CA2 may be attributed to the enrichment of phosphatases such as STEP (striatal-enriched protein tyrosine phosphatase), which might impede tau hyperphosphorylation. The enrichment of the well-known neuroprotective agent neutrophin-3 in CA2 may also confer resistance to damage in ischemic events as it has been found to protect cultured hippocampal neurons from these insults^{141,142}.

Consistent with its resistance to damage to hypoxia and ischemia, CA2 neurons also are resistant to cell loss following epileptic seizures^{110,135,140,143,144}, and several signaling proteins enriched in hippocampal CA2, possibly including RGS14, may act in concert to confer protection. The high expression levels of Ca²⁺ buffering proteins and active Ca²⁺ handling processes in CA2 pyramidal neurons are believed to reduce the seizure-induced activation of Ca²⁺-dependent apoptotic pathways resulting in limited cell death¹⁴⁵. RGS14 may contribute to the unique Ca²⁺ buffering and extrusion properties in CA2 neurons by its binding Ca²⁺/CaM, similar to PCP4/Pep-19. Adenosine is known to have anticonvulsant effects, and the preferential sparing of CA2 in models of temporal lobe epilepsy have also been attributed to activation of A1R by adenosine released during seizures^{73,146}. RGS14 may contribute to adenosine's actions in CA2 by engaging G α i signaling pathways downstream of A1R. Amigo2, also highly enriched in and restricted

in its expression to area CA2¹⁴⁷, may contribute to the neuroprotection of pyramidal neurons similar to its capacity to promote neuronal survival in response to Ca²⁺ signals in the cerebellum¹⁴⁸. Moreover, decreased levels of ERK phosphorylation observed in CA2 compared to CA1 after experimentally induced seizure may be a critical component of CA2 survival strategy. RGS14 binding of active H-Ras to suppress ERK signaling may contribute to the reduced ERK activation in this case. How RGS14 engages these proteins and pathways to contribute to CA2 stability and survival is currently unknown, but ongoing studies are assessing the functional role of RGS14 in seizure activity and cell survival.

A deep literature on neuronal plasticity shows that brain regions exhibiting synaptic plasticity do so at the expense of increased susceptibility to damage, indicating a trade-off between these two features. Consistent with this idea, the complement of signaling proteins that uniquely limit plasticity in area CA2, most notably RGS14, may serve an adaptive mechanism to ensure this region's survival from neuronal injury. This hypothesis would suggest that although CA2 may store memories under specific circumstances, the information encoded within this region serve a critical function that mandates its survival. We expect that area CA2 will be implicated in additional human neuropsychiatric conditions as mnemonic functions of this region are further defined. The recently described role of area CA2 in social memory^{95,106,135–137,148} suggests that dysfunction in CA2 could be a central feature in human disorders characterized by impaired social information processing, such as Autism Spectrum Disorders, Rett Syndrome, and schizophrenia.

Based on these findings, we hypothesize that RGS14 restricts CA2 plasticity to allow selective learning and memory encoding under specific conditions, and that its presence is required to discriminate which forms of learning and memory to encode. Of note, microarray data confirms that RGS14 is highly expressed in nonhuman primate and human CA2^{133,134}, and this conserved expression pattern could suggest that RGS14 also suppresses LTP in primate CA2. If RGS14 indeed plays a pivotal role in selective memory storage, then genetic mutations that eliminate RGS14 function could either enhance cognitive function or, alternatively, be maladaptive by potentially allowing indiscriminant memory storage or cognitive inflexibility. Consistent with this notion, RGS14 was recently identified as a candidate gene involved in fear learning suggesting it could have a potential role in human posttraumatic stress disorder (PTSD)¹¹¹. Studies are in progress to define a functional role for RGS14 in these behaviors and associated disorders.

4.6 RGS14: more than just a suppressor of learning and memory?

While RGS14 expression is highest in hippocampal CA2, RGS14 protein is also expressed in other regions of the mouse brain, providing possible insight to its other functions in brain⁴². In the hippocampus, RGS14 expression increases during postnatal development in fasciola cinerea (FC) – the region located at the midline of the brain neighboring CA1. While the specific functions of the FC are currently unknown, the molecular markers used to identify hippocampal CA2 are curiously also expressed in the FC. A recent study suggests that area CA2 and FC comprise one region in the anterior hippocampus, which becomes separated in the posterior segment of the hippocampus into the medial FC and lateral CA2 by the interjection of CA1¹⁴⁷. Spurious immunolabeling of

RGS14 also is observed in CA1 neurons although its expression is not consistently detected in this region. RGS14 functions in regions of adult brain outside area CA2 currently are unknown.

Outside the hippocampus, RGS14 expression is also upregulated during postnatal development in pyramidal neurons of the anterior olfactory nucleus (AON) and piriform cortex. These brain regions are included in a collective group of brain structures referred to as the primary olfactory cortex. In mammals, the olfactory bulb initially processes odorants and sends direct projections to the primary olfactory cortex. The primary olfactory cortex processes input provided by the olfactory bulb and associates odorants with episodic events¹⁰⁴. RGS14 protein is found in neurons with pyramidal morphology in the orbital and entorhinal cortices, both of which receive input from primary olfactory cortex. Thus, RGS14 is well positioned to modulate olfactory processing in mice and the association of these stimuli with specific memories. Olfaction is an essential component of mammalian social behavior, and ongoing experiments are assessing the role of RGS14 in social learning and odorant association.

In contrast to our findings that RGS14 naturally inhibits novel object recognition⁷, one study reported that RGS14 enhances object recognition memory when introduced as recombinant protein into other brain areas¹⁵¹. RGS14 is not natively expressed in rodent visual cortex⁴⁴. However, Lopez-Aranda et al. (2009) reported that ectopic over expression of RGS14 in this region in rats promotes the conversion of short-term object recognition memory to stable, long-term memory. This puzzling finding that RGS14 enhances recognition memory differs from our work demonstrating that native RGS14 naturally inhibits novel objection recognition memory in CA2 neurons⁷. It is possible that

unnatural expression of RGS14 modulates this form of memory by perturbing G protein, H-Ras/MAPK, and/or Ca^{2+} signaling leading to augmentation of plasticity in visual cortex neurons. How RGS14 alters the activity of neurons in visual cortex and the cellular mechanisms underlying this effect are currently unknown.

Despite these findings with ectopically expressed RGS14, the question still remains whether native RGS14 suppresses activity-dependent plasticity (i.e. LTP) in neuronal populations outside of hippocampal CA2. One striking observation is that RGS14 protein subcellular localization differs dramatically between CA2 pyramidal neurons and other regions, despite consistent labeling of neurons with pyramidal morphology⁴². In CA2 pyramidal neurons RGS14 immunoreactivity intensely labels the postsynaptic dendrites and spines; however, RGS14 protein is localized to the soma and apical dendrites in other brain regions during development⁴². The lower levels of RGS14 immunoreactivity and differences in subcellular localization suggest RGS14 may serve distinct functions in areas outside of CA2 during this critical period of development.

4.7 Summary and Perspectives

The findings discussed here highlight the defined roles of RGS14 in cell signaling, hippocampus physiology, and animal behavior. As with other members of the RGS protein family, RGS14 negatively regulates canonical GPCR/G protein signaling by serving as a GAP for $\text{G}\alpha$ -GTP subunits through its conserved RGS domain. The unusual domain structure of RGS14 allows it to bridge these conventional G protein pathways with unconventional G protein signaling through its GPR motif as well as MAPK signaling by virtue of tandem RBDs. RGS14 is able to functionally integrate these pathways in cells to impact specific downstream signaling events, and RGS14 function is

subject to complex regulation by binding partners and other factors. We reviewed the defined physiological role of RGS14 as an inherent factor restricting plasticity in the peculiar CA2 pyramidal neurons within the hippocampus. These recently distinguished neurons were historically thought to be a mere transition zone in the hippocampus, despite distinct molecular composition and differential pathology in neurological conditions. However, mice lacking RGS14 display a nascent capacity for plasticity specific to CA2 and also have enhanced spatial learning and object recognition memory. Very recent reports have linked hippocampal CA2 to additional behaviors including temporal order of events and social behavior. Future behavioral studies will identify potential roles for RGS14 in these behaviors mediated by CA2 plasticity. Further elucidating the functional significance of RGS14 expression in other brain areas and peripheral tissues should provide additional insight into this unusual RGS protein.

Still the question remains as to why a gene would exist that seemingly only functions to inhibit learning and memory. Similar to rodents, RGS14 expression levels are highest in human and non-human primate CA2^{133,134}, suggesting it may serve an evolutionarily conserved function in this hippocampal subregion. We propose that RGS14 serves as a tightly regulated filter to selectively permit memory storage in CA2 under specific conditions. Loss of RGS14 function in CA2 of humans could potentially result in enhanced cognition or, alternatively, maladaptive consequences such as indiscriminant memory encoding or runaway excitation of CA2 neurons. Moreover, RGS14 and/or CA2 dysfunction could have consequences on social information processing. Consistent with this idea, variations in the copy number of alleles for the chromosomal location containing the human RGS14 gene are clinically linked to Autism

Spectrum Disorder as well as developmental delay¹⁵². These findings underscore the importance of RGS14 and its host CA2 neurons in human cognitive function.

References

1. Hepler, J. R. & Gilman, A. G. G proteins. *Trends Biochem. Sci.* **17**, 383–387 (1992).
2. Simon, M. I., Strathmann, M. P. & Gautam, N. Diversity of G proteins in signal transduction. *Science* **252**, 802–8 (1991).
3. Hamm, H. E. & Gilchrist, A. Heterotrimeric G proteins. *Curr. Opin. Cell Biol.* **8**, 189–196 (1996).
4. Wettschureck, N. & Offermanns, S. Mammalian G proteins and their cell type specific functions. *Physiol. Rev.* **85**, 1159–204 (2005).
5. Hepler, J. R. Emerging roles for RGS proteins in cell signalling. *Trends Pharmacol. Sci.* **20**, 376–382 (1999).
6. Hollinger, S. & Hepler, J. R. Cellular regulation of RGS proteins: modulators and integrators of G protein signaling. *Pharmacol. Rev.* **54**, 527–59 (2002).
7. Neitzel, K. L. & Hepler, J. R. Cellular mechanisms that determine selective RGS protein regulation of G protein-coupled receptor signaling. *Semin. Cell Dev. Biol.* **17**, 383–389 (2006).
8. Abramow-Newerly, M., Roy, A. A., Nunn, C. & Chidiac, P. RGS proteins have a signalling complex: Interactions between RGS proteins and GPCRs, effectors, and auxiliary proteins. *Cell. Signal.* **18**, 579–591 (2006).
9. McCoy, K. L. & Hepler, J. R. Regulators of G protein signaling proteins as central components of G protein-coupled receptor signaling complexes. *Prog. Mol. Biol. Transl. Sci.* **86**, 49–74 (2009).
10. Willars, G. B. Mammalian RGS proteins: multifunctional regulators of cellular signalling. *Semin. Cell Dev. Biol.* **17**, 363–76 (2006).
11. Ross, E. M. & Wilkie, T. M. GTPase-activating proteins for heterotrimeric G proteins: regulators of G protein signaling (RGS) and RGS-like proteins. *Annu. Rev. Biochem.* **69**, 795–827 (2000).
12. Snow, B. E., Antonio, L., Suggs, S., Gutstein, H. B. & Siderovski, D. P. Molecular cloning and expression analysis of rat Rgs12 and Rgs14. *Biochem. Biophys. Res. Commun.* **233**, 770–7 (1997).
13. Traver, S. *et al.* RGS14 is a novel Rap effector that preferentially regulates the GTPase activity of G α h. *Biochem. J.* **350 Pt 1**, 19–29 (2000).
14. Hollinger, S., Taylor, J. B., Goldman, E. H. & Hepler, J. R. RGS14 is a bifunctional regulator of G α h α i/o activity that exists in multiple populations in brain. *J. Neurochem.* **79**, 941–9 (2001).
15. Cho, H., Kozasa, T., Takekoshi, K., De Gunzburg, J. & Kehrl, J. H. RGS14, a GTPase-activating protein for G α h, attenuates G α h- and G α 13-mediated signaling pathways. *Mol. Pharmacol.* **58**, 569–76 (2000).
16. Kiel, C. *et al.* Recognizing and Defining True Ras Binding Domains II: In Silico Prediction Based on Homology Modelling and Energy Calculations. *J. Mol. Biol.* **348**, 759–775 (2005).
17. Shu, F., Ramineni, S. & Hepler, J. R. RGS14 is a multifunctional scaffold that integrates G protein and Ras/Raf MAPkinase signalling pathways. *Cell. Signal.* **22**, 366–76 (2010).
18. Vellano, C. P., Brown, N. E., Blumer, J. B. & Hepler, J. R. Assembly and function of the regulator of G protein signaling 14 (RGS14)·H-Ras signaling complex in

- live cells are regulated by Gai1 and Gai-linked G protein-coupled receptors. *J. Biol. Chem.* **288**, 3620–31 (2013).
19. Evans, P. R. & Hepler, J. R. Regulator of G protein Signaling 14 (RGS14) interacts with calmodulin (CaM) in a calcium-dependent manner. in *Society for Neuroscience* 44.04 (2012).
 20. Kimple, R. J. *et al.* RGS12 and RGS14 GoLoco Motifs Are G iInteraction Sites with Guanine Nucleotide Dissociation Inhibitor Activity. *J. Biol. Chem.* **276**, 29275–29281 (2001).
 21. Mittal, V. & Linder, M. E. The RGS14 GoLoco domain discriminates among Galphai isoforms. *J. Biol. Chem.* **279**, 46772–8 (2004).
 22. Shu, F., Ramineni, S., Amyot, W. & Hepler, J. R. Selective interactions between Gi alpha1 and Gi alpha3 and the GoLoco/GPR domain of RGS14 influence its dynamic subcellular localization. *Cell. Signal.* **19**, 163–76 (2007).
 23. Vellano, C. P. *et al.* Activation of the regulator of G protein signaling 14-Gai1-GDP signaling complex is regulated by resistance to inhibitors of cholinesterase-8A. *Biochemistry* **50**, 752–62 (2011).
 24. Vellano, C. P., Lee, S. E., Dudek, S. M. & Hepler, J. R. RGS14 at the interface of hippocampal signaling and synaptic plasticity. *Trends Pharmacol. Sci.* **32**, 666–674 (2011).
 25. Lee, S. E. *et al.* RGS14 is a natural suppressor of both synaptic plasticity in CA2 neurons and hippocampal-based learning and memory. *Proc. Natl. Acad. Sci. U. S. A.* **107**, 16994–8 (2010).
 26. Zhao, P., Nunn, C., Ramineni, S., Hepler, J. R. & Chidiac, P. The Ras-binding domain region of RGS14 regulates its functional interactions with heterotrimeric G proteins. *J. Cell. Biochem.* **114**, 1414–1423 (2013).
 27. Hepler, J. R., Cladman, W., Ramineni, S., Hollinger, S. & Chidiac, P. Novel activity of RGS14 on Goalpha and Gialpha nucleotide binding and hydrolysis distinct from its RGS domain and GDI activity. *Biochemistry* **44**, 5495–502 (2005).
 28. Blumer, J. B. & Lanier, S. M. Activators of G Protein Signaling Exhibit Broad Functionality and Define a Distinct Core Signaling Triad. *Mol. Pharmacol.* **85**, 388–396 (2014).
 29. Sato, M., Blumer, J. B., Simon, V. & Lanier, S. M. ACCESSORY PROTEINS FOR G PROTEINS: Partners in Signaling. *Annu. Rev. Pharmacol. Toxicol.* **46**, 151–187 (2006).
 30. Willard, F. S., Kimple, R. J. & Siderovski, D. P. Return of the GDI: The GoLoco Motif in Cell Division. *Annu. Rev. Biochem.* **73**, 925–951 (2004).
 31. Hampoelz, B. & Knoblich, J. A. Heterotrimeric G Proteins: New Tricks for an Old Dog. *Cell* **119**, 453–456 (2004).
 32. Vellano, C. P., Maher, E. M., Hepler, J. R. & Blumer, J. B. G protein-coupled receptors and resistance to inhibitors of cholinesterase-8A (Ric-8A) both regulate the regulator of g protein signaling 14 RGS14·Gai1 complex in live cells. *J. Biol. Chem.* **286**, 38659–69 (2011).
 33. Cho, H., Kim, D.-U. & Kehrl, J. H. RGS14 is a centrosomal and nuclear cytoplasmic shuttling protein that traffics to promyelocytic leukemia nuclear bodies following heat shock. *J. Biol. Chem.* **280**, 805–14 (2005).

34. Tall, G. G., Krumins, A. M. & Gilman, A. G. Mammalian Ric-8A (Synembryn) Is a Heterotrimeric Galpha Protein Guanine Nucleotide Exchange Factor. *J. Biol. Chem.* **278**, 8356–8362 (2003).
35. Tall, G. G. & Gilman, A. G. Resistance to inhibitors of cholinesterase 8A catalyzes release of Galphai-GTP and nuclear mitotic apparatus protein (NuMA) from NuMA/LGN/Galphai-GDP complexes. *Proc. Natl. Acad. Sci. U. S. A.* **102**, 16584–9 (2005).
36. Thomas, C. J., Tall, G. G., Adhikari, A. & Sprang, S. R. Ric-8A Catalyzes Guanine Nucleotide Exchange on G α i Bound to the GPR/GoLoco Exchange Inhibitor AGS3. *J. Biol. Chem.* **283**, 23150–23160 (2008).
37. Oner, S. S. *et al.* Regulation of the AGS3·G α i signaling complex by a seven-transmembrane span receptor. *J. Biol. Chem.* **285**, 33949–58 (2010).
38. Oner, S. S., Maher, E. M., Breton, B., Bouvier, M. & Blumer, J. B. Receptor-regulated interaction of activator of G-protein signaling-4 and Galphai. *J. Biol. Chem.* **285**, 20588–94 (2010).
39. Hollinger, S. & Hepler, J. R. Methods for measuring RGS protein phosphorylation by G protein-regulated kinases. *Methods Mol. Biol.* **237**, 205–19 (2004).
40. Hollinger, S., Ramineni, S. & Hepler, J. R. Phosphorylation of RGS14 by protein kinase a potentiates its activity toward G $\beta\gamma$. *Biochemistry* **42**, 811–819 (2003).
41. Hornbeck, P. V. *et al.* PhosphoSitePlus: a comprehensive resource for investigating the structure and function of experimentally determined post-translational modifications in man and mouse. *Nucleic Acids Res.* **40**, D261–D270 (2012).
42. Evans, P. R., Lee, S. E., Smith, Y. & Hepler, J. R. Postnatal developmental expression of regulator of G protein signaling 14 (RGS14) in the mouse brain. *J. Comp. Neurol.* **522**, 186–203 (2014).
43. Larminie, C. *et al.* Selective expression of regulators of G-protein signaling (RGS) in the human central nervous system. *Mol. Brain Res.* **122**, 24–34 (2004).
44. López-Aranda, M. F., Acevedo, M. J., Carballo, F. J., Gutiérrez, A. & Khan, Z. U. Localization of the GoLoco motif carrier regulator of G-protein signalling 12 and 14 proteins in monkey and rat brain. *Eur. J. Neurosci.* **23**, 2971–2982 (2006).
45. Grafstein-Dunn, E., Young, K. H., Cockett, M. I. & Khawaja, X. Z. Regional distribution of regulators of G-protein signaling (RGS) 1, 2, 13, 14, 16, and GAIP messenger ribonucleic acids by in situ hybridization in rat brain. *Mol. Brain Res.* **88**, 113–123 (2001).
46. Corkin, S. What's new with the amnesic patient H.M.? *Nat. Rev. Neurosci.* **3**, 153–160 (2002).
47. Whitlock, J. R., Heynen, A. J., Shuler, M. G. & Bear, M. F. Learning induces long-term potentiation in the hippocampus. *Science* **313**, 1093–7 (2006).
48. Gruart, A., Muñoz, M. D. & Delgado-García, J. M. Involvement of the CA3-CA1 Synapse in the Acquisition of Associative Learning in Behaving Mice. *J. Neurosci.* **26**, 1077–1087 (2006).
49. Grant, S. G. N. & Silva, A. J. Targeting learning. *Trends Neurosci.* **17**, 71–75 (1994).
50. van Strien, N. M., Cappaert, N. L. M. & Witter, M. P. The anatomy of memory: an interactive overview of the parahippocampal-hippocampal network. *Nat. Rev.*

- Neurosci.* **10**, 272–82 (2009).
51. Kerchner, G. A. & Nicoll, R. A. Silent synapses and the emergence of a postsynaptic mechanism for LTP. *Nat. Rev. Neurosci.* **9**, 813–825 (2008).
 52. Murakoshi, H. & Yasuda, R. Postsynaptic signaling during plasticity of dendritic spines. *Trends Neurosci.* **35**, 135–143 (2012).
 53. Xia, Z. & Storm, D. R. The role of calmodulin as a signal integrator for synaptic plasticity. *Nat. Rev. Neurosci.* **6**, 267–76 (2005).
 54. Zhu, J. J., Qin, Y., Zhao, M., Van Aelst, L. & Malinow, R. Ras and Rap Control AMPA Receptor Trafficking during Synaptic Plasticity. *Cell* **110**, 443–455 (2002).
 55. Thomas, G. M. & Huganir, R. L. MAPK cascade signalling and synaptic plasticity. *Nat. Rev. Neurosci.* **5**, 173–183 (2004).
 56. Harvey, C. D., Yasuda, R., Zhong, H. & Svoboda, K. The spread of Ras activity triggered by activation of a single dendritic spine. *Science* **321**, 136–40 (2008).
 57. Lynch, G., Larson, J., Kelso, S., Barrionuevo, G. & Schottler, F. Intracellular injections of EGTA block induction of hippocampal long-term potentiation. *Nature* **305**, 719–721 (1983).
 58. Lisman, J., Yasuda, R. & Raghavachari, S. Mechanisms of CaMKII action in long-term potentiation. *Nat. Rev. Neurosci.* **13**, 169–82 (2012).
 59. Patterson, M. A., Szatmari, E. M. & Yasuda, R. AMPA receptors are exocytosed in stimulated spines and adjacent dendrites in a Ras-ERK-dependent manner during long-term potentiation. *Proc. Natl. Acad. Sci.* **107**, 15951–15956 (2010).
 60. N6, R. L. de. Studies on the structure of the cerebral cortex. II. Continuation of the study of the ammonic system. *J. für Psychol. und Neurol.* (1934).
 61. Jones, M. W. & McHugh, T. J. Updating hippocampal representations: CA2 joins the circuit. *Trends Neurosci.* **34**, 526–535 (2011).
 62. Caruana, D. a., Alexander, G. M. & Dudek, S. M. New insights into the regulation of synaptic plasticity from an unexpected place: Hippocampal area CA2. *Learn. Mem.* **19**, 391–400 (2012).
 63. Zhao, M., Choi, Y.-S., Obrietan, K. & Dudek, S. M. Synaptic plasticity (and the lack thereof) in hippocampal CA2 neurons. *J. Neurosci.* **27**, 12025–12032 (2007).
 64. Pizzorusso, T. *et al.* Reactivation of ocular dominance plasticity in the adult visual cortex. *Science* **298**, 1248–51 (2002).
 65. Brückner, G., Grosche, J., Hartlage-Rübsamen, M., Schmidt, S. & Schachner, M. Region and lamina-specific distribution of extracellular matrix proteoglycans, hyaluronan and tenascin-R in the mouse hippocampal formation. *J. Chem. Neuroanat.* **26**, 37–50 (2003).
 66. Yamamoto, M., Marshall, P., Hemmendinger, L. M., Boyer, A. B. & Caviness, V. S. Distribution of glucuronic acid-and-sulfate-containing glycoproteins in the central nervous system of the adult mouse. *Neurosci. Res.* **5**, 273–98 (1988).
 67. Lein, E. S., Callaway, E. M., Albright, T. D. & Gage, F. H. Redefining the boundaries of the hippocampal CA2 subfield in the mouse using gene expression and 3-dimensional reconstruction. *J. Comp. Neurol.* **485**, 1–10 (2005).
 68. Lein, E. S. *et al.* Genome-wide atlas of gene expression in the adult mouse brain. *Nature* **445**, 168–76 (2007).
 69. Willard, F. S. *et al.* Regulator of G-Protein Signaling 14 (RGS14) Is a Selective H-Ras Effector. *PLoS One* **4**, e4884 (2009).

70. Seress, L. *et al.* Distribution, morphological features, and synaptic connections of parvalbumin- and calbindin D_{28k}-immunoreactive neurons in the human hippocampal formation. *J. Comp. Neurol.* **337**, 208–230 (1993).
71. Leranth, C. & Ribak, C. E. Calcium-binding proteins are concentrated in the CA2 field of the monkey hippocampus: a possible key to this region's resistance to epileptic damage. *Exp. Brain Res.* **85**, (1991).
72. Simons, S. B., Escobedo, Y., Yasuda, R. & Dudek, S. M. Regional differences in hippocampal calcium handling provide a cellular mechanism for limiting plasticity. *Proc. Natl. Acad. Sci. U. S. A.* **106**, 14080–4 (2009).
73. Kohara, K. *et al.* Cell type-specific genetic and optogenetic tools reveal hippocampal CA2 circuits. *Nat. Neurosci.* **17**, 269–79 (2014).
74. Maglóczy, Z., Acsády, L. & Freund, T. F. Principal cells are the postsynaptic targets of supramammillary afferents in the hippocampus of the rat. *Hippocampus* **4**, 322–334 (1994).
75. Chevaleyre, V. & Siegelbaum, S. A. Strong CA2 pyramidal neuron synapses define a powerful disinaptic cortico-hippocampal loop. *Neuron* **66**, 560–72 (2010).
76. Cui, Z., Gerfen, C. R. & Young, W. S. Hypothalamic and other connections with dorsal CA2 area of the mouse hippocampus. *J. Comp. Neurol.* **521**, 1844–1866 (2013).
77. Haglund, L., Swanson, L. W. & Köhler, C. The projection of the supramammillary nucleus to the hippocampal formation: An immunohistochemical and anterograde transport study with the lectin PHA-L in the rat. *J. Comp. Neurol.* **229**, 171–185 (1984).
78. Vertes, R. P. PHA-L analysis of projections from the supramammillary nucleus in the rat. *J. Comp. Neurol.* **326**, 595–622 (1992).
79. Ochiishi, T. *et al.* High level of adenosine A1 receptor-like immunoreactivity in the CA2/CA3a region of the adult rat hippocampus. *Neuroscience* **93**, 955–967 (1999).
80. Kiss, J., Csáki, Á., Bokor, H., Shanabrough, M. & Leranth, C. The supramammillo-hippocampal and supramammillo-septal glutamatergic/aspartatergic projections in the rat: a combined [3H]d-aspartate autoradiographic and immunohistochemical study. *Neuroscience* **97**, 657–669 (2000).
81. Rowland, D. C. *et al.* Transgenically Targeted Rabies Virus Demonstrates a Major Monosynaptic Projection from Hippocampal Area CA2 to Medial Entorhinal Layer II Neurons. *J. Neurosci.* **33**, 14889–14898 (2013).
82. Llorens-Martín, M., Jurado-Arjona, J., Avila, J. & Hernández, F. Novel connection between newborn granule neurons and the hippocampal CA2 field. *Exp. Neurol.* **263**, 285–292 (2015).
83. Buralossi, A. *et al.* Microcircuits of Functionally Identified Neurons in the Rat Medial Entorhinal Cortex. *Neuron* **70**, 773–786 (2011).
84. Couey, J. J. *et al.* Recurrent inhibitory circuitry as a mechanism for grid formation. *Nat. Neurosci.* **16**, 318–324 (2013).
85. Schmidt-Hieber, C. & Häusser, M. Cellular mechanisms of spatial navigation in the medial entorhinal cortex. *Nat. Neurosci.* **16**, 325–331 (2013).

86. Evans, P. R., Dudek, S. M. & Hepler, J. R. Regulator of G Protein Signaling 14: A Molecular Brake on Synaptic Plasticity Linked to Learning and Memory. *Prog. Mol. Biol. Transl. Sci.* **133**, 169–206 (2015).
87. Dudek, S. M., Alexander, G. M. & Farris, S. Rediscovering area CA2: unique properties and functions. *Nat. Rev. Neurosci.* **17**, 89–102 (2016).
88. Vellano, C. P., Brown, N. E., Blumer, J. B. & Hepler, J. R. Assembly and Function of the Regulator of G protein Signaling 14 (RGS14) H-Ras Signaling Complex in Live Cells Are Regulated by G_{i1} and G_i-linked G Protein-coupled Receptors. *J. Biol. Chem.* **288**, 3620–3631 (2013).
89. Snow, B. E., Antonio, L., Suggs, S., Gutstein, H. B. & Siderovski, D. P. Molecular Cloning and Expression Analysis of RatRgs12 and Rgs14. *Biochem. Biophys. Res. Commun.* **233**, 770–777 (1997).
90. Bernstein, L. S. *et al.* RGS2 binds directly and selectively to the M1 muscarinic acetylcholine receptor third intracellular loop to modulate Gq/11 α signaling. *J. Biol. Chem.* **279**, 21248–56 (2004).
91. Kimple, A. J., Bosch, D. E., Giguere, P. M. & Siderovski, D. P. Regulators of G-Protein Signaling and Their G Substrates: Promises and Challenges in Their Use as Drug Discovery Targets. *Pharmacol. Rev.* **63**, 728–749 (2011).
92. Mural, R. J. *et al.* A comparison of whole-genome shotgun-derived mouse chromosome 16 and the human genome. *Science* **296**, 1661–71 (2002).
93. Holmseth, S. *et al.* The Density of EAAC1 (EAAT3) Glutamate Transporters Expressed by Neurons in the Mammalian CNS. *J. Neurosci.* **32**, 6000–6013 (2012).
94. Manning, C. F. *et al.* Benefits and Pitfalls of Secondary Antibodies: Why Choosing the Right Secondary Is of Primary Importance. *PLoS One* **7**, e38313 (2012).
95. DeVito, L. M. *et al.* Vasopressin 1b Receptor Knock-Out Impairs Memory for Temporal Order. *J. Neurosci.* **29**, 2676–2683 (2009).
96. Wilson, D. A. & Rennaker, R. L. *Cortical Activity Evoked by Odors. The Neurobiology of Olfaction* (2010).
97. Wilson, D. A. & Sullivan, R. M. Cortical Processing of Odor Objects. *Neuron* **72**, 506–519 (2011).
98. Fiala, J. C., Feinberg, M., Popov, V. & Harris, K. M. Synaptogenesis via dendritic filopodia in developing hippocampal area CA1. *J. Neurosci.* **18**, 8900–11 (1998).
99. Scorza, C. A. *et al.* Morphological and electrophysiological properties of pyramidal-like neurons in the stratum oriens of Cornu ammonis 1 and Cornu ammonis 2 area of *Proechimys*. *Neuroscience* **177**, 252–268 (2011).
100. Benes, F. M., Kwok, E. W., Vincent, S. L. & Todtenkopf, M. S. A reduction of nonpyramidal cells in sector CA2 of schizophrenics and manic depressives. *Biol. Psychiatry* **44**, 88–97 (1998).
101. Kirino, T. Delayed neuronal death in the gerbil hippocampus following ischemia. *Brain Res.* **239**, 57–69 (1982).
102. Sadowski, M. *et al.* Pattern of neuronal loss in the rat hippocampus following experimental cardiac arrest-induced ischemia. *J. Neurol. Sci.* **168**, 13–20 (1999).
103. Sloviter, R. S. Permanently altered hippocampal structure, excitability, and inhibition after experimental status epilepticus in the rat: The ?dormant basket

- cell? hypothesis and its possible relevance to temporal lobe epilepsy. *Hippocampus* **1**, 41–66 (1991).
104. Parker, C. C., Sokoloff, G., Cheng, R. & Palmer, A. A. Genome-Wide Association for Fear Conditioning in an Advanced Intercross Mouse Line. *Behav. Genet.* **42**, 437–448 (2012).
 105. Simons, S. B., Caruana, D. A., Zhao, M. & Dudek, S. M. Caffeine-induced synaptic potentiation in hippocampal CA2 neurons. *Nat. Neurosci.* **15**, 23–5 (2012).
 106. Pagani, J. H. *et al.* Role of the vasopressin 1b receptor in rodent aggressive behavior and synaptic plasticity in hippocampal area CA2. *Mol. Psychiatry* **20**, 490–9 (2015).
 107. Carstens, K. E., Phillips, M. L., Pozzo-Miller, L., Weinberg, R. J. & Dudek, S. M. Perineuronal Nets Suppress Plasticity of Excitatory Synapses on CA2 Pyramidal Neurons. *J. Neurosci.* **36**, 6312–20 (2016).
 108. Brown, N. E. *et al.* Integration of G Protein α ($G\alpha$) Signaling by the Regulator of G Protein Signaling 14 (RGS14). *J. Biol. Chem.* **290**, 9037–9049 (2015).
 109. Zhou, Y. *et al.* Identification of the Calmodulin Binding Domain of Connexin 43. *J. Biol. Chem.* **282**, 35005–35017 (2007).
 110. Vellano, C. P., Maher, E. M., Hepler, J. R. & Blumer, J. B. G protein-coupled receptors and resistance to inhibitors of cholinesterase-8A (Ric-8A) both regulate the regulator of G protein signaling 14 (RGS14)??G?? i1 complex in live cells. *J. Biol. Chem.* **286**, 38659–38669 (2011).
 111. Xu, P., Duong, D. M. & Peng, J. Systematical Optimization of Reverse-Phase Chromatography for Shotgun Proteomics. *J. Proteome Res.* **8**, 3944–3950 (2009).
 112. Huang, D. W., Sherman, B. T. & Lempicki, R. A. Bioinformatics enrichment tools: paths toward the comprehensive functional analysis of large gene lists. *Nucleic Acids Res.* **37**, 1–13 (2009).
 113. Huang, D. W., Sherman, B. T. & Lempicki, R. A. Systematic and integrative analysis of large gene lists using DAVID bioinformatics resources. *Nat. Protoc.* **4**, 44–57 (2009).
 114. Goswami, D. *et al.* Time window expansion for HDX analysis of an intrinsically disordered protein. *J. Am. Soc. Mass Spectrom.* **24**, 1584–92 (2013).
 115. Pascal, B. D. *et al.* HDX workbench: software for the analysis of H/D exchange MS data. *J. Am. Soc. Mass Spectrom.* **23**, 1512–21 (2012).
 116. Stoppini, L., Buchs, P. A. & Muller, D. A simple method for organotypic cultures of nervous tissue. *J. Neurosci. Methods* **37**, 173–82 (1991).
 117. McAllister, A. K. Biolistic transfection of neurons. *Sci. STKE* **2000**, pl1 (2000).
 118. Lee, S.-J. R., Escobedo-Lozoya, Y., Sztatmari, E. M. & Yasuda, R. Activation of CaMKII in single dendritic spines during long-term potentiation. *Nature* **458**, 299–304 (2009).
 119. Geusebroek, J. M., Cornelissen, F., Smeulders, A. W. & Geerts, H. Robust autofocusing in microscopy. *Cytometry* **39**, 1–9 (2000).
 120. Sugar, J. D., Cummings, A. W., Jacobs, B. W. & Robinson, D. B. A Free Matlab Script for Spatial Drift Correction. *Microsc. Today* **22**, 40–47 (2014).
 121. Aoyagi, Y. *et al.* A Rapid Optical Clearing Protocol Using 2,2'-Thiodiethanol for Microscopic Observation of Fixed Mouse Brain. *PLoS One* **10**, e0116280 (2015).

122. Yap, K. L. *et al.* Calmodulin target database. *J. Struct. Funct. Genomics* **1**, 8–14 (2000).
123. Matsuzaki, M., Honkura, N., Ellis-Davies, G. C. R. & Kasai, H. Structural basis of long-term potentiation in single dendritic spines. *Nature* **429**, 761–6 (2004).
124. Nishiyama, J. & Yasuda, R. Biochemical Computation for Spine Structural Plasticity. *Neuron* **87**, 63–75 (2015).
125. Abel, T. *et al.* Genetic demonstration of a role for PKA in the late phase of LTP and in hippocampus-based long-term memory. *Cell* **88**, 615–26 (1997).
126. Malenka, R. C. *et al.* An essential role for postsynaptic calmodulin and protein kinase activity in long-term potentiation. *Nature* **340**, 554–7 (1989).
127. Zhai, S., Ark, E. D., Parra-Bueno, P. & Yasuda, R. Long-distance integration of nuclear ERK signaling triggered by activation of a few dendritic spines. *Science* **342**, 1107–11 (2013).
128. San Antonio, A., Liban, K., Ikrar, T., Tsyganovskiy, E. & Xu, X. Distinct physiological and developmental properties of hippocampal CA2 subfield revealed by using anti-Purkinje cell protein 4 (PCP4) immunostaining. *J. Comp. Neurol.* **522**, 1333–1354 (2014).
129. Dityatev, A., Schachner, M. & Sonderegger, P. The dual role of the extracellular matrix in synaptic plasticity and homeostasis. *Nat. Rev. Neurosci.* **11**, 735–746 (2010).
130. Young, W. S., Li, J., Wersinger, S. R. & Palkovits, M. The vasopressin 1b receptor is prominent in the hippocampal area CA2 where it is unaffected by restraint stress or adrenalectomy. *Neuroscience* **143**, 1031–1039 (2006).
131. Pagani, J. H., Lee, H.-J. & Young, W. S. Postweaning, forebrain-specific perturbation of the oxytocin system impairs fear conditioning. *Genes, Brain Behav.* **10**, 710–719 (2011).
132. Meyer-Lindenberg, A., Domes, G., Kirsch, P. & Heinrichs, M. Oxytocin and vasopressin in the human brain: social neuropeptides for translational medicine. *Nat. Rev. Neurosci.* **12**, 524–538 (2011).
133. Arai, A. & Lynch, G. *Factors regulating the magnitude of long-term potentiation induced by theta pattern stimulation.* *Brain Research* **598**, (1992).
134. Dunwiddie, T. V & Masino, S. A. The role and regulation of adenosine in the central nervous system. *Annu. Rev. Neurosci.* **24**, 31–55 (2001).
135. Caldwell, H. K., Wersinger, S. R. & Young, W. S. The role of the vasopressin 1b receptor in aggression and other social behaviours. *Prog. Brain Res.* **170**, 65–72 (2008).
136. Hitti, F. L. & Siegelbaum, S. A. The hippocampal CA2 region is essential for social memory. *Nature* **508**, 88–92 (2014).
137. Alexander, G. M. *et al.* Social and novel contexts modify hippocampal CA2 representations of space. *Nat. Commun.* **7**, 10300 (2016).
138. Lu, L., Igarashi, K. M., Witter, M. P., Moser, E. I. & Moser, M.-B. Topography of Place Maps along the CA3-to-CA2 Axis of the Hippocampus. *Neuron* **87**, 1078–92 (2015).
139. Mankin, E. A., Diehl, G. W., Sparks, F. T., Leutgeb, S. & Leutgeb, J. K. Hippocampal CA2 activity patterns change over time to a larger extent than between spatial contexts. *Neuron* **85**, 190–201 (2015).

140. Kay, K. *et al.* A hippocampal network for spatial coding during immobility and sleep. *Nature* **531**, 185–190 (2016).
141. Serradeil-Le Gal, C. *et al.* An overview of SSR149415, a selective nonpeptide vasopressin V(1b) receptor antagonist for the treatment of stress-related disorders. *CNS Drug Rev.* **11**, 53–68 (2005).
142. Allen Brain Institute: Allen Human Brain Atlas.
143. NIH Blueprint Non-Human Primate (NHP) Atlas.
144. Dam, A. M. Epilepsy and Neuron Loss in the Hippocampus. *Epilepsia* **21**, 617–629 (1980).
145. Ishizawa, T. *et al.* Selective neurofibrillary degeneration of the hippocampal CA2 sector is associated with four-repeat tauopathies. *J. Neuropathol. Exp. Neurol.* **61**, 1040–7 (2002).
146. Benes, F. M., Sorensen, I. & Bird, E. D. Reduced Neuronal Size in Posterior Hippocampus of Schizophrenic Patients. *Schizophr. Bull.* **17**, 597–608 (1991).
147. Gao, X.-M. *et al.* Ionotropic Glutamate Receptors and Expression of N-Methyl-D-Aspartate Receptor Subunits in Subregions of Human Hippocampus: Effects of Schizophrenia. *Am. J. Psychiatry* **157**, 1141–1149 (2000).
148. Piskorowski, R. A. *et al.* Age-Dependent Specific Changes in Area CA2 of the Hippocampus and Social Memory Deficit in a Mouse Model of the 22q11.2 Deletion Syndrome. *Neuron* **89**, 163–76 (2016).
149. Maxwell, W. L. *et al.* There is differential loss of pyramidal cells from the human hippocampus with survival after blunt head injury. *J. Neuropathol. Exp. Neurol.* **62**, 272–9 (2003).
150. Sloviter, R. S. ‘Epileptic’ brain damage in rats induced by sustained electrical stimulation of the perforant path. I. Acute electrophysiological and light microscopic studies. *Brain Res. Bull.* **10**, 675–697 (1983).
151. Vigers, A. J., Baquet, Z. C. & Jones, K. R. Expression of neurotrophin-3 in the mouse forebrain: insights from a targeted LacZ reporter. *J. Comp. Neurol.* **416**, 398–415 (2000).
152. Cheng, B. & Mattson, M. P. NT-3 and BDNF protect CNS neurons against metabolic/excitotoxic insults. *Brain Res.* **640**, 56–67 (1994).
153. Young, D. & Dragunow, M. Neuronal Injury Following Electrically Induced Status Epilepticus with and without Adenosine Receptor Antagonism. *Exp. Neurol.* **133**, 125–137 (1995).
154. Williamson, A. & Spencer, D. D. Electrophysiological characterization of CA2 pyramidal cells from epileptic humans. *Hippocampus* **4**, 226–237 (1994).
155. Sloviter, R. S. Calcium-binding protein (calbindin-D28k) and parvalbumin immunocytochemistry: Localization in the rat hippocampus with specific reference to the selective vulnerability of hippocampal neurons to seizure activity. *J. Comp. Neurol.* **280**, 183–196 (1989).
156. Winn, H. R., Welsh, J. E., Rubio, R. & Berne, R. M. Changes in brain adenosine during bicuculline-induced seizures in rats. Effects of hypoxia and altered systemic blood pressure. *Circ. Res.* **47**, 568–577 (1980).
157. Laeremans, A. *et al.* AMIGO2 mRNA expression in hippocampal CA2 and CA3a. *Brain Struct. Funct.* **218**, 123–130 (2013).
158. Ono, T., Sekino-Suzuki, N., Kikkawa, Y., Yonekawa, H. & Kawashima, S. Alivin

- 1, a novel neuronal activity-dependent gene, inhibits apoptosis and promotes survival of cerebellar granule neurons. *J. Neurosci.* **23**, 5887–96 (2003).
159. López-Aranda, M. F. *et al.* Role of layer 6 of V2 visual cortex in object-recognition memory. *Science* **325**, 87–9 (2009).
160. Landrum, M. J. *et al.* ClinVar: public archive of relationships among sequence variation and human phenotype. *Nucleic Acids Res.* **42**, D980–D985 (2014).